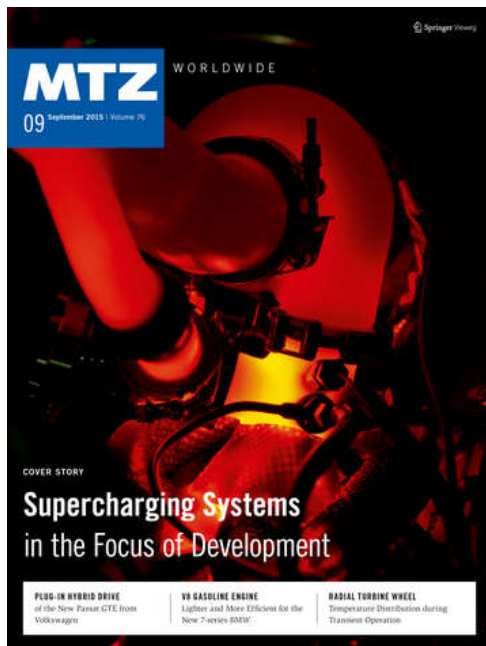


personal buildup for

## Force Motors Limited Library



mtzw 9/2015, as epaper released on 03.08.2015  
<http://http:www.mtz-worldwide.com>

content:

page 1: Cover. p.1

page 2: Contents. p.2

page 3: Editorial. p.3

page 4: Verdichter. p.4-9

page 10: Aufladung. p.10-15

page 16: Passat. p.16-23

page 24: Ansaugdrossel. p.24-29

page 30: Emissionen. p.30-33

page 34: 7er\_BMW. p.34-41

page 42: Imprint. p.42

page 43: Peer\_review. p.43

page 44: Energieeffizienz. p.44-49

page 50: Radialturbinenrad. p.50-55

**copyright**

The PDF download of contributions is a service for our subscribers. This compilation was

created individually for Force Motors Limited Library. Any duplication, renting, leasing, distribution and publicreproduction of the material supplied by the publisher, as well as making it publicly available, is prohibited without his permission.

**MTZ**

WORLDWIDE

09 September 2015 | Volume 76

personal buildup for Force Motors Limited Library

COVER STORY

# Supercharging Systems in the Focus of Development

**PLUG-IN HYBRID DRIVE**

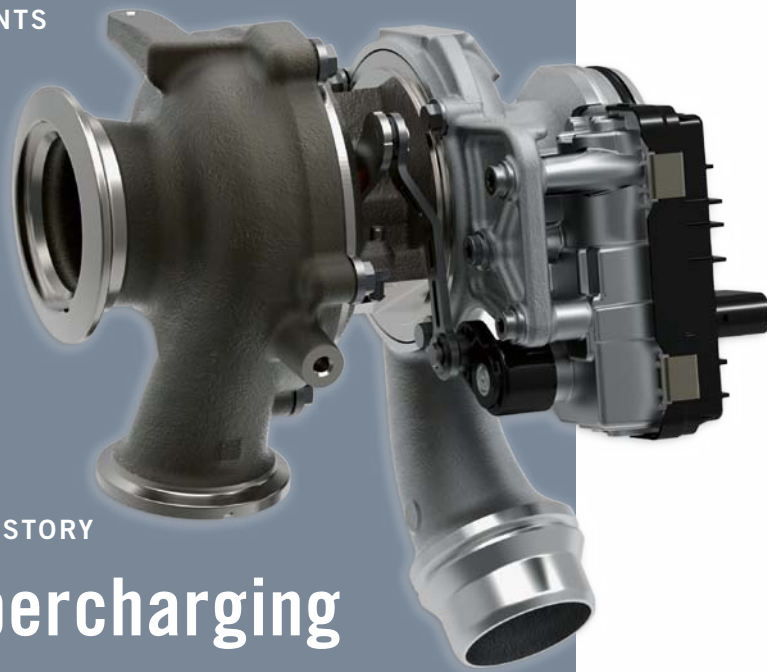
of the New Passat GTE from  
Volkswagen

**V8 GASOLINE ENGINE**

Lighter and More Efficient for the  
New 7-series BMW

**RADIAL TURBINE WHEEL**

Temperature Distribution during  
Transient Operation



## COVER STORY

# Supercharging Systems in the Focus of Development

Supercharging is and always has been the best means of improving the power output, torque and efficiency of internal combustion engines. However, the trend towards downsizing – a smaller engine displacement combined with an exhaust gas turbo-charger – reaches its limits when it comes to low-end torque. Manufacturers and suppliers are intensively working on solutions to improve driveability by increasing starting torque.

**4** The Electric Supercharger – Challenge, Conception and Implementation  
Stefan Rothgang, Michael Pachmann, Sven Nigrin, Markus von Scheven [Pierburg]

**10** Multistage Supercharging for Downsizing with Reduced Compression Ratio  
René Berndt, René Pohlke, Christopher Severin, Matthias Diezemann [IAV]

**DEVELOPMENT****ELECTRIFICATION OF THE DRIVE**

**16** The Plug-in Hybrid Drive of the VW Passat GTE  
Hanno Jelden, Norbert Pelz, Heiko Haußmann, Manfred Kloft [Volkswagen]

**EMISSIONS**

**24** Optimisation of Boosting Stage and LP EGR System through Pre-swirl Throttle  
Urs Hanig, Nicolai Halder, Mihai Miclea-Bleiziffer, Jerry Song [BorgWarner]

**30** Emission Reduction – A Solution of Lubricant Composition, Calibration and Mechanical Development  
Jens Hadler, Christian Lensch-Franzen, Marcus Gohl, Tobias Mink [APL]

**GASOLINE ENGINES**

**34** The V8 Gasoline Engine for the New 7-series BMW  
Johann Schopp, Rainer Düngen, Martin Wetzel, Thomas Spieß [BMW]

**RESEARCH**

**43** Peer Review

**ALTERNATIVE DRIVES**

**44** Advanced Development of Hybrid Drivetrains  
Friedrich Brezger [KIT]

**SUPERCHARGING**

**50** Temperature Distribution in a Radial Turbine Wheel during Transient Operation  
Mathias Diefenthal, Christian Rakut, Hailu Tadesse, Manfred Wirsum [RWTH Aachen]

**RUBRICS | SERVICE**

**3** Editorial  
**42** Imprint, Scientific Advisory Board

**COVER FIGURE** © Volkswagen Motorsport  
**FIGURE ABOVE** © Bosch Mahle Turbo Systems

---

# Under Pressure

---

Dear Reader,

can you remember your very first car? Even today, I still have vivid memories of mine. It was back in 2000, while I was still at school, when I scraped all my money together and eagerly placed 5000 Deutschmarks on the previous owner's kitchen table, after tough but fruitful negotiations. In return, I became the registered keeper of a small Japanese car that had been launched in 1987 and was already a rarity. The reason was that this sports version had a three-cylinder 993 cc petrol engine equipped with twelve valves and a turbocharger. The maximum output of 74 kW, which had to pull just 810 kg of unladen weight, was a source of great enjoyment for me. At 3500 rpm, a green lamp with a stylised turbocharger would light up between the speedometer and the rev counter. The maximum boost pressure, and at the same time the full potential of 130 Nm of torque, would then come in with a powerful kick – and that's just how I felt it.

What I could not have known at the time was that downsizing, the engine concept in this small car, would become more relevant today than ever before. And, across brands, models and vehicle classes, would become a key element for reducing fleet fuel consumption and complying with CO<sub>2</sub> emissions legislation. The green turbo lamp has long since been banished from the dashboard. Today, drivers want supercharging systems that have the widest possible operating range to ensure a

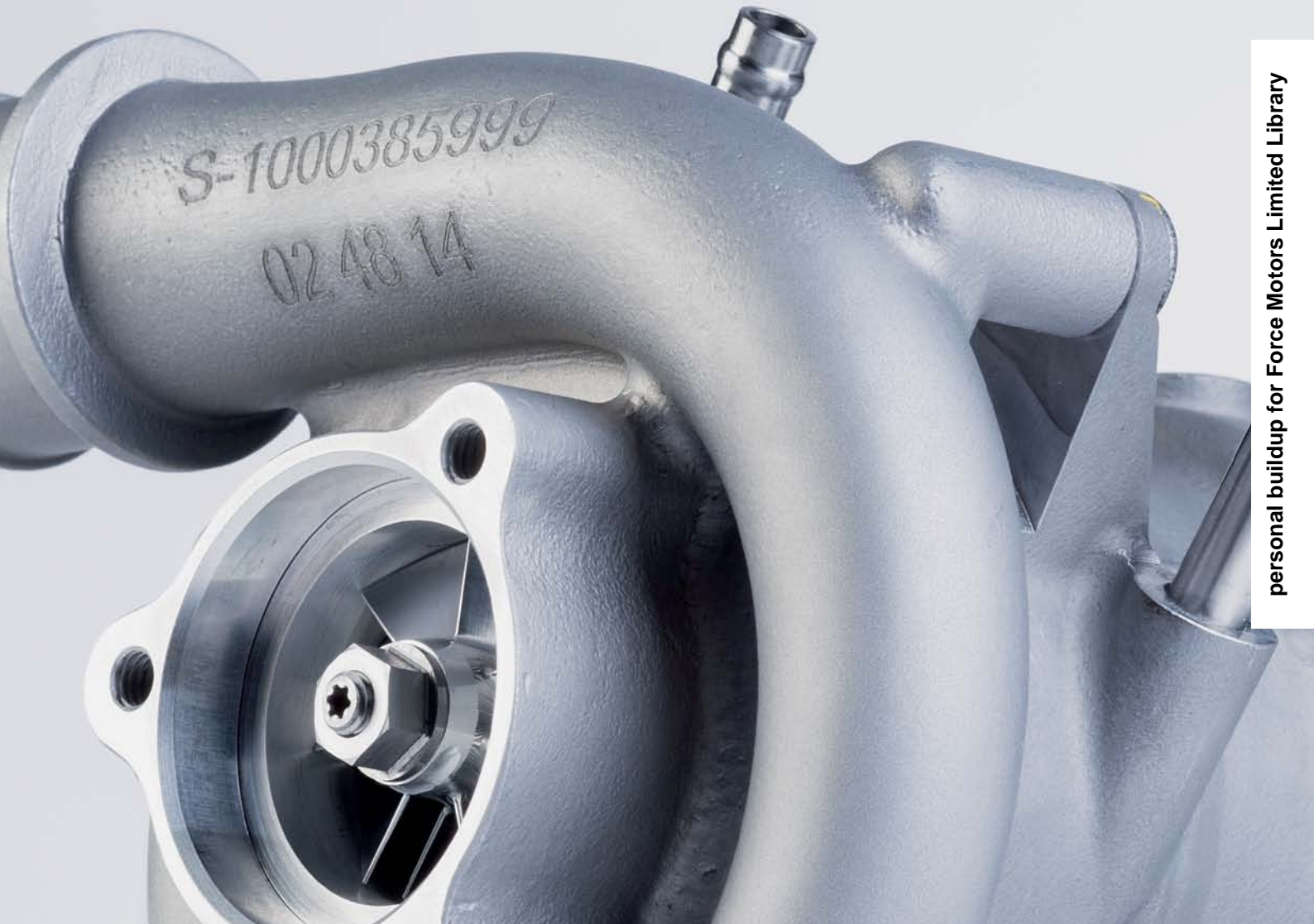
correspondingly even, balanced torque curve. And the aim is to raise low-end torque in particular. Only in this way will further downsizing with even higher specific power outputs be able to fully replace an engine with a larger displacement. OEMs, suppliers and engineering service providers are working intensively on various solutions. Particular focus is on multi-stage supercharging systems which not only use an exhaust gas turbocharger but also have an electrically powered compressor. Some of the latest approaches and research findings are described in our Cover Story on page 4.

Best regards,



**Dipl.-Journ. (FH) Martin Westerhoff**  
Deputy Editor in Chief





# The Electric Supercharger Challenge, Conception and Implementation

Electric superchargers enable improvement in CO<sub>2</sub> and pollutant emissions while simultaneously enhancing the driveability and subjective driving experience. Based on the technical challenges, the Pierburg GmbH introduces the in house developed electrical air charger.

## AUTHORS



**Dipl.-Ing. Stefan Rothgang**  
is Senior Manager for  
Auxiliaries & Alternative Drives  
in the Advanced Engineering  
of the Pierburg GmbH  
in Neuss (Germany).



**Dipl.-Ing. Michael Pachmann**  
is Head of the Emission Controls  
Business Unit at the Pierburg GmbH  
in Neuss (Germany).



**Dipl.-Ing. Sven Nigrin**  
is Electronic Development Engineer  
for Auxiliaries & Alternative Drives  
in the Advanced Engineering of the  
Pierburg GmbH in Neuss (Germany).



**Markus von Scheven, M. Sc.**  
is E-Engine Development Engineer  
for Auxiliaries & Alternative Drives  
in the Advanced Engineering of the  
Pierburg GmbH in Neuss (Germany).

## ELECTRICALLY SUPPORTED ENGINE SUPERCHARGING

In addition to perceivable features like acceleration and power characteristics, end customers especially cite low fuel consumption as a criterion when buying a new vehicle. This and further reduced CO<sub>2</sub> emission limits from 130 to 95 g/km represent the central challenges for the manufacturers in developing vehicles and their powertrains.

While these overall development goals had long been considered almost irreconcilable with one another, the paradigm shift from singular powertrain combustion engines to a partially electrified powertrain offers entirely new design possibilities.

Vehicle electrical systems with suitably adjusted voltage and ampacity thus enable the use of high-performance mechatronic components that can be operated flexibly and independently from the operational status of the combustion engine. Downsizing and downspeeding concepts employ this flexibilisation within the context of a partial electrification of the supercharging process, in which a purely electrical supercharger is added to supplement the conventional supercharging unit. The result is a considerably accelerated build-up of supercharging pressure from low revolution speeds. The high torque thereby made available enables one to experience performance previously known only from purely electric powertrains [1, 2, 3].

As an established supplier of 12-, 48-V and high-voltage components, Pierburg GmbH has added a supercharging so-called “electric Air Charger” (eAC) to its product portfolio in order to take advantage of the evident market potential. The challenges encountered in developing the eAC – as well as the problem-solving approaches and differentiating features – shall be described in greater detail in the following.

## POSITIONING THE ELECTRIC SUPERCHARGER IN THE AIRFLOW

The eAC can be freely positioned anywhere within the airflow stream, the setup is solely based on the technical requirements. Comparably short, temporary usages for rapid availability of supercharging pressures characterise the scope of application for the component,

thereby making it an ideal part of a multistage supercharging system. The intermittent mode of operation of the eAC makes it sensible to use a parallelly arranged bypass installation, which either connects to the eAC in series with the exhaust-driven supercharger or guides the air directly to the engine without passing through the eAC.

Presenting a simplified airflow intake path, **FIGURE 1** indicates possible mounting positions for the eAC, which are evaluated in a matrix. Each mounting position presents both beneficial and disadvantageous, partially contrary effects in the interaction between component and combustion engine. In addition to the improved response time, similar to

that of a naturally aspirated engine, and reduced pre-catalyst exhaust gas emissions through adjusted engine air conditions, increased exhaust gas recirculation rates are obtainable depending on the position. Moreover, the overall efficiency of the electric supercharger in positions 3 and 4 can be positively influenced due to the fact that the compressor maps of the eAC can be narrower resulting in higher efficiency. Furthermore, high air pressures and air temperatures that might place stress on the components must be taken into consideration early in the design phase of the eAC. The depositions of the oil bearing system of an upstream supercharging unit and blow-by gases with elements of

engine oil, fuel and water vapour likewise exert critical effects on components. The same applies for discharges from the low-pressure EGR section, with sediments from GPF/DPF systems as well as corrosive reagents.

**TARGET DESIGN PARAMETERS**

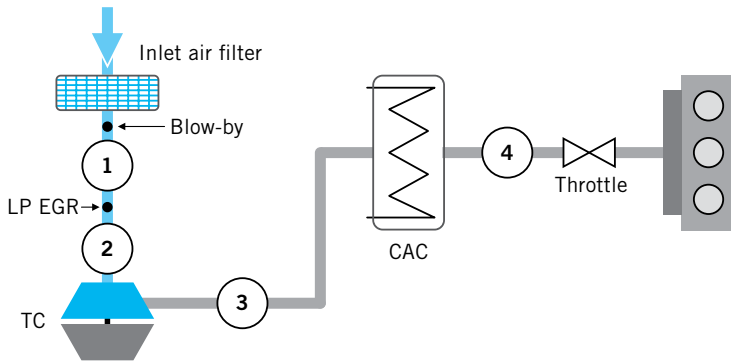
The highest possible utility value of an electric supercharger is measured based on the following target requirements:

- high acceleration/rotational speed gradients
- high aerodynamic capacities/high overall efficiency
- smallest possible outer dimensions
- low component costs.

In addition, one must ensure functionality over the course of the entire engine service life.

In accordance with Eq. 1, the eAC converts electrical energy into drive shaft torque, which translates into acceleration and flow capacity in transient phases:

<b>Eq. 1</b>	$M_{E-motor} = M_{Flow} + M_{Acceleration}$
	with $M_{Acceleration} = J \cdot \dot{\omega}$



Characteristic	Position			
	4	3	2	1
Transient behaviour of combustion engine	++	+	0	0
Average compressor efficiency	++	+	-	0
Enabler for emission reduction	++	+	0	-
Risk of fouling / corrosion / formation of lacquer	0	-	+	++
Thermomechanical stress	0	-	+	++

The mass inertia of the rotating system, consisting of the rotor unit and compressor wheel, proves to be the main factor for achieving high rotor accelerations. Here the compressor wheel shows the greatest potential for reducing mass inertia, so that its constructive design and dimensioning must take that into account. Tests confirm that designing the wheel for high nominal rotational speeds helps to achieve lower  $T_{90}$  acceleration times.  $T_{90}$  is defined as period the eAC needs after a certain speed step to reach 90 % of the new setpoint.

This runs up against rotational speed restrictions, like the permissible component stress, which especially results from the temperature load on the compressor wheel as well as the available wheel and rotor materials, particularly the materials for fixing the rotor magnets. Also limiting rotational speeds are the permissible velocities of the roller bearings used for mounting the rotor which, instead of the plain bearings normally used in exhaust-driven superchargers, are employed to eliminate the need for an oil supply.

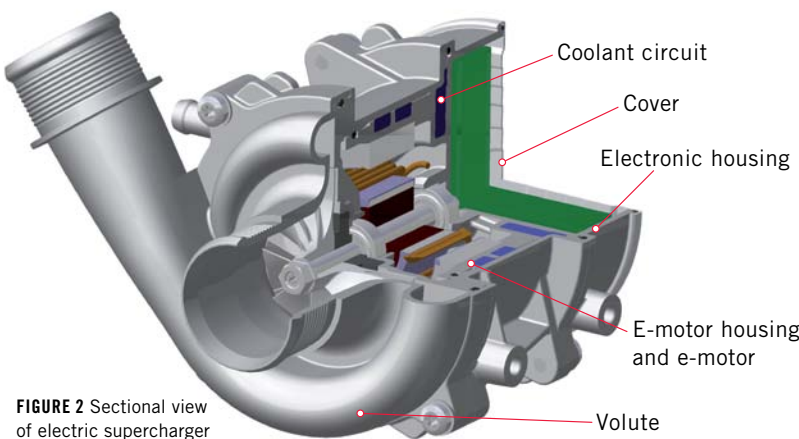


**FIGURE 2** Sectional view of electric supercharger



			12 V	48 V
Aero-dynamics	Operating point ( $\pi$ , $\dot{m}$ )	- ; kg/h	1.25; 150	1.45; 300
	Acceleration $T_{90}$	ms	<350	<250
	Rated speed eAC (max.)	rpm	70k	65k
Electronics	Voltage level	V	12	48
	Current steady-state	A	150	105
	Max. current transient <1 s	A	200	150
	Max. el. power supply	kW	2.4	7.2
	El. power supply steady-state	kW	1.8	5.0
Mechanics	Accumulated run time / lifetime	h	>1500/6000	
	Max. speed-up no.	-	>1.5 Mio.	
	Max. actuating frequency	%	100	
	Max. air pressure / temperature intake manifold	bar/°C	3.5-4/190	

FIGURE 3 Electric supercharger specification

The available drive shaft materials, the distances from the centre of the bearing to the centre of gravity of the compressor wheel as well as the bearing and housing stiffnesses define the resonance frequency profile of the rotor. This limits the rotational speed of the rotor which has to stay subcritical. A nominal rotational speed of between 65,000 and 70,000 rpm was selected as the best compromise for the eAC.

### CONSTRUCTION AND SPECIFICATION

The ball bearings (with retainers made of PEEK and a high-performance lubricant), which cannot be manufactured as self-sealing due to the high rotational speeds, are inserted in a pre-stressed fixed/movable bearing combination and special holding fixtures of the outer ring for tolerance compensation and rotation prevention.

Among the range of materials for manufacturing compression wheels, high-performance plastic materials are

excluded due to the expected thermal and dynamic mechanical stress. Added to that is a limited degree of freedom in the design of a wheel made from plastic material resulting from manufacturing limitations, which in turn limits the efficiency for the supercharger stage.

For this reason, the compressor wheels were designed as a milled aluminium component and developed with an optimised hub length and rear contour by employing the most modern, internal CAE methods as well as verifications on laboratory and engine test benches. Mass inertias of less than 50 % of the nominal values of conventional compression wheels were achieved in this way. Small clearances to reduce gap losses between wheel and contour as well as the desired high-pressure die casting demoldability of the entire volute are additional features of the supercharger unit, FIGURE 2.

The design and dimensioning of the other eAC components is based on the design of the electric motor. The electric motor itself consists of the wound stator, the electrically active rotor segment and

the power electronics (PE). The latter includes the power element with the semiconductors, the control board (galvanically separated from the power element with CAN/LIN interface) and the intermediate circuit.

The electric motor, controlled and rpm-regulated by the PE, can be designed in different ways. A permanently excited and symmetrically designed synchronous motor, used within the company on numerous occasions, was selected for the eAC. The limited available space – and thus the high motor efficiency required – were decisive in the selection process. Additional requirements are low noise radiation and a low price for components. Above all, this demands an efficient and small-sized PE as well as a low need for intermediate circuit capacities.

Furthermore, the motor design leads on the one hand to cost-effective fabrication due to the possible simplification of the clearances and tolerances between rotor and stator, while on the other hand leading to significantly less pronounced radial force components with enormous advantages in the NVH.

The eAC design constructed in this way enables good scalability of individual systems in order to realise both 12- and 48-V models with 2 and/or 5 kW electric power ratings. FIGURE 3 shows the current specification figures of the application available in hardware.

### THERMAL COMPONENT STRESS

Despite high efficiency factors of the individual components, the electric power conversion induces thermal losses, which need to be taken care of to protect the electric motor and the PE. As an example, FIGURE 4 shows the given efficiency chain with a power input of 5 kW, of which about 485 W becomes lost as waste heat,

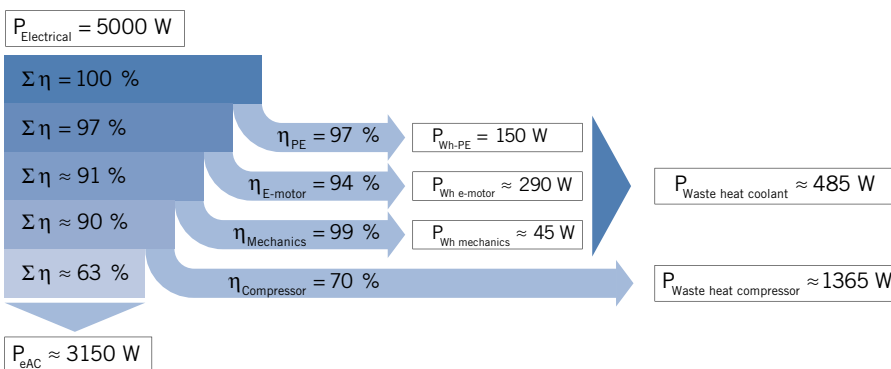


FIGURE 4 Efficiency chain of electric supercharger at optimum operating point

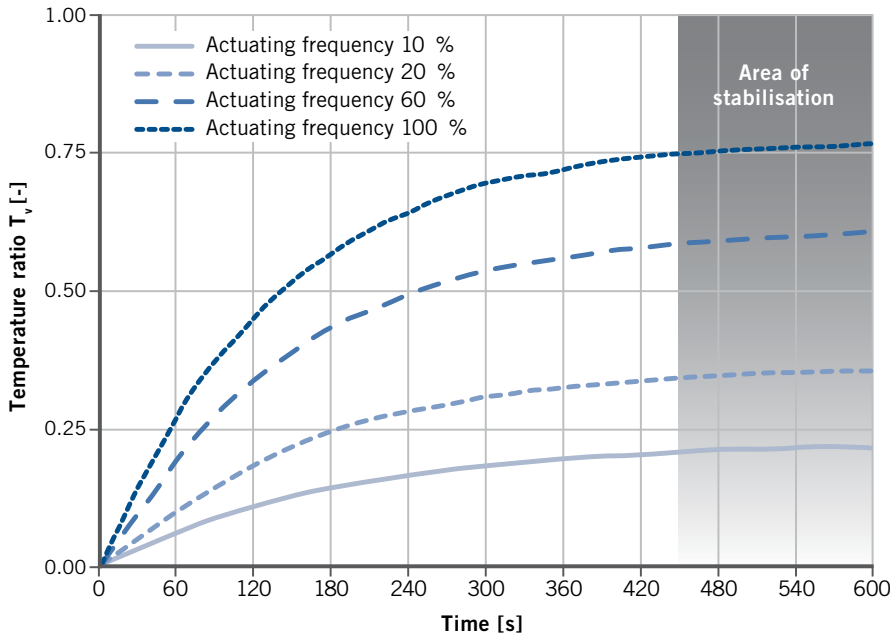


FIGURE 5 Temperature ratio of the electric motor over runtime and actuation frequency

primarily in the electric motor and the PE. A circulating coolant duct placed between the electric motor and its housing ensures direct cooling of the elements needing protection. Temperature sensors on the coils and semiconductors enable a control strategy to additionally protect the elements against damage.

The thereby achievable actuating frequency (AF) as a quotient of runtime over nominal rotation speed and idling time can assume values of up to 100 %. FIGURE 5 shows the actuating frequencies plotted over time relative to the temperature ratio of the engine, coolant and permissible temperature limit with the definition according to Eq. 2:

Eq. 2	$T_v = \frac{T_{E-motor} - T_{Coolant}}{T_{Limit} - T_{Coolant}}$
-------	---

The absolute switch-on time per cycle made possible by the eAC is dependent upon various constraints and can extend into minutes.

**SEALING**

The apparent impracticality of using abrasive seals for insertion between the eAC housing and rotor due to the high rotational speeds exposes the risk that stresses like reagents, high air temperatures and air pressures will find their way along the rotor shaft into the electric supercharger. All individual components

affected, such as the non-self-sealing bearings, the electric motor and the PE, would be irreversibly damaged by erosion, corrosion and bearing lubricant discharge. Common countermeasures such as labyrinth seals, shaft seal rings or centrifugal discs prove inadequate. A sealing concept was therefore developed, which relies on proven components in a new overall functionality. This ensures that no air and reagent contamination exchange occurs between the interior of the eAC and the intake manifold. The durability of the eAC is thereby ensured and separate static sealing measures, especially of the PE, can be eliminated.

**BYPASSING**

The temporary interconnection of the eAC in the airflow stream takes place via a bypass device, which is as throttle-free, compression-sealed and flexible as possible in its operating behaviour. Common spring-loaded, passive one-way valves are discretely opened and generate flow losses, which lead to increased losses in gas exchange. Strategies for preventing pump phenomena (through the recirculation of compressed air) are also impossible.

Therefore an electric, continuous and counterrotatingly pivotable control butterfly valve with fail-safe function was developed, which was especially dedicated to the aim of high system integration. In this way, the bypass valve and other functionalities can be combined into one unit.

Moreover, a specially developed seal seat protects against residual leakage at a level comparable with a heavy-duty butterfly valve. In one design variation the bypass valve was additionally integrated into the outlet of the volute, creating a very compact overall housing, which is advantageous in meeting most ambitious cost and package targets.

**CONCLUSION AND OUTLOOK**

Due to its modular structure and availability in 12-V and 48-V component versions, the presented electric supercharger fulfils the operating requirements for both diesel and gasoline engines. Integrated into the design were innovative solutions for increasing reliability and durability as well as enabling the possibility of long operating times. The eAC is designed for usage in combination with a conventional turbocharger for improving transient response. Tuning the entire air system specifically to the eAC yields the greatest improvements in all target parameters.

**REFERENCES**

[1] Knirsch, S.; Weiss, U.; Zülch, S.; Kilger, M: Electric Supercharging in the Audi RS 5 TDI Concept. In: MTZ worldwide 76 (2015), No. 1, pp. 14-19  
 [2] Aymanns, R.; Uhlmann, R.; Nebbia, C.; Plum, T.: Electric Supercharging, New Opportunities with Higher System Voltage. In: MTZ worldwide 75 (2014), No. 7-8, pp. 4-11  
 [3] Forissier, M.; Zechmair, D.; Weber, O.; Criddle, M.; Durrieu, D.; Picron, V.; Menegazzi, P.; Surbled, K.; Wu, Y.: The Electric Supercharger. 34<sup>th</sup> Vienna Motor Symposium, 2013

2g  
less CO<sub>2</sub>  
per km

**FTE**  
automotive

personal buildup for Force Motors Limited Library



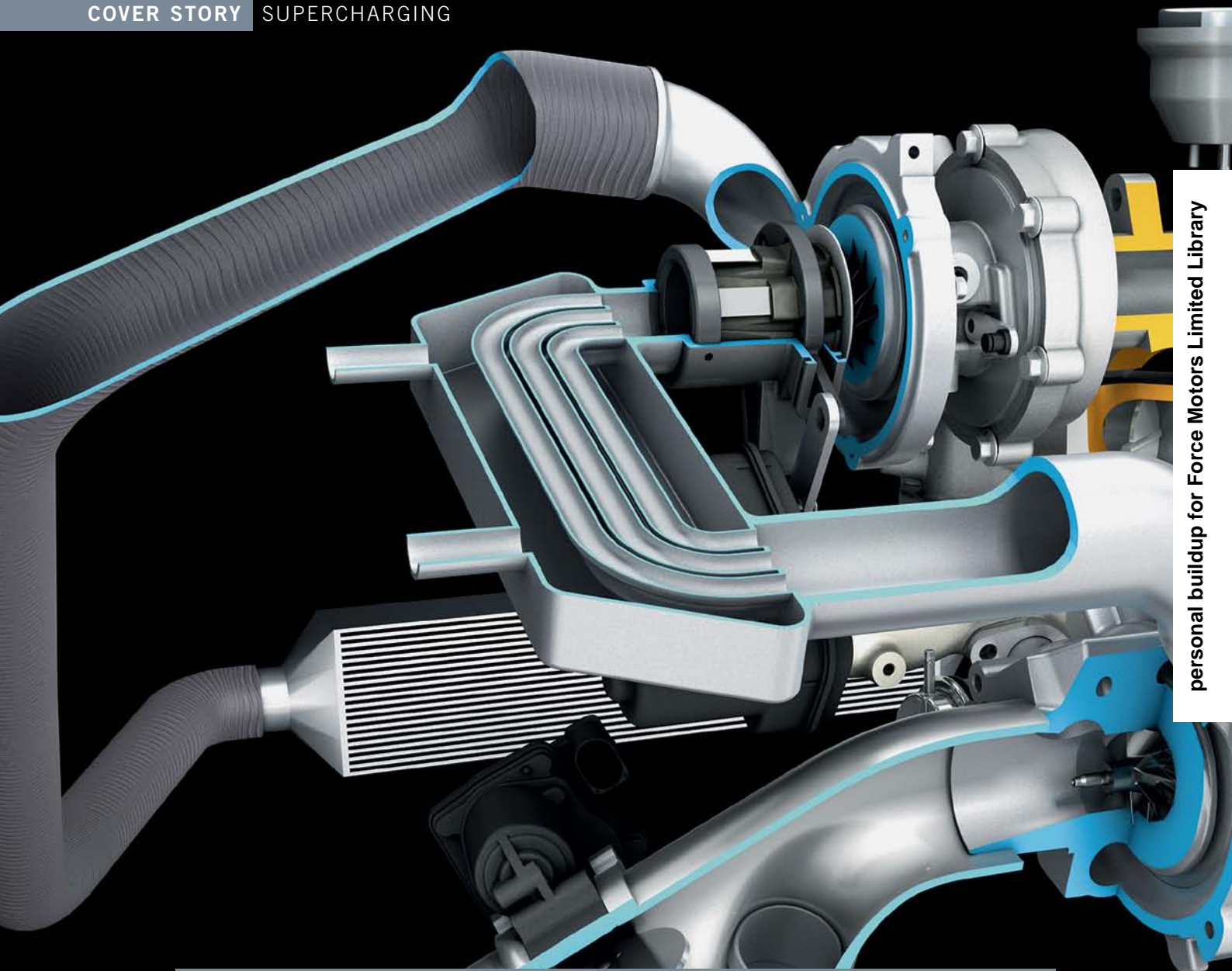
Lightweight and more efficient:  
Developed by FTE automotive

FTE automotive – Innovation drives

While working with a customer on an innovative gearbox we achieved significantly reduced CO<sub>2</sub> emissions with this electrically powered oil pump made of high-performance plastic.

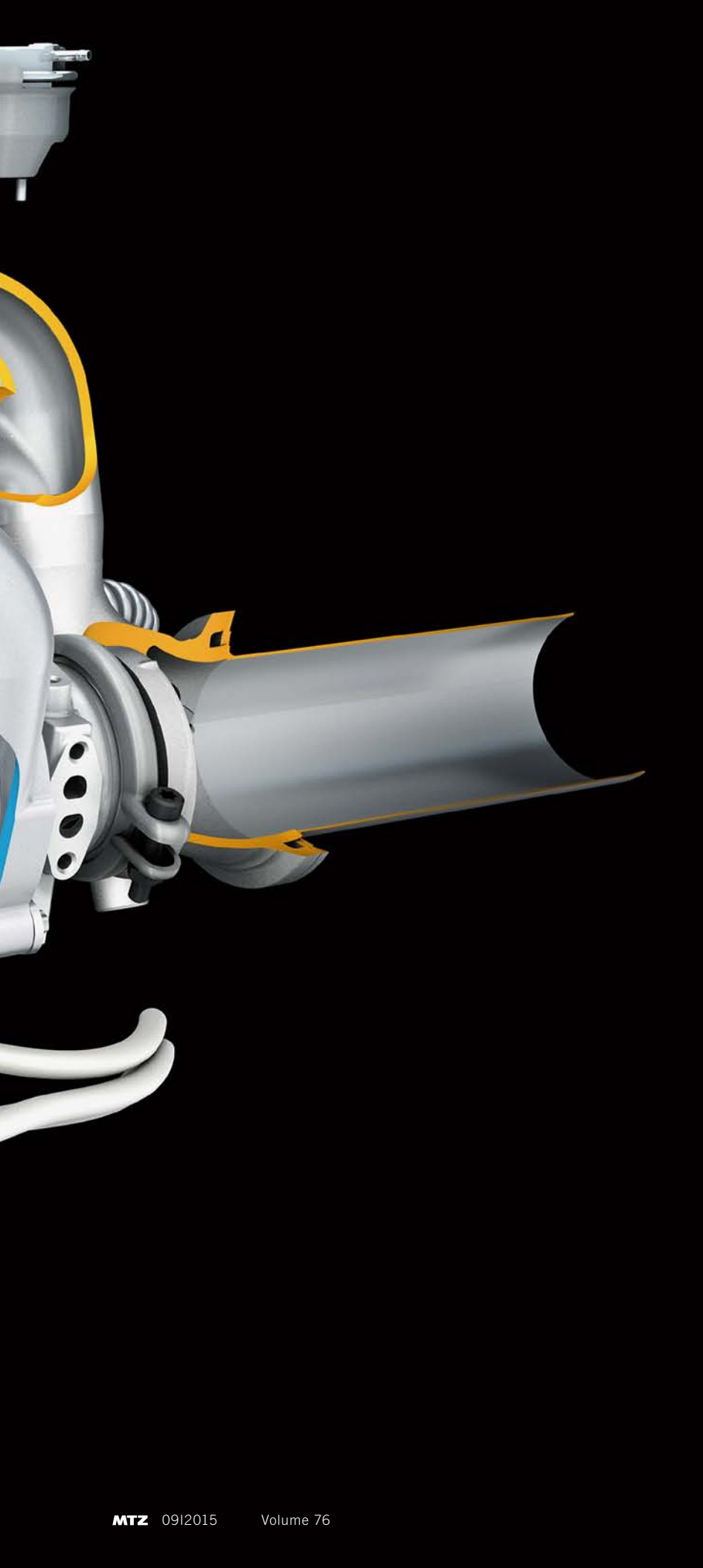
We could be taking the next step with you.

➤ [www.fte.de](http://www.fte.de)



# Multistage Supercharging for Downsizing with Reduced Compression Ratio

Downsizing remains one of the key technologies for reducing CO<sub>2</sub> emissions in diesel engines. A variable compression ratio makes it possible to achieve a further increase in specific power output while staying within the thermo-mechanical stress limits, although this is necessarily linked with a further rise in boost pressures. Against this background, IAV has examined the potential of multi-stage supercharging for achieving a specific power output of 110 kW/l on the basis of steady-state and transient simulations.



## AUTHORS



**Dr.-Ing. René Berndt**  
is Team Manager in Air Path Concepts, Business Area Powertrain Mechatronics Diesel, at the IAV GmbH in Berlin (Germany).



**Dipl.-Ing. René Pohlke**  
is Development Engineer in Diesel Engine Concepts, Business Area Powertrain Mechatronics Diesel, at the IAV GmbH in Berlin (Germany).



**Dr.-Ing. Christopher Severin**  
is Head of the System Development and Combustion Concepts Department, Business Area Powertrain Mechatronics Systems, at the IAV GmbH in Gifhorn (Germany).



**Dipl.-Ing. Matthias Diezemann**  
is Senior Technical Consultant in Technology Scouting, Business Area Powertrain Mechatronics Diesel, at the IAV GmbH in Berlin (Germany).

## DYNAMIC BEHAVIOUR AND RESPONSIVENESS POSES MAJOR CHALLENGE

Nowadays, the development of modern passenger car diesel engines is defined more than ever by endeavors to reduce fuel consumption while also meeting statutory emission ceilings and improving power density. However, these goals are at odds to the extent that those meas-

ures with a positive effect in one direction come with drawbacks in relation to the others. Combining consistent downsizing approaches with higher supercharging rates is increasingly making this balancing act work.

Given its high level of market penetration in Europe among passenger car and truck drive systems, the diesel engine can be instrumental in quickly reducing fleet CO<sub>2</sub> emission levels on a lasting basis. Downsizing remains one of the key technologies for IAV, even if the thermo-mechanical loads, such as peak cylinder pressure and exhaust emission temperature, have reached their limits. In this context, a variable compression ratio (VCR) makes it possible to observe these limits while further increasing specific engine output.

This increase is automatically contingent on further increasing boost pressure. A rating of 110 kW/l requires a two-stage supercharging concept (P2S, permanent two-stage) at the point of nominal power output. Particular attention is given here to reaching a compromise between an adequate supply of boost pressure in the low-end torque (LET) and part-load range with a higher compression ratio ( $\epsilon$ ) on the one hand and the pressure ratio to volume flow behaviour needed on the other to reach the specific power output target at full load with reduced  $\epsilon$ . It is against this backdrop that the dynamic behaviour and responsiveness of such a power output concept poses a major challenge.

**MULTISTAGE SUPERCHARGING CONCEPTS**

Five supercharging concepts are under consideration for an in-line four-cylinder passenger car diesel engine with a displacement of 2.2 l which meet the above-mentioned goals. They are compared and evaluated below by means of 1-D simulation. Unlike the basic configuration, the engine is equipped with a VCR system. For the purpose of analysis, the engine is operated at part load with  $\epsilon = 20$  and at high load with  $\epsilon = 11$ . The following table summarises the base engine's technical specifications:

- stroke / bore: 99 mm / 83 mm
- geometric compression ratio (basis): 16.2
- number of valves: 4
- maximum injection pressure: 2000 bar
- maximum cylinder pressure: 190 bar
- maximum exhaust gas temperature upstream of the turbine: 835 °C
- supercharging concept (production configuration): regulated two-stage (R2S) from BorgWarner Turbo Systems).

The potential provided by the various supercharging concepts in conjunction with the described base engine is ascertained in steady-state full-load investigations involving transient acceleration rates.

**FIGURE 1** shows schematic diagrams presenting the concepts under review at component level. Common to all systems is the fact that boost pressure at the point of nominal power output is built up in two stages as the level required lies above that

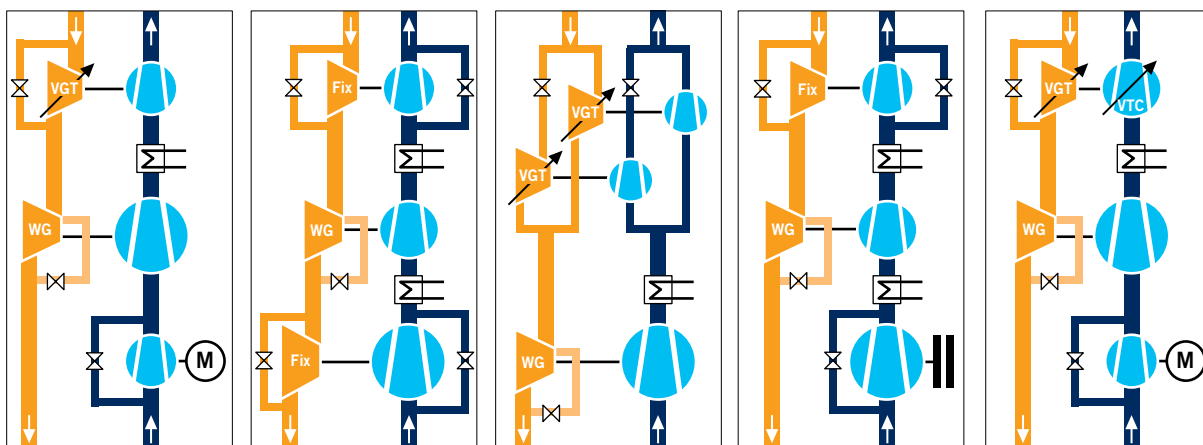
which radial compressors of passenger car size are capable of providing in one stage [1]. Apart from layout 4, this is achieved by connecting exhaust gas turbochargers (ETC) in series. To achieve efficient part-load and response behaviour, these ETC combinations are linked in layout 1 and layout 5 with an electrically driven compressor (48-V systems) in low-pressure (LP) position, also connected in series. By way of alternative, a third ETC is used in layout 2 in serial high-pressure (HP) position. In layout 3 – the so-called Tri-Turbo concept (R3S) presented by BMW and BorgWarner Turbo Systems [2] – two ETCs are connected in parallel in the HP position. Depending on the requisite boost pressure and flow rate, the HP turbochargers are operated either in single (part load) or parallel mode (full load).

Layout 4 shows a consistent fuel consumption and emission concept. At part load, two-stage turbocharging of appropriately small rating delivers the necessary boost pressure. At full load, a mechanically coupled flow compressor in LP position performs this function in combination with the intermediate pressure stage while bypassing the HP stage.

Compared to layout 1, layout 5 additionally has a variable trim compressor (VTC) at the HP stage.

**MODEL AND SIMULATION ENVIRONMENT**

Potential was examined here using a 1-D GTPower simulation model of the base



**Layout 1** Serial TwinTurbo w/ LET-eCompressor  
**Layout 2** Serial TriTurbo  
**Layout 3** Parallel TriTurbo R3S  
**Layout 4** Serial TwinTurbo w/ RP-mCompressor  
**Layout 5** Serial TwinTurbo w/ HP-VTC + LET-eCompressor

**FIGURE 1** Supercharging concepts for providing Ps = 110 kW/l (VGT: variable geometry turbocharger, WG: waste gate, VTC: variable trim compressor)

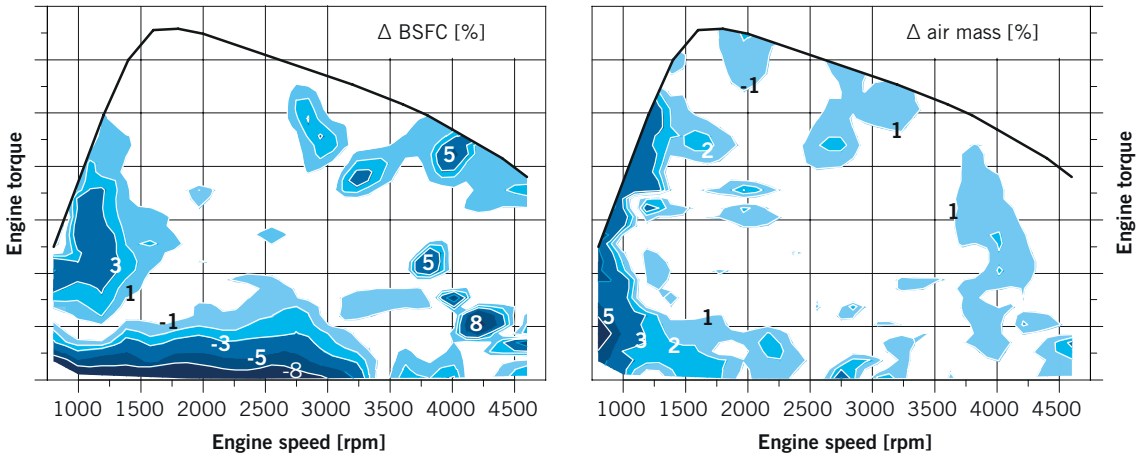


**FIGURE 2** Steady-state, map-wide computation/measurement-based comparison of specific fuel consumption and air mass flow rate for the base engine in production configuration

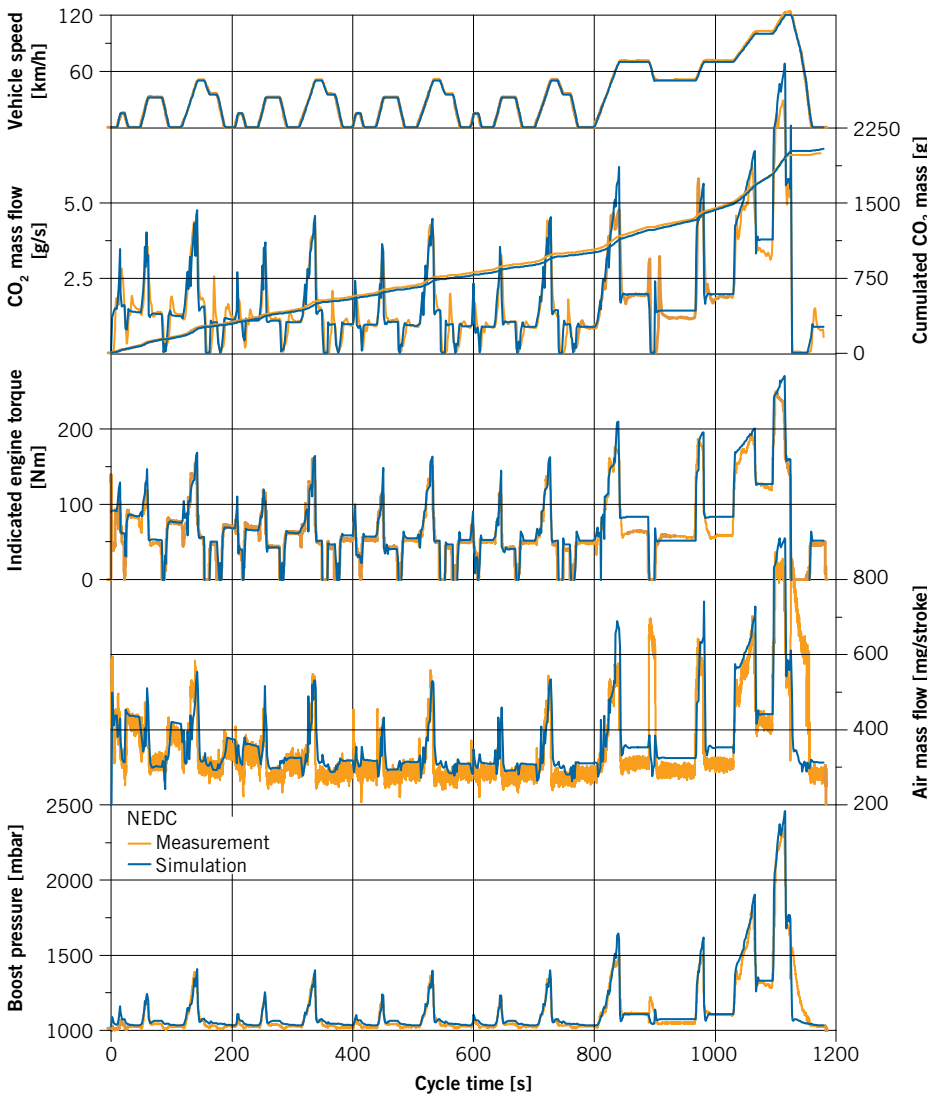


**FIGURE 3** Simulation/measurement-based comparison of the NEDC for the base engine in production configuration

parison, cycle simulation in **FIGURE 3** also shows good correlation.

In simulation, the flow and efficiency behaviour of the turbo machine is usually reproduced by means of maps. The maps provided by the manufacturer are not suitable on account of the concept-specific layout of each individual turbo machine. Instead, it must be possible to describe compressor and turbine behaviour on the basis of scalable, harmoniously progressing and layout-neutral maps. To do this, IAV has developed an empirical scaling method on the basis of extensive measurement data which provides the capability of generating map sets of the same kind for any machine size. Only this way is it possible to compare the supercharging systems objectively and free from layout details specific to the concept underlying the machines used.

#### COMPARISON OF CONCEPTS DURING FULL-LOAD STEADY-STATE OPERATION

The size of the two-stage ETC combinations ensuring operation at nominal power output is determined by the requisite boost pressure and flow rate. This means that there are fixed boundary conditions for rating this supercharger subgroup, leaving stage splitting as the only freely definable parameter.

The above-mentioned scaling method was used to generate optimum flow rate and efficiency maps for the associated compressors and turbine that reach the target value of 110 kW/l with minimum fuel consumption and slightly adjusted limit values ( $p_{cyl, max} = 200 \text{ bar}$ ,  $T_{3, max} = 850 \text{ }^\circ\text{C}$ ) in comparison to the base engine configuration, **FIGURE 4**.

engine which is verified with measurement results both in a steady and transient state. Colourless areas in the com-

parison of steady-state maps in **FIGURE 2** represent a  $\pm 1 \%$  deviation by the simulation from the value measured. In com-

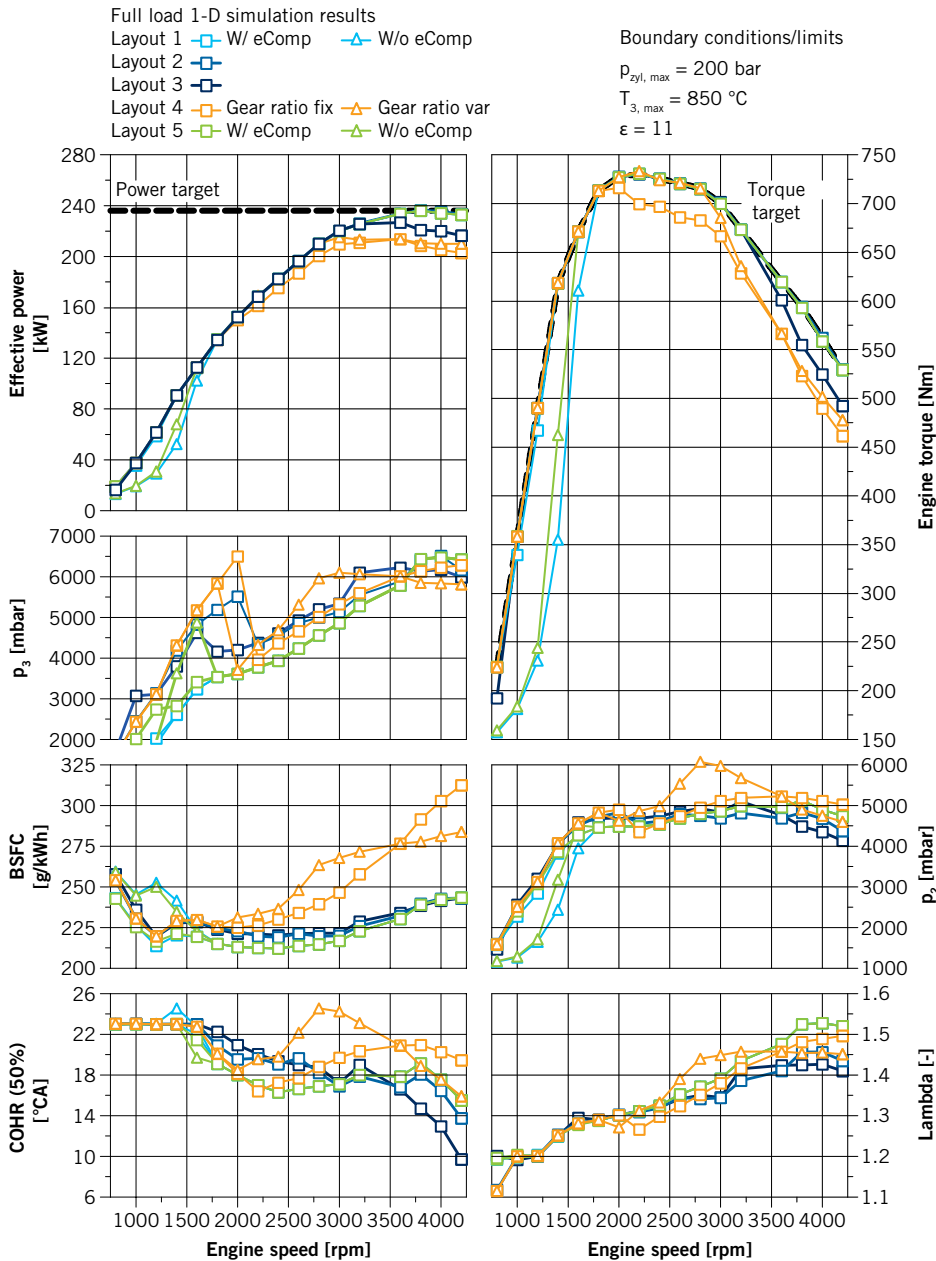


FIGURE 4 Steady-state full-load potential of multistage supercharging concepts

Concepts 1, 2 and 5 reach the power target with their two series-connected ETCs. The LP stage can in each case be calibrated irrespectively of any LET demands. Layout 3 produces a slightly different power output because with the full-load rating it is necessary to find a compromise between the lower and the upper flow range.

Compared to the potential nominal power output, layout 4 lags a long way behind. As from an engine speed of 2000 rpm, the power output required from a mechanically coupled LP stage ( $P_{max} \sim 40$  kW) prevents the target value from

being reached under the requested boundary conditions.

The target for full-load torque behaviour in the lower engine speed range (LET range) comes from a single-stage supercharged 3.0-l six-cylinder engine. These target values can only be reached by rating an additional supercharging component (e-compressor in layouts 1 and 5, HP ETC in layouts 2 and 4, single operating mode for the HP stage in layout 3). This completely describes the hardware as well as the layout boundary conditions for the various supercharging concepts.

Concepts 1 and 5 only reach the target profile of steady-state LET with the aid of the electrically driven compressor, although this component is not rated for steady-state operation. In the dynamic case, the e-compressor reaches the steady-state parameters faster than ETC systems which are associated with significant differences between target and actual values owing to the moment of inertia and dependency on exhaust gas mass flow. The bypassable HP stages of layouts 2 and 4 can be configured independently of the nominal power demand, making it possible to achieve the requisite torque behaviour without a problem.

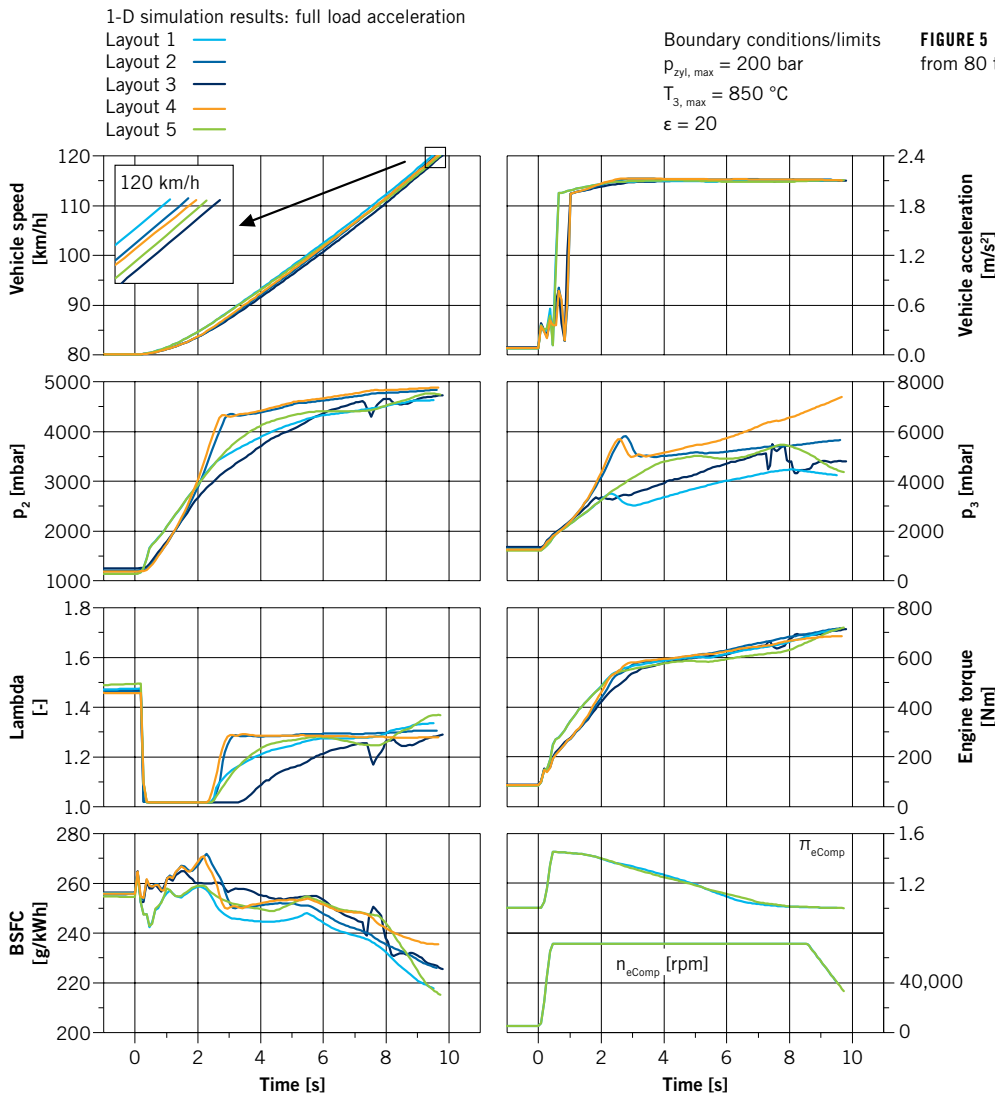
In addition to the above-described turbo machine layout, two options for the gear ratio of the mechanically driven compressor were examined for concept 4. Although a fixed gear ratio comes with benefits on the cost and efficiency side, a compromise must be made between the maximum permissible compressor speed and power target. Although this conflict can be resolved with a variable ratio, it in turn gives rise to disadvantages in relation to costs and levels of efficiency.

**COMPARISON OF CONCEPTS DURING TRANSIENT OPERATION**

To estimate the potentials during dynamic vehicle operation, simulations were carried out to determine elasticity behaviour. Attention focused on an acceleration from 80 to 120 km/h with constant gear ratio and an engine starting speed of  $n = 1280$  rpm.

Given the e-compressor’s spontaneous response, concepts 1 and 5 provide better boost pressure and torque for the first two seconds of acceleration, FIGURE 5. As from second 2, layouts 2 and 4 reach a higher boost pressure on account of the altogether higher boost pressure potential from smaller HP stages. Although concept 3 starts with single operation in the HP stage, the relatively large LP stage limits an even faster built-up of boost pressure and prevents the HP stages from quickly switching over into parallel operating mode.

As both e-compressor systems manage without the relatively small HP stage in comparison to concepts 2 and 4, they produce benefits in terms of exhaust gas backpressure and consequently with regard to charge cycle work.



Direct comparison of concepts 1 and 5 reveals better boost pressure build-up for the VTC system. This is because of the extended map area near the surge limit. This, however, comes at the expense of a close VTG position and thus higher exhaust gas back pressures.

The third turbine stage lacking in concept 4 is the reason for initial benefits in boost pressure development over layout 2. In the further course, however, the serial TriTurbo provides greater flexibility as the HP stage can be bypassed earlier.

### SUMMARY AND OUTLOOK

The potential of multistage supercharging for producing a specific power output of 110 kW/l was examined in this article on the basis of steady-state and transient simulation. Under review were five super-

charging concepts which were evaluated on an in-line four-cylinder passenger car engine with a displacement of 2.2 l.

At steady-state full load those concepts are at an advantage which are capable of implementing two-stage exhaust-gas turbochargers without having to make any compromise in relation to possible LET or part-load demands (concepts 1, 2 and 5).

An additional assessment at part load becomes necessary in particular if spreading the map of the turbo machines in favour of an ambitious nominal power target in the part-load range comes with the risk of only providing little boost pressure potential.

The examinations therefore carried out in addition at part load showed that the e-compressor systems should be combined with LP EGR. The R3S concept shows advantages as soon as both HP stages can

be operated in parallel. With the serial TriTurbo, the LP stage must be strictly bypassed during part-load operation.

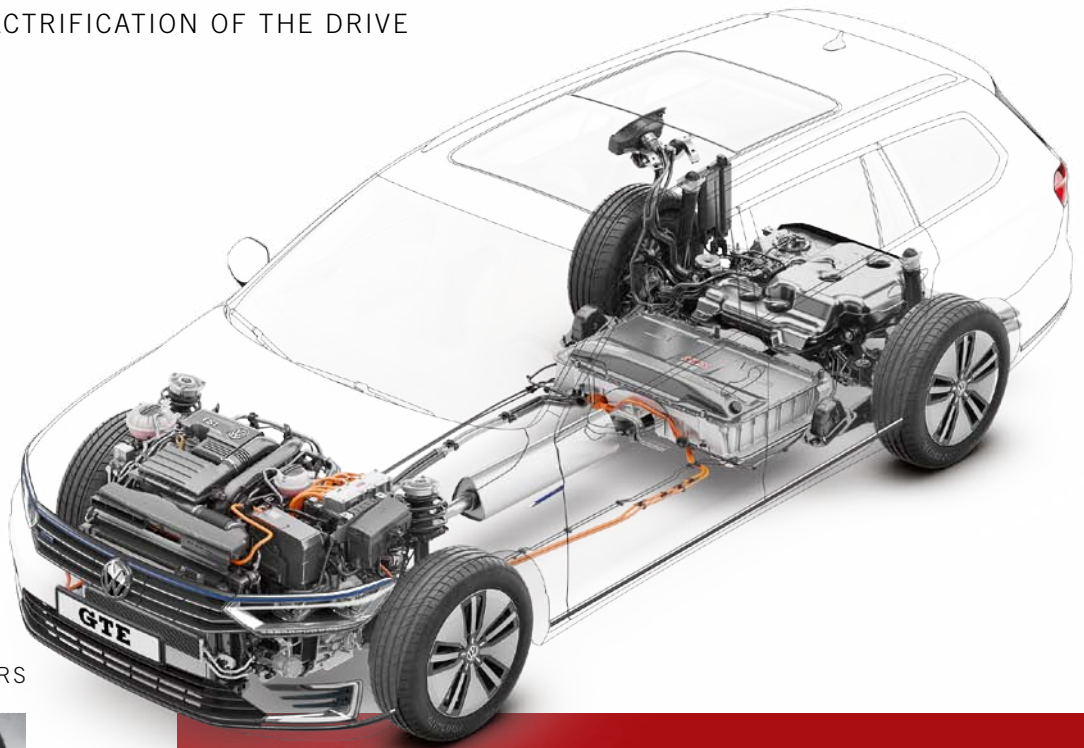
The elasticity tests revealed clear advantages for the e-compressor concepts. In conjunction with a VTC adjustment in HP position, further potentials are produced in terms of boost pressure behaviour. The serial TriTurbo provides a high level of flexibility and can be rated to meet demands.

### REFERENCES

- [1] Brauer, M.; Schramm, C.; Werler, A.; Diezemann, M.; Severin, Ch.; Kratzsch, M.; Neukirchner, H.; Buschmann, G.; Blumenröder, K.: Kontinuierliche variable Verdichtung für Downsizing-Dieselmotoren – Lösungswege zur Verbesserung von Wirkungsgrad, Emissionen und Performance. 36<sup>th</sup> International Vienna Motor Symposium, 2015
- [2] Schmitt, F.: Leistungsstarke Turboaufladung für Pkw-Dieselmotoren. BorgWarner Knowledge Library, 2014

## THANKS

The authors extend their warmest thanks to Carolin Remus and Isaak Darby, both IAV GmbH, for their support in drawing up the simulation results and for their valuable contributions to this publication.



AUTHORS



**Dipl.-Ing. Hanno Jelden** is Head of the Drivetrain Electronics Department within Engine Development at the Volkswagen AG in Wolfsburg (Germany).



**Dipl.-Ing. Norbert Pelz** is Head of the Drivetrain Control Systems Department within Engine Development at the Volkswagen AG in Wolfsburg (Germany).



**Dipl.-Ing. Heiko Haußmann** is Technical Project Manager for the Passat GTE within Engine Development at the Volkswagen AG in Wolfsburg (Germany).



**Dipl.-Ing. Manfred Kloft** is Head of the Subdivision for Advance Development Petrol Engines within Engine Development at the Volkswagen AG in Wolfsburg (Germany).

## The Plug-in Hybrid Drive of the VW Passat GTE

In 2015, Volkswagen presents the first Passat with a plug-in hybrid drive, the Passat GTE, based on the Volkswagen modular matrix for electrified drives. The Passat GTE is offered as a saloon and estate car. It is driven by a 1.4-l TSI engine with 115 kW and an electric motor with an output of 85 kW. Power is transmitted, as per the Volkswagen Golf GTE, via the DQ400E 6-speed dual-clutch gearbox, which can transmit torque of up to 400 Nm. The lithium-ion high-voltage battery with an energy content of 9.9 kWh has been newly developed for the Passat GTE and enables an electric range of up to 50 km.

### A VERSATILE COMBINATION

Political frameworks, social requirements, continuous reduction of fuel consumption and CO<sub>2</sub> emissions, as well as a more intense competitive situation, all impact the development of future drive concepts. It is therefore Volkswagen's objective to develop drives that enable

sustainable mobility, while at the same time offering driving fun and comfort. Electric drives, with their potential for the reduction of CO<sub>2</sub> emissions, are thus an important key aspect for development activities at Volkswagen.

The most compelling attributes of electric vehicles are their performance and emissions-free drive, particularly

in urban traffic. Plug-in hybrids combine the benefits of electric drive with those of the internal combustion engine. This combination serves a number of usage profiles – from electric-driven city vehicle to long-distance vehicle with all the familiar performance features.

Since 2010, Volkswagen has launched series production of two full hybrids (Touareg Hybrid, Jetta Hybrid), two plug-in hybrids (XL1, Golf GTE) and two electric vehicles (e-Up!, e-Golf). With the Passat GTE, Volkswagen is presenting a further production vehicle with plug-in hybrid drive. This car is the next important milestone in the company's electro-mobility strategy [1, 2, 3].

### VEHICLE ARCHITECTURE AND POWERTRAIN

The powertrain of the Passat GTE is designed as a parallel hybrid, meaning that the internal combustion engine and electric motor share a single drive shaft and deliver their driving force via the transmission to the drive axle in parallel or independently of one another. The arrangement here combines a 1.4-l TSI engine from the EA211 range with the DQ400E 6-speed dual-clutch gearbox. It combines the newly developed electric motor, the de-coupler (K0 engine clutch between the TSI engine and the motor) as well as the base transmission, to create a highly integrated, compact assembly. In order to integrate the hybrid powertrain into the Passat vehicle architecture, the TSI engine has been moved to the right by 57.5 mm compared with a conventional drive.

The hybrid drive enables the vehicle to be powered by the internal combustion engine or the electric motor independently of one another or together. In electric drive mode, the Passat GTE achieves already good performance with its 85 kW electric motor and, with the battery fully charged, an electric range of up to 50 km. The hybrid mode – when the internal combustion engine and the electric motor work together to drive the Passat GTE – delivers sporty performance combined with low fuel consumption. In addition, the internal combustion engine provides drivers with all familiar long-distance features and comforts.

Serving as the electric energy storage system is a liquid-cooled lithium-ion

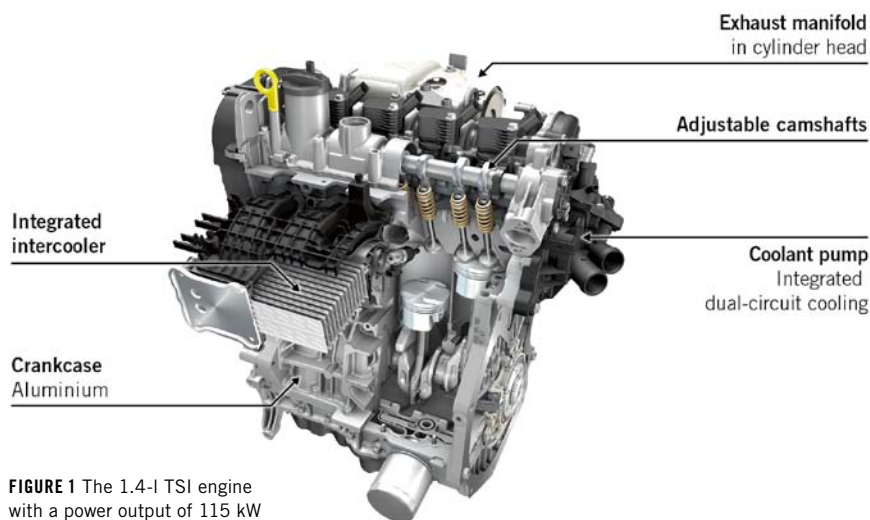


**FIGURE 1** The 1.4-l TSI engine with a power output of 115 kW

high-voltage battery with an energy content of 9.9 kWh. For external charging from the AC grid, there is a charging socket in the radiator grille and a charging device in the engine compartment. The fuel tank is a pressurised system with a capacity of 50 l.

The braking system operates with an electrically controlled brake servo unit. The braking input from the driver is distributed as required between the hydraulic brakes and the electric motor, which then functions as a generator (recuperation). This means that the vehicle's kinetic energy can be used during braking to charge the high-voltage battery.

#### 1.4L TSI ENGINE

The innovative and efficient 1.4l TSI engine, **FIGURE 1**, is used in its base form in many vehicles from the modular transverse matrix (MQB). For its use in the Passat GTE, the power output of the internal combustion engine has been raised to 115 kW. The big-end bearing, pistons, exhaust valves and spark plugs have been adapted accordingly. Further, targeted design measures have been implemented to fulfil requirements that are specific to hybrid technology. These include an immediate availability and full power reserves upon start of the combustion engine when ending an electric drive, as well as stability when it comes to the avoidance of inactive periods in electric drive mode.

The main bearings are treated with a polymer coating. The piston rings are nitrided for surface hardness using

the PVD (Physical Vapour Deposition) process. The bearing shells and piston clearance are adapted accordingly.

The cylinder barrels are powder coated using the APS (Atmospheric Plasma Spray) process. This delivers an especially good coating quality, even in the case of small cylinder bores. In order to ensure good adhesion of the coating, a new laser process developed by Volkswagen gently roughens the aluminium cylinder barrels. This achieves a high adhesive tensile strength.

The plasma coating enables flexible reaction to demands such as heightened resistance to corrosion and wear. Frequent cold starts with immediate performance demands are safely met through targeted tribological characteristics. The thin layer of metallic material ensures good heat transfer to the coolant. The multi-stage honing process takes place under tension with a torque plate fastened to it and generates a particularly smooth surface finish. The use of a fine-grained spray powder creates a large number of pits that are not interconnected. They serve as lubrication pockets for retention of the engine oil.

The piston ring seals the small lubricant pockets as it passes over them, so that the oil is unable to escape. The enclosed lubricant becomes pressurised inside this micro-pressure-chamber system, thus guaranteeing optimum slip between the piston ring and the surface of the cylinder barrel. This ensures retention of low-friction and low-wear hydrodynamic lubrication characteristics all the way down to low sliding speeds close to the pistons'

## DEVELOPMENT ELECTRIFICATION OF THE DRIVE

dead-centre positions. It also reduces particulate emissions from the lubricant film. The REM image, **FIGURE 2**, shows the real surface of a honed plasma layer.

### HYBRID TRANSMISSION

The DQ400E transmission developed by Volkswagen, **FIGURE 3**, incorporates a high-power electric motor, a de-coupler and a 6-speed dual-clutch gearbox into a single, highly integrated unit. This design enables the combination of transversely mounted internal combustion engines with an electric motor to create a parallel hybrid. The DQ400E has already been successfully used in series production in the Golf GTE.

As with the well-known DSG transmission, the flow of power is split between two partial gearboxes via the coaxially arranged drive shafts, each equipped with a clutch. In order to create packaging space for the electric motor integrated into the transmission unit, the gear set has an extremely compact design.

Control is via mechatronics, in the form of an electro-hydraulic control module. To enable on-demand energy management, the hydraulic system consists of one high-pressure and one low-pressure section with operating pressures of 40 and 5 bar respectively. An electrically driven, intermittent dual oil pump supplies both subsystems with the necessary oil pressure on a continuously variable basis.



**FIGURE 2** Hydro-dynamic lubrication of the cylinder barrels with APS coating

The multiple clutch system, which runs in oil, consists of the drive clutches K1 and K2 and the engine clutch K0. The compact actuating unit for the engine clutch is in the clutch space between the electric motor's rotor mount and the input shaft. The rotor

mount is part of both the electric motor and the drive clutch.

The overall efficiency of the transmission is extremely high due to low drag torques, fixed/floating bearings for the drive shafts and actuation of the drive clutch via concentric dual-ring pistons, paired with on-demand energy management for the hydraulics.

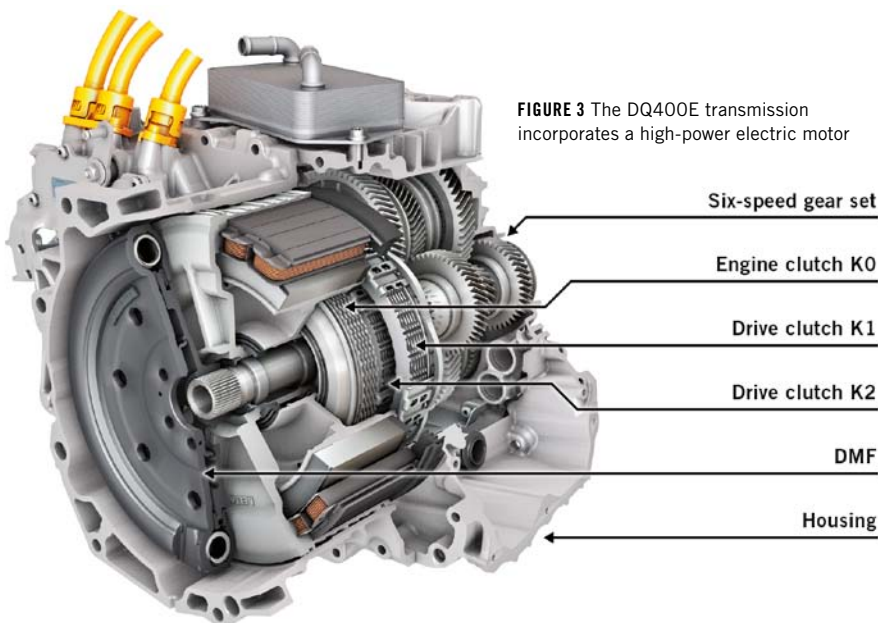


**FIGURE 3** The DQ400E transmission incorporates a high-power electric motor

### ELECTRIC MOTOR

The Passat GTE features a newly developed, three-phase, permanent-magnet synchronous motor with a maximum output of 85 kW. This motor, **FIGURE 4**, is an integral part of the DQ400E transmission and located within the so-called hybrid module on the input shaft between the K0 engine clutch and the K1/K2 drive clutches.

The rotor consists of laminated one-piece stamped and coated electrical sheets, which incorporate the permanent magnets. The stator, in contrast, is made from 24 individual segments, each wrapped with a copper coil and pressed into the cooling jacket. This design development increases

the lamination factor, improving efficiency within the same packaging space. A resolver calculates the position of the rotor and its rotational speed, which are necessary input parameters for control of the phase currents by the power electronics. The motor is integrated into the low-temperature circuit and cooling channels in the casing serve it with a water/glycol mixture.

**POWER ELECTRONICS**

The power electronics, **FIGURE 5**, use phase currents to regulate the torque generated by the electric motor. When it is running as a motor, it uses high-performance insulated-gate bipolar transistors (IGBT) to convert the direct current from the high-voltage battery into three-phase

**FIGURE 5** The power electronics are reduced in packaging space



alternating current of variable frequency and amplitude. In generator mode (recuperation), the alternating current is rectified to charge the high-voltage battery. The power electronics in the Passat GTE have been further developed to incorporate the latest semi-conductor technology and highly integrated low-inductance structural technology. Together with innovative thermal connection of the power semi-conductor to the cooling circuit, achieved through a tight bond between the power module and the heat sink, it has also been possible to reduce

packaging space, despite the improvement in performance figures. The permissible DC voltage range is between 250 and 450 V, while maximum phase current is 450 A and constant phase current more than 200 A.

A DC/DC converter is also integrated into the power electronics for isolated supply of the 12-V vehicle network. Due to the increased comfort requirements of the Passat GTE, its maximum output has been raised to 3 kW. The DC/DC converter has a modular design and can be equipped as required for use in future hybrid and electric vehicles with lower on-board electrical requirements.

**HIGH-VOLTAGE BATTERY**

The electrochemical energy storage system used in the Passat GTE is a modular lithium-ion high-voltage battery, **FIGURE 6**, designed for fully electric and hybrid operation of a plug-in hybrid vehicle. It consists of 96 prismatic cells with a capacity of 28 Ah each. Divided into eight modules of twelve cells each, this results in a rated energy content of 9.9 kWh at a rated voltage of 352 V.

To save space, the high-voltage battery is packaged compactly beneath the vehicle floor. This arrangement means the interior of the Passat and Passat Estate

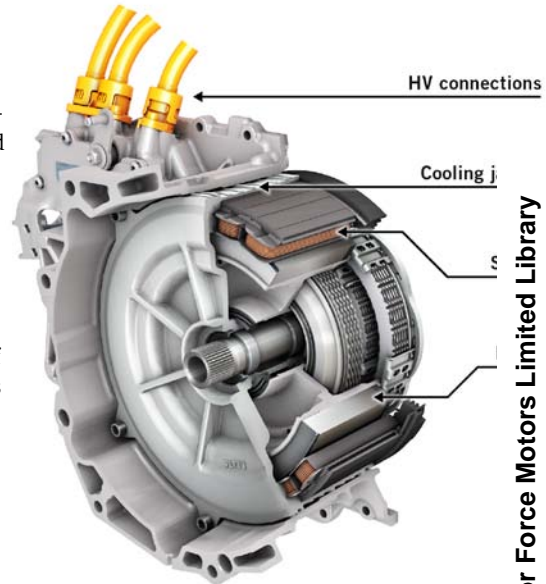
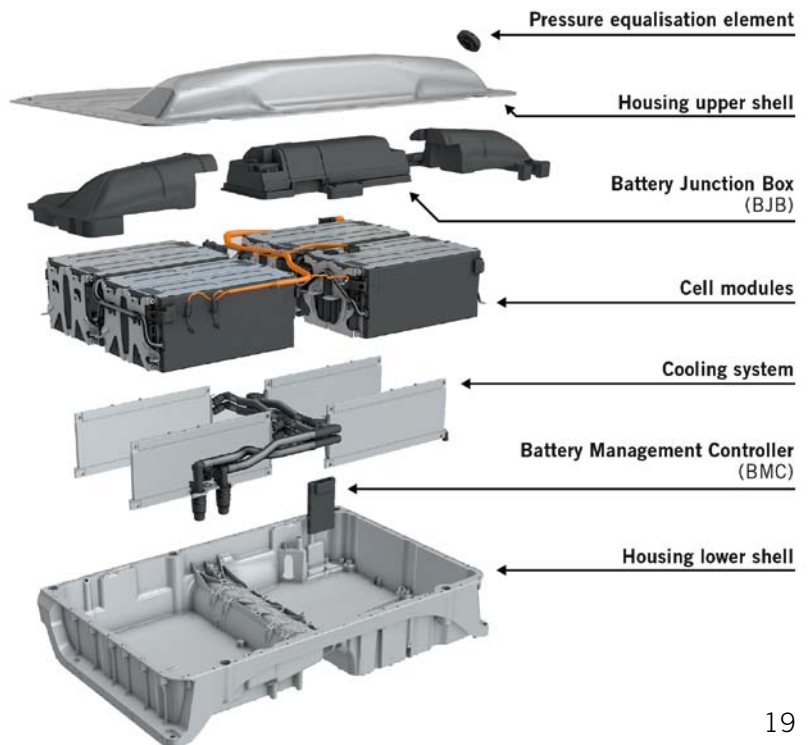


**FIGURE 4** The three-phase, permanent-magnet synchronous motor with an output of 85 kW

are not restricted in any way. The housing for the high-voltage battery consists of an upper section made from sheet aluminium and a lower section made from cast aluminium. Alongside the cell modules, the high-voltage battery also incorporates the battery management controller (BMC) and the battery junction box (BJB) containing the switching and measurement elements for the battery's high-voltage part.

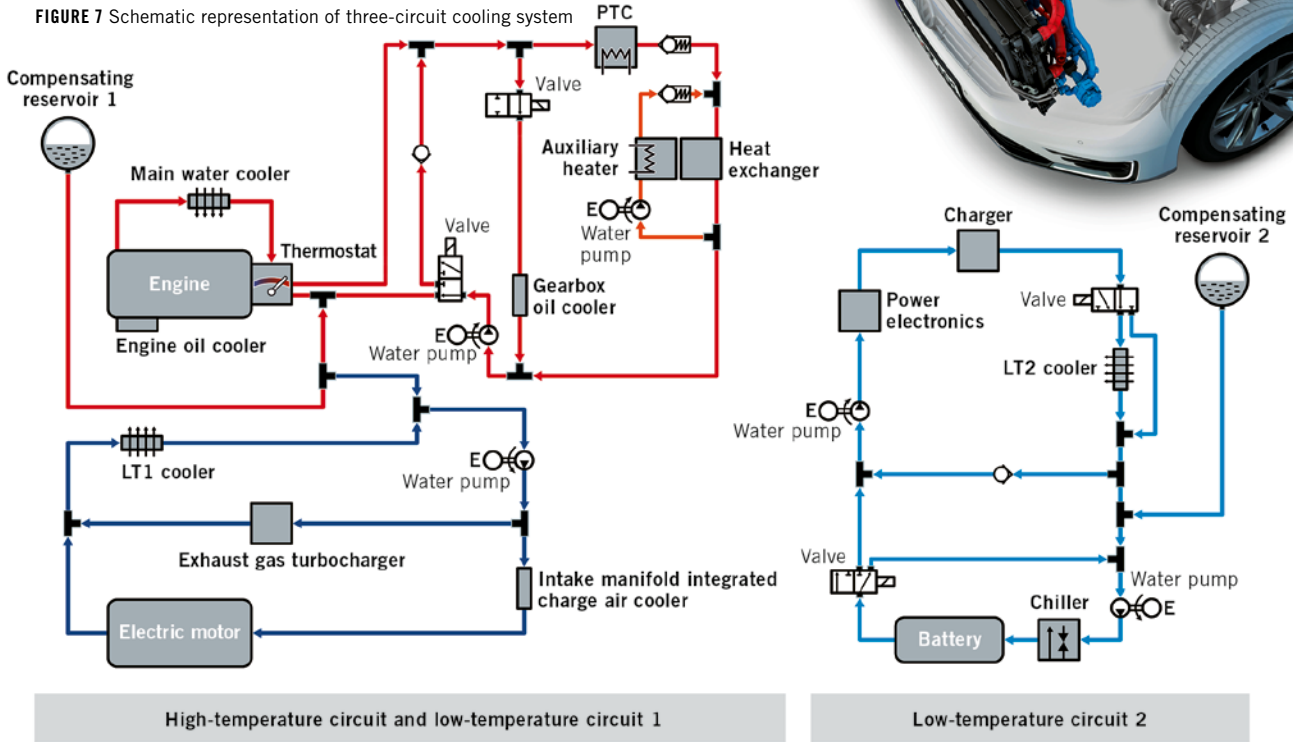
**FIGURE 6** Structure of the lithium-ion high-voltage battery



# DEVELOPMENT ELECTRIFICATION OF THE DRIVE



FIGURE 7 Schematic representation of three-circuit cooling system



personal buildup for Force Motors Limited Library

## THREE-CIRCUIT COOLING SYSTEM

The topology of the cooling system for the Passat GTE, **FIGURE 7**, is carried over from the Golf GTE, although the cooling system has been adapted to the requirements of the powertrain and the vehicle. Inflow to the radiator has been optimised to suit the requirements of the Passat GTE through appropriate shaping of the radiator grille. This compensates for the increased cooling requirements arising from the higher system output, greater vehicle weight and higher towing load. The only modifications necessary are to the radiator for low-temperature circuit 2, due to the structure and packaging position of the power electronics.

## PLUG-IN OPERATING STRATEGY

Volkswagen has expanded its hybrid operating strategy to incorporate the requirements of a plug-in hybrid. New functions for drive control and driveline management are developed within the framework of the Group's function matrix, **FIGURE 8**, and existing functions are optimised for full hybrids.

Catalyst warm-up takes place independently of the driving profile. When the K0 clutch is open, the internal combustion engine runs under zero load up



- Control, TSI engine**  
Engine control unit (ECU)
- Control, electric motor**  
Power electronics (PE)
- Torque coordination**
- Drivability functions**  
Load cycling, vibration damping
- Hybrid coordinator**  
Operating modes, charging strategy
- Torque distribution ICE - EM**  
Hybrid load point shifting, recuperation
- Start/Stop control**  
with DQ400E
- Display functions**  
Energy flow, power meter
- Operating mode selection**
- External input from assistance functions**  
ESC, ACC/FAS, GRA
- External charging**  
AC
- Driver input**  
Drive pedal, brake pedal
- High-voltage battery management**
- Thermal management**

FIGURE 8 Group function matrix and hybrid control for the MQB plug-in hybrid

# Heavy-Duty, On- and Off-Highway Engines

Sustainable concepts put to the test

10th International MTZ Conference

24 and 25 November 2015

Speyer | Germany

---

## NEW DIESEL, GAS AND DUAL-FUEL ENGINES

Working Process and Design Concepts

---

## COMPLETE SYSTEM OPTIMIZATION

Engine and Component Design

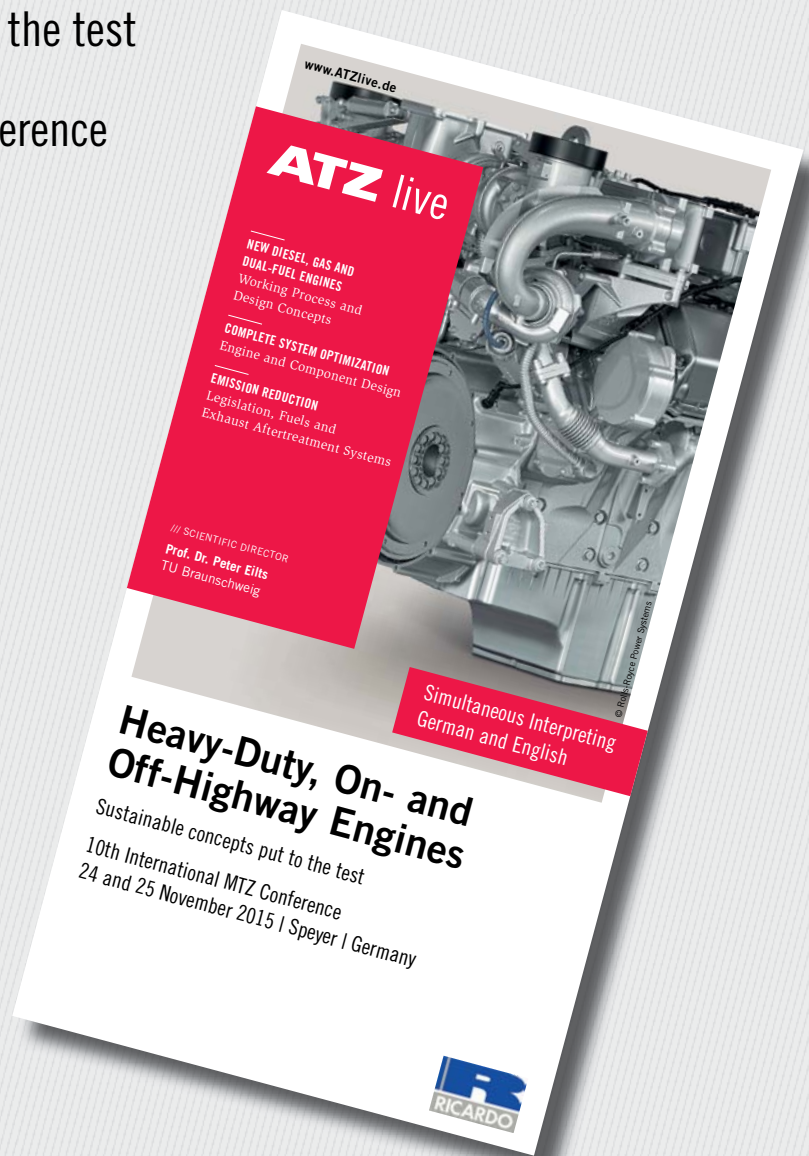
---

## EMISSION REDUCTION

Legislation, Fuels and Exhaust Aftertreatment Systems

/// SCIENTIFIC DIRECTOR

**Prof. Dr. Peter Eilts**  
TU Braunschweig



/// KINDLY SUPPORTED BY



**ATZ** live  
Abraham-Lincoln-Straße 46  
65189 Wiesbaden | Germany

Phone +49 611 7878-131  
Fax +49 611 7878-452  
ATZlive@springer.com

PROGRAM AND REGISTRATION  
[www.ATZlive.com](http://www.ATZlive.com)



FIGURE 9 Left tube of the Active Info Display with variable read-outs

to a preferred, pre-set rev level. The electric motor provides the torque which the driver demands.

In electric mode, the Passat GTE operates as a purely electric vehicle. In this operating mode, there are periods during which the internal combustion engine is inactive. During these operating phases, the drive management regulates the lubrication of the internal combustion engine by intermittently refilling the oil gallery. The internal combustion engine is also run briefly at pre-determined intervals in order to ensure lubrication for component protection.

**PLUG-IN OPERATING MODES**

The following five operating modes are available:

- E mode: Once the vehicle is ready for operation, the Passat GTE starts in E

mode. The electric drive supplies all propulsion up to a top speed of 130 km/h. In certain cases, for example when the outside temperature is extremely low or the high-voltage battery has very low charge, the internal combustion engine starts at the beginning of the driving cycle.

- Hybrid mode: In hybrid mode, the internal combustion engine and the electric motor run at the same time or alternately in order to achieve good performance combined with low fuel consumption. The charge status of the high-voltage battery is kept at a medium level through switching operation of the electric motor between motor and generator. This uses a total of around one eighth of the capacity of the high-voltage battery.
- Battery charge mode: In battery charge mode, the internal combus-

tion engine charges the high-voltage battery through the generator function of the electric motor. This means that the charge status of the high-voltage battery can be increased, for example, during cross-country driving, to ensure sufficient energy is available for electric-only operation in the next zero-emissions zone.

- GTE mode: In GTE mode, parallel operation of the internal combustion engine and the electric motor delivers particularly sporty performance. The driver has at his/her disposal an overall system torque of 400 Nm and system output of 160 kW. During this time, the charge status of the high-voltage battery is constantly maintained within an upper-medium bandwidth.
- B drive: B drive facilitates a preset value for defined motor recuperation when the accelerator pedal is in the 0 position. By making small adjustments to the angle of the accelerator pedal, the driver can influence the degree of recuperation and thus vehicle deceleration.

**DISPLAY CONCEPT**

Volkswagen offers the Passat GTE with an optional high-resolution display, known as the 12.3-inch large Active Info Display, in place of the conventional instrument panel, FIGURE 9. All instru-

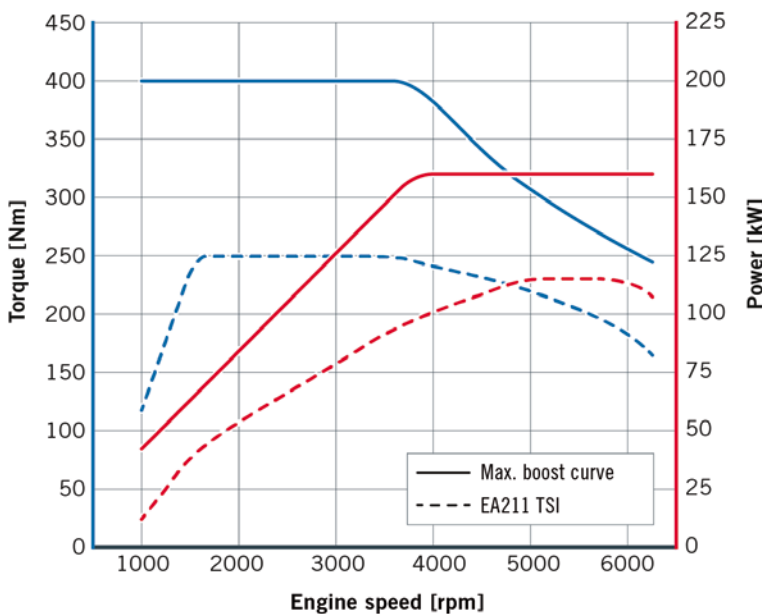


FIGURE 10 Technical data of the Passat GTE

**Technical data**

- Internal combustion engine: 115 kW / 250 Nm
- Electric motor: 85 kW / 330 Nm
- System: 160 kW / 400 Nm
- Energy content HV battery: 9.9 kWh
- Electrical range: approx. 50 km
- Electricity consumption: 12.2 / 12.4 kWh/100 km <sup>1)</sup>
- Acceleration 0 – 100 km/h: 7.4 s
- Top speed: 225 km/h
- Fuel consumption: 1.6 l / 100 km
- CO<sub>2</sub> emissions: 37 / 39 g/km <sup>1)</sup>
- Kerb weight: 1647 / 1660 kg <sup>1)</sup>

<sup>1)</sup> Saloon / estate

ments and dedicated gauges and read-outs are generated digitally, with the power meter and/or the rev counter on the left and the speedometer on the right. The resolution of  $1440 \times 540$  pixels delivers an exceptionally precise, interactive and high-quality graphical representation of all details. The Active Info Display shows relevant driver information, depending on the selected operating mode and individual settings.

#### TECHNICAL DATA

The Passat GTE is an exceptionally sporty yet efficient plug-in hybrid, as indicated by the performance and consumption figures, **FIGURE 10**. With the 85 kW electric drive, it reaches an electric top speed of 130 km/h. The lithium-ion high-voltage battery, which can be charged via the external electricity grid, has an energy content of 9.9 kWh and provides power for an electrical range of up to 50 km. In GTE mode, the TSI and electric motor deliver a system output of 160 kW and accelerate the Passat GTE from 0 to 100 km/h in just 7.4 s. It reaches a top speed of 225 km/h.

The fuel consumption of the Passat GTE is dependent upon the route profile and the operating mode. In purely electrical operation, the electrical consumption is 12.2 kWh/100 km. In mixed operation, with two-thirds electric-only and one-third hybrid driving, the average fuel consumption in the NEDC is 1.6 l/100 km. This equates to CO<sub>2</sub> emissions for the Passat GTE of 37 g/km.

#### SUMMARY

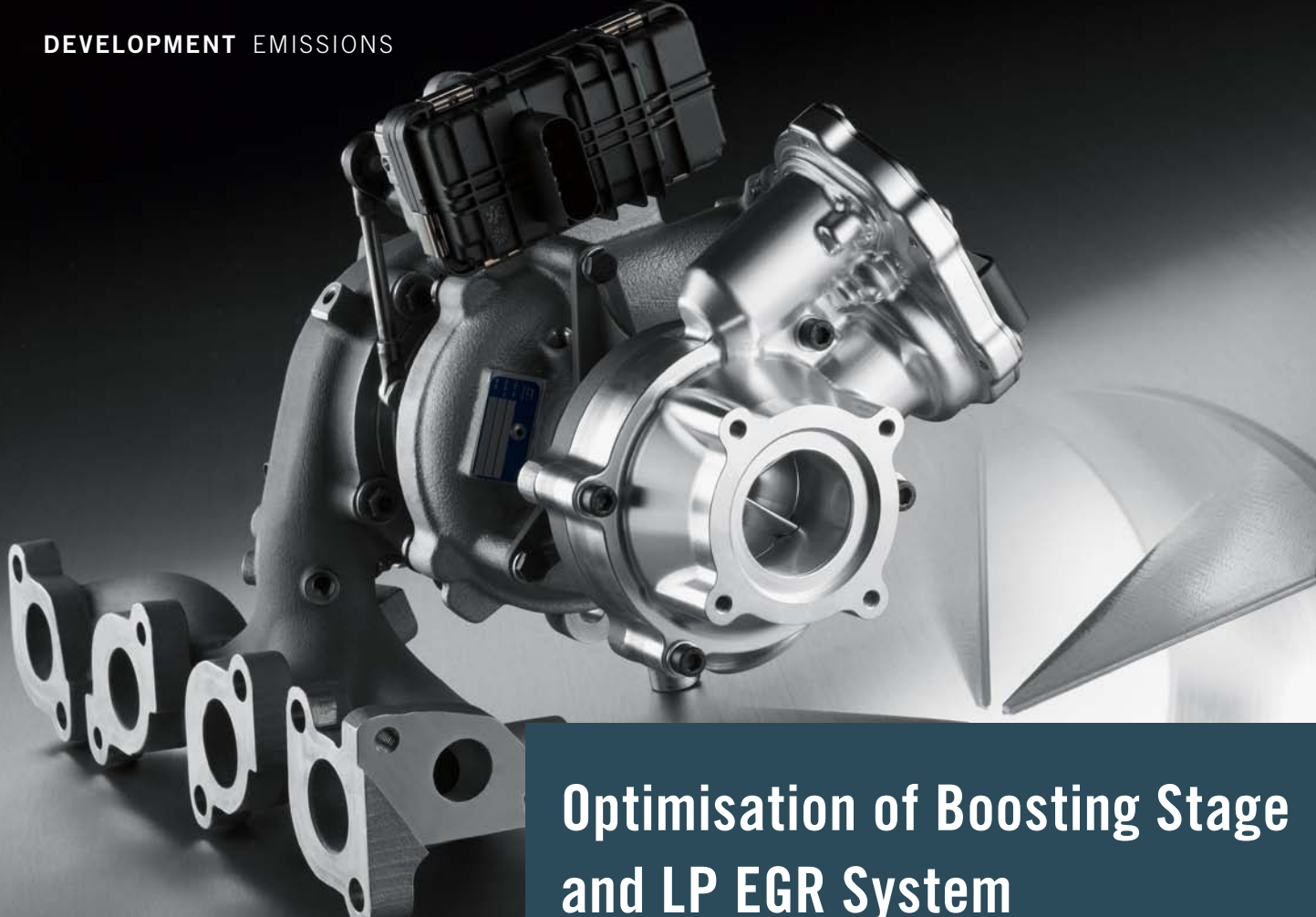
The plug-in hybrid in the Volkswagen Passat GTE combines the apparently contradictory. With an electrical range of around 50 km, it can drive economically and with zero local emissions. At the same time, the Passat GTE has unrestricted long-distance capabilities, thanks to its efficient TSI engine. Both drives together deliver sporty performance. And, at all times, it remains fully suited to everyday use, with the wide-ranging usability familiar from Volkswagen vehicles.

The drive system of the Volkswagen Passat GTE is part of a modular matrix, the components of which enable the construction of a number of different drive systems for hybrid and electric vehicles.

The control software for the new drive systems has also been derived from a modular approach. With the aid of these modular drive and control matrix, is it possible to achieve significant reductions in effort and costs when it comes to the development of new drive systems. This is a major prerequisite for the broader market penetration of hybrid and electric vehicles.

#### REFERENCES

- [1] Zillmer, M.; Neußer, H.-J.; Jelden, H.; Lück, P.; Kruse, G.: The Electric Drive of the Volkswagen e-up! – A Step Towards Modular Electrification of the Powertrain. 34<sup>th</sup> International Vienna Motor Symposium, 2013
- [2] Hadler, J.; Neußer, H.-J.; Szengel, R.; Middelndorf, H.; Theobald, J.; Möller, N.: The New TSI. 33<sup>rd</sup> International Vienna Motor Symposium, 2012
- [3] Jelden, H.; Philipp, K.; Weiß, N.; Keßler, A.: The Plug-In Hybrid of the Volkswagen Modular Transverse Matrix. In: MTZ 75 (2014), No. 4, pp. 40-47



# Optimisation of Boosting Stage and LP EGR System through Pre-swirl Throttle

personal buildup for Force Motors Limited Library

## SYSTEM LAYOUT TO PROVIDE A NEW SOLUTION

In [1] the IST (inlet swirl throttle) was introduced as a new component to provide multiple benefits. Through its location close upstream the TC compressor it has the ability to greatly impact the engine breathing system. The diesel engine used for system optimisation is the same as described in [1]. With 2.0-l displacement, a rated power of 100 kW and dual loop EGR it represents a state-of-the-art architecture. In its delivery

Driven by emissions legislation, need for CO<sub>2</sub> reduction, and customer demand for vehicle agility, passenger car diesel engines incorporate a combination of low pressure exhaust gas recirculation (LP EGR) and exhaust gas turbochargers (TC). BorgWarner has identified the combination of TC and a so-called inlet swirl throttle (IST) as a new way to optimise the engine for emissions, performance and cost.

## AUTHORS



**Dipl.-Ing. Urs Hanig** is Program Manager for Pass Car Systems at BorgWarner in Ludwigsburg (Germany) and Member of BorgWarner's Corporate Advanced R&D Organization.



**Nicolai Halder, B. Eng.** is Design Engineer R&D at BorgWarner Emissions Systems in Esslingen (Germany).



**Dipl.-Ing. Mihai Miclea-Bleiziffer** is Development Engineer for Compressor Stage Aerodynamics at BorgWarner Turbo Systems in Kirchheimbolanden (Germany).



**Jerry Song, Ph.D.** is Technical Specialist for Controls and Simulation at BorgWarner in Auburn Hills (USA) and Member of BorgWarner's Corporate Advanced R&D Organization.

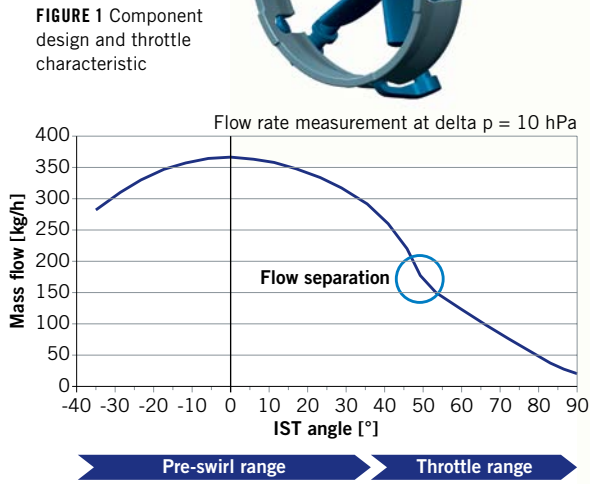
state it is equipped with a butterfly type exhaust throttle. Key element of the system optimisation is a switch from exhaust throttle to IST. When switching from exhaust throttle to inlet swirl type, three main modes of operation can be identified for IST:

- mode 1: part load LP EGR throttling and mixing
- mode 2: low speed, high load compressor stability improvement
- mode 3: rated power turbo speed reduction.

In [1] steady-state fuel economy improvements were shown when operating a first generation IST prototype along with the stock TC. In order to evaluate the full engine benefits, the boosting system was modified and a second generation IST prototype fit for improved geometrical coupling. The TC optimisation aimed at forming a new boosting stage with IST as an integral part and can be characterised by application of latest turbine technology to provide high turbine power at low engine speeds, adaption of the compressor housing to integrate IST and compressor surge specific instrumentation.

**COMPONENT DESIGN AND THROTTLING CHARACTERISTICS**

IST represents a throttle valve and is installed at the compressor inlet, right in front of the LP EGR inlet position. It consists of several parts with housing functionalities and inner elements to drive the vanes which are exposed to fresh air flow, **FIGURE 1**. Inside the inlet housing a Direct Current (DC) motor with a two-stage spur



gear transmission, a failsafe spring mechanism and a non-contacting position feedback sensor are located. This solution provides a compact and robust actuation system. A low friction, low play solution was chosen to synchronise the motion of all vanes. It relies on the known principle of an actuation ring and individual levers connected to the vane shaft ends.

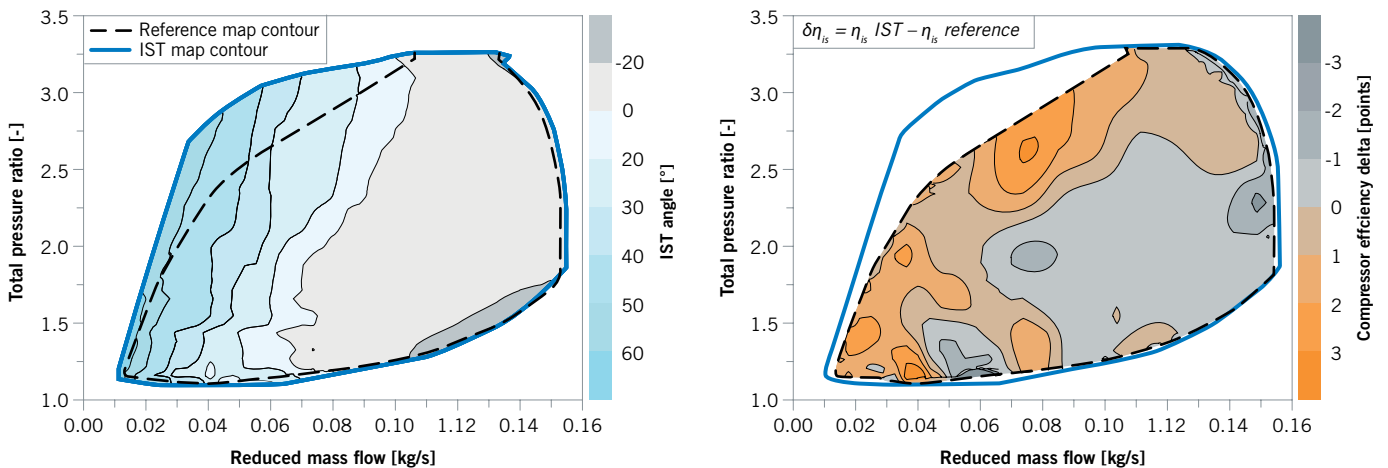
Vaness with symmetrical profiles and a particular vane chamber contour lead to high aerodynamic reliability and low pressure losses in the wide open position. The throttle characteristic is shown in **FIGURE 1**. For small vane angles pressure loss is kept on a low level. Increasing pitch-angle leads to transition from pre-swirl generation to throttling. A change in slope characterises the point at which the flow starts to separate from the vanes. In fully closed position the gaps around

the vanes determine the remaining air mass flow.

**COMPRESSOR IMPACT**

Previous attempts to apply inlet guide vanes to automotive TC compressors have shown that both map size and compressor efficiency are affected by pre-swirl. If positive pre-swirl is applied at the wheel's inlet the map is shifted to the left hand side. This behaviour is caused by the reduction of the incidence angle. By applying positive pre-swirl there are two other basic effects at the compressor's inlet: the inlet relative velocity is reduced and the total wheel work is reduced. The first effect can lead to an efficiency increase since the reduced velocity in the blade channel reduces friction losses [2]. Due to the reduced wheel work, the compressor has

**FIGURE 2** Compressor map comparison with IST vane angle positions and efficiency impact



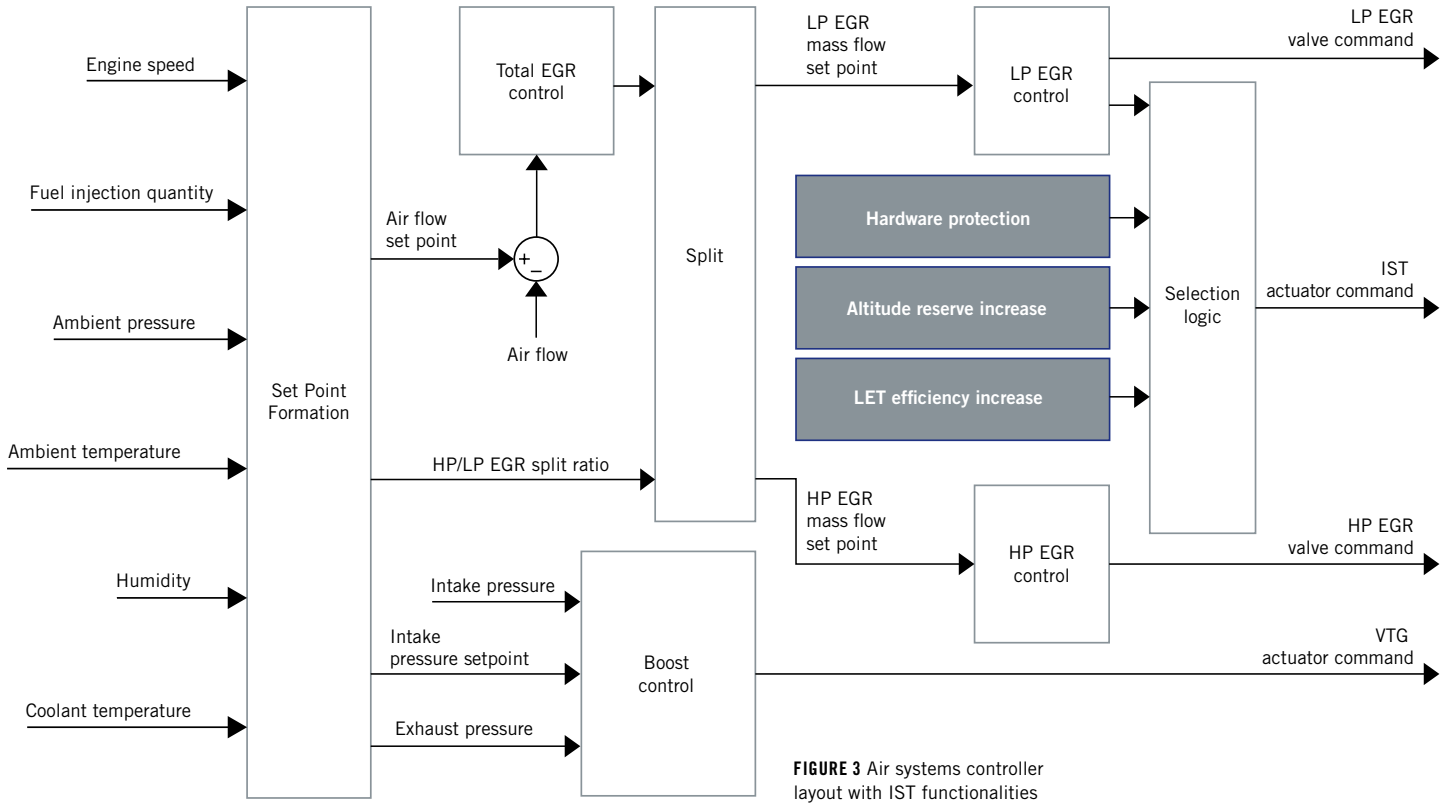


FIGURE 3 Air systems controller layout with IST functionalities

to run at higher speeds in order to achieve the desired pressure ratio. In **FIGURE 2** a comparison of compressor map envelopes is shown. To generate a reference the prototype compressor was measured with an ideal cone section instead of IST. The measurements with IST were carried out with multiple vane angle posi-

tions. A combined map was deduced from the single individual maps. Gain in map width is visible for both low flow and high flow conditions. The vane angles which return best results are highlighted within the map. Efficiencies are compared within **FIGURE 2** as well. The negative impact of added flow losses can be limited

by using optimal vane angles. IST leads to benefits of up to three efficiency points.

**CONTROLS APPROACH**

The BorgWarner air systems controller for a dual loop EGR diesel engine [3] was chosen to control IST during engine

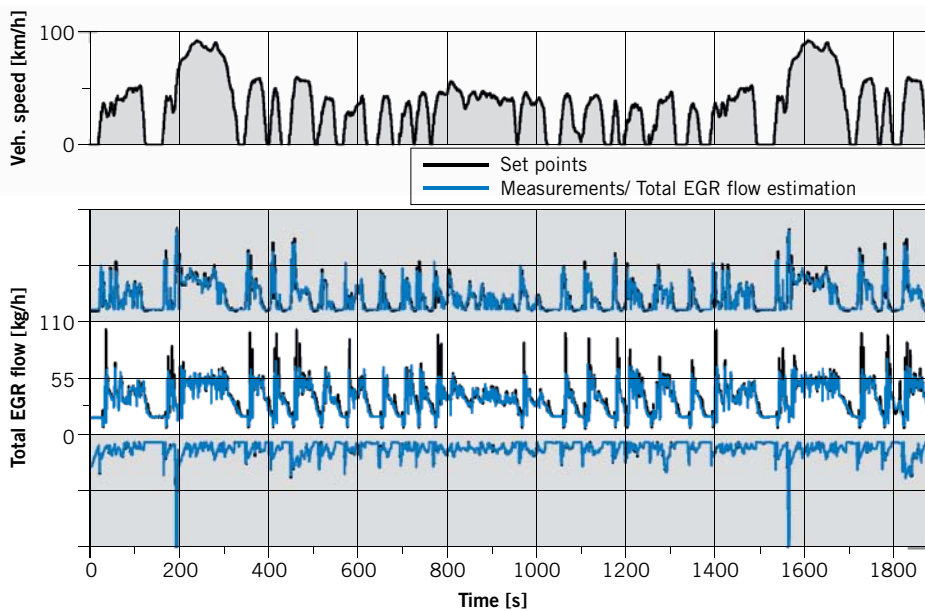


FIGURE 4 FTP-75 air systems controller performance

operation. It was modified to drive LP EGR using IST for intake throttling. The modification was achieved through 1-D controls-plant co-simulations. In combination with the low and high pressure EGR valves, IST can target and achieve the desired total amount of EGR flow and split. It also meets the boost pressure and air flow targets for the engine assisted by the Variable Turbine Geometry (VTG). In **FIGURE 3** the controller layout is shown with outputs to all mentioned actuators. In addition to the basic EGR and boost functionalities the controller was expanded with features to provide additional IST benefits. In the low-end torque region, IST improves surge margin and also increases charging efficiencies, while delivering similar mass flow and boost pressure levels.

Furthermore it improves LP EGR mixing while throttling for LP EGR. A selection logic constantly monitors the engine state and sets IST into the appropriate mode of operation. Besides managing

benefits, the selection logic also ensures safe engine operation. Compressor oiling can be avoided by restricting the rate and range of IST movements. After integration of IST into the controller layout, it was calibrated for high performance during a certification cycle. **FIGURE 4** shows set points and measured values during Federal Test Procedure (FTP) 75. IST operates within its throttling range. Boost pressure and total EGR flow are continuously achieved.

### ENGINE EVALUATION

The potential of IST was evaluated through steady-state tests and FTP-75 cycles on an engine dyno. To deduct the impact of the adapted turbine individually from IST, three turbocharger setups were tested. Setup 1 features a baseline stock TC. In setup 2 the new turbine technology and the base compressor are used. In setup 3 the new turbine technology, the base compressor and IST are used.

As IST drives LP EGR, the exhaust throttle has been replaced with a pipe section.

**FIGURE 5** shows the results for the full load investigations with all three setups. Differences between the setups become apparent in the low-end torque area. The reference full load curve was measured with setup 1. Maximum torque was reached at 1750 rpm. Resulting from the near closed state of the VTG at low speed full load, it was not possible to increase low end torque.

In setup 2 the optimised turbine provides substantially more turbine power. This power can be used to drive the compressor to higher pressure ratio and thus increased low-end torque (LET). A requirement for compressor operation at higher pressure ratio is stable operation with a margin to the surge line. As shown in [4] the dynamic pressure situation upstream the compressor indicates the state of stability. Analysis of the pressure pulsations in the range below 200 Hz at 1375 rpm and 16 bar shows a

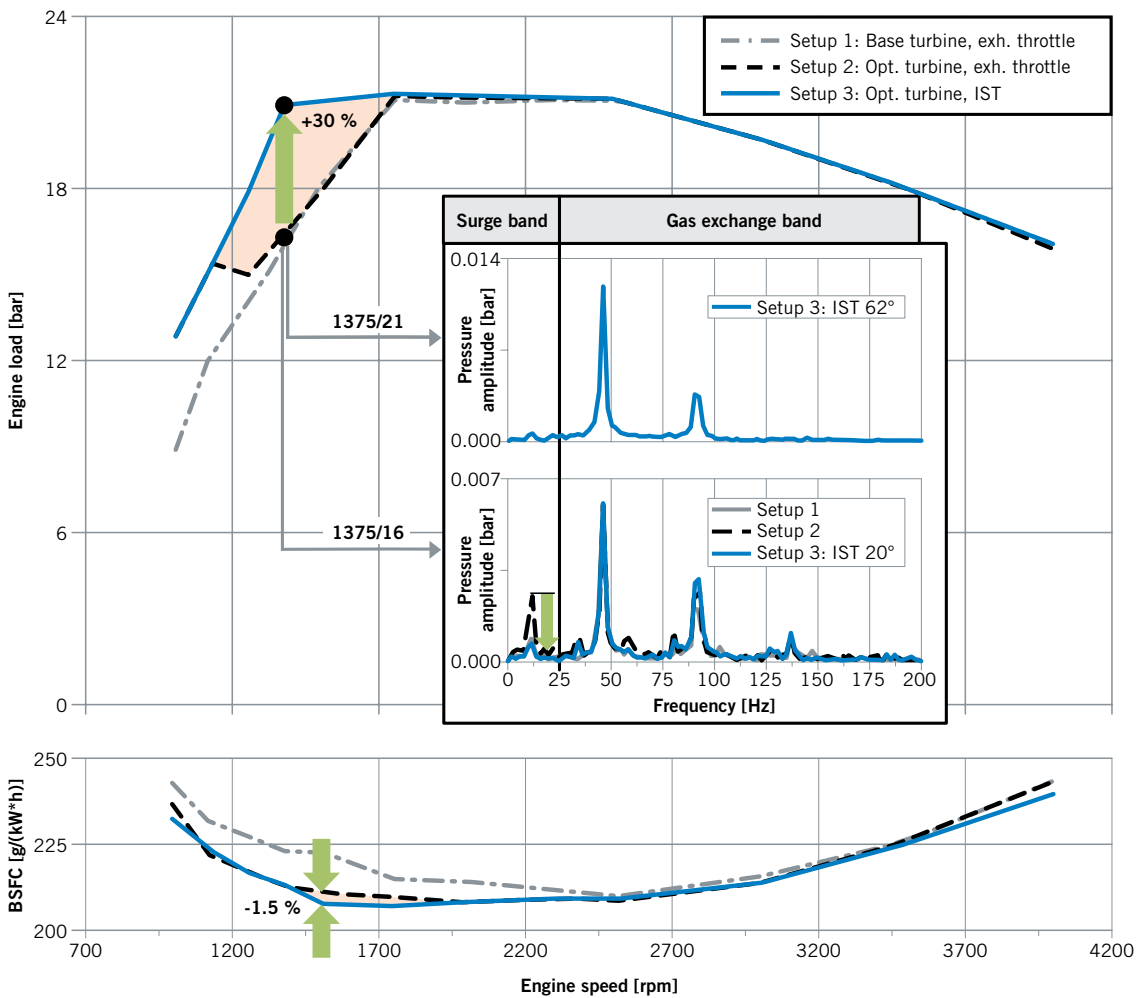


**FIGURE 5** Steady state full load engine dyno results

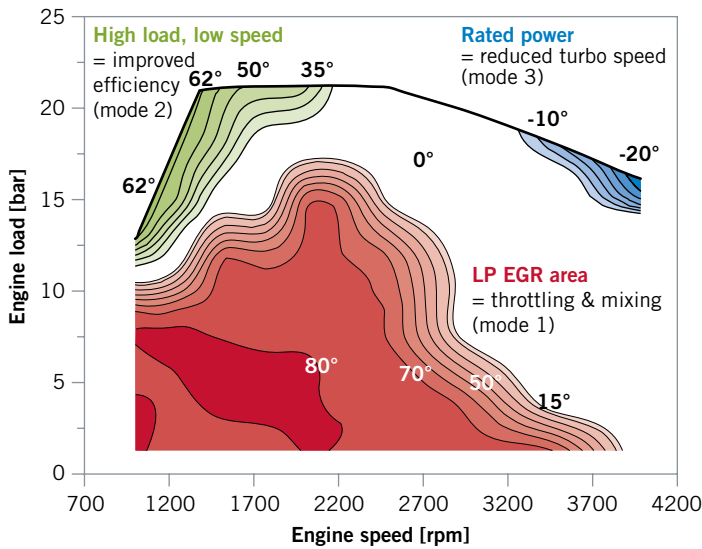
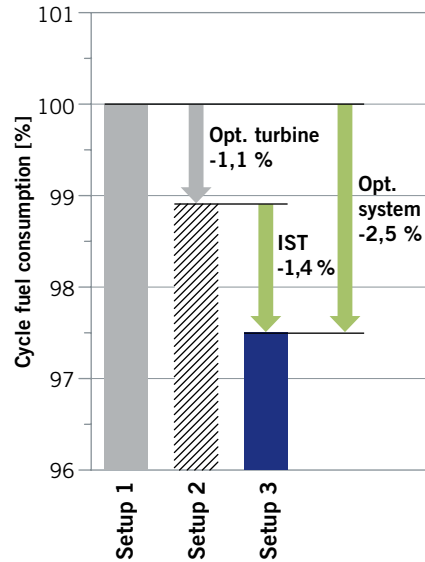


FIGURE 6 Engine dyno results for applied IST vane angles and FTP-75 fuel economy



pressure amplitude peak at surge frequency. This trace of instability is a clear indicator of compressor operation close to the stability boundary. The remaining distance to the surge line was considered application reserve. The relative instability of the compressor prevented increased load despite the availability of turbine power.

When running setup 3 with IST, compressor stability is no longer an issue. Depending on the need for stabilisation, sufficient pre-swirl levels can be applied to prevent fluctuations. Application of 20° IST angle leads to stabilisation of the compressor at 1375 rpm and 16 bar. The same level of stability can be maintained up to 21 bar through 62° vane angle, leading to a low-end torque increase of 30 %. Full load Brake Specific Fuel Consumption (BSFC) is reduced for setup 2 and 3 compared to setup 1 while exhaust lambda never drops below 1.25. IST can provide additional 1.5 % BSFC benefit through improved compressor efficiency in the low-end torque area. VTG application reserve remains at stock level for setup 2 and 3. At 4000 rpm and full load all

three setups reach rated power. The exhaust back pressure levels as well as exhaust temperatures stay below the specified limits.

The overall IST vane angle strategy for the examined system is illustrated in FIGURE 6. During part load operation IST acts as a throttle and operates at angles greater than 70°. During low speed, high load operation the compressor is stabilised by up to 62° positive pre-swirl. In the area of maximum turbo speed mild negative angles of -20° are applied to increase altitude reserve. Each operating mode can be applied on its own. The transition between modes can be achieved by seamlessly opening IST or blending angle areas into each other. FIGURE 6 compares FTP-75 fuel efficiency results for all three setups. Introducing latest turbine technology improved fuel efficiency by 1.1 % with IST providing 1.4 % gain on top. The optimised system lowers cycle fuel consumption by 2.5 %.

**THERMODYNAMIC ADVANTAGE**

Through extensive component and engine testing a new way to optimise the air path

of a diesel engine was evaluated. Benefits were proven in terms of CO<sub>2</sub> emissions as well as engine performance. Through application of an IST and appropriate integration into the boosting stage, a multi benefit solution outside the frame of component optimisation is provided. Despite the presumed disadvantage of intake throttling on engine thermodynamics, the application of a swirl inducing throttle can lead to fuel efficiency benefits compared to exhaust throttling. Future analysis of IST in a gasoline engine is considered, where scavenging limitations for Real Driving Emissions (RDE) compliance make widened compressor maps even more attractive.

**REFERENCES**

[1] Hanig, U.; Becker, M.: Intake Throttle and Pre-swirl Device for Low-Pressure EGR Systems. In: MTZ worldwide 76 (2015), No. 1, pp. 26-31  
 [2] Eckert, B.; Schnell, E.: pAxial- und Radialkompressoren. Second Edition. p. 385 Berlin, Heidelberg, New York: Springer-Verlag, 1980  
 [3] Shutty, J.; Kienzle, D.; Wenzel, W.; Becker, M.: Air System Management to Improve a Diesel Engine. SAE Technical Paper 2011-01, Detroit, 2011  
 [4] Müller, D.; Grigoriadis, P.: Dynamische Pumpgrenze. Final report FVV project No. 845, Frankfurt, 2007

**ATZ** live

# Spotlight on Powertrain and Vehicle Engineering.

personal buildup for Force Motors Limited Library

## ATZlive Conferences for Vehicle and Engine Specialists

**G** **DER ANTRIEB VON MORGEN**

MTZ-Fachtagung

**INTERNATIONAL ENGINE CONGRESS**

Engine Technology in the Vehicle

**DRIVER ASSISTANCE SYSTEMS**

International ATZ Conference

**G** **KAROSSERIEBAUTAGE HAMBURG**

ATZ-Fachtagung

**CHASSIS.TECH PLUS**

International Munich Chassis Symposium

**G** **VPC – SIMULATION UND TEST**

MTZ-Fachtagung

**G** **LADUNGSWECHSEL IM VERBRENNUNGSMOTOR**

MTZ-Fachtagung

**G** **WERKSTOFFTECHNIK IM AUTOMOBILBAU**

ATZ-Fachtagung

**HEAVY-DUTY, ON- AND OFF-HIGHWAY ENGINES**

International MTZ Conference

**AUTOMOTIVE ACOUSTICS CONFERENCE**

International ATZ Conference

**G** **REIBUNGSMINIMIERUNG IM ANTRIEBSSTRANG**

ATZ-Fachtagung

/// CONFERENCES MARKED WITH A **G** WILL BE HELD IN GERMANY

**ATZ** live  
Abraham-Lincoln-Straße 46  
65189 Wiesbaden | Germany

Phone +49 611 7878 131  
Fax +49 611 7878 452  
ATZlive@springer.com

PROGRAM AND REGISTRATION  
[www.ATZlive.de](http://www.ATZlive.de)

# Emission Reduction

## A Solution of Lubricant Composition, Calibration and Mechanical Development

In combustion engines, the piston group system mainly determines the mechanical and thermodynamic losses and exhaust emissions resulting from the lubricant oil, like particles and hydrocarbons. To understand the tribological processes and the different oil transport and emission mechanisms better, APL Group has developed a method to reduce oil-caused pollutant emissions and irregular combustion phenomena with targeted-oriented measures.

### TARGET-ORIENTED COMBINATION OF MEASURES

To reduce CO<sub>2</sub> emissions in combustion engines significantly, a targeted combination of different measures in the areas of oil formulation, calibration and mechanical development is necessary [1, 2]. Especially under the boundary conditions of the through legislation limited pollutant emissions, like unburned hydrocarbons and particles this pose a huge challenge.

The generation of hydrocarbons from the oil from the functional group of piston – piston rings – cylinder wall depends on a number of combustion-related, geometrical, thermal and dynamic influencing factors. The corresponding oil transport and oil emission mechanisms, as well as the particle

emission from the lubricating oil and resulting pre-ignition phenomena are not yet fully explored.

In the trade-off between minimum oil consumption and adequate lubrication of the piston group tribosystem for minimum friction loss, it is indispensable to know the connections and influencing factors[3]. This is especially relevant under the boundary conditions of the legislation in Europe from 2017, where the pollutant emissions are no longer evaluated in New European Drive Cycle (NEDC), but under more realistic test conditions like the Worldwide harmonized Light duty Test Cycle (WLTC) and under Real Driving Emissions (RDE) conditions. In this connection, high specific power requires a careful matching of the mechanical components with cor-

responding system robustness over life-time. Here the lubricating oil must also be considered as a design element.

### OIL TRANSPORT AND OIL EMISSION MECHANISMS

In the analysis of the piston group, the combustion chamber should be considered as an open system in which lubricating oil can be brought into the cylinder charge. For this there are two important sources, **FIGURE 1**:

- The lubrication oil which is left over on the cylinder wall as an oil film from the piston rings in the downwards movement of the piston.
- The oil mass flow from the cavities in the ring land and the top land.

### AUTHORS



**Prof. Dr.-Ing. Jens Hadler**  
is CEO of the APL GmbH  
in Landau (Germany).



**Dipl.-Ing. Christian  
Lensch-Franzen**  
is Head of Engineering at the  
APL GmbH in Landau (Germany).



**Dr.-Ing. Marcus Gohl**  
is Team Leader Mechanical  
Development in Engineering at the  
APL GmbH in Landau (Germany).



**Dipl.-Ing. Tobias Mink**  
is Project Engineer Mechanical  
Development in Engineering at the  
APL GmbH in Landau (Germany).

The amount of oil entering is determined from the oil supply and the transport due to mass forces and gas dynamic towards the combustion chamber. Increased amounts of reverse blow-by gas from the area between the rings favour the oil entry as well as an impaired sealing effect of the piston rings from limited conformability or increased cylinder distortion. The oil supply can be significantly increased from additional oil from the piston cooling nozzles. In the following these mechanisms are described through an example with a modified oil formulation.

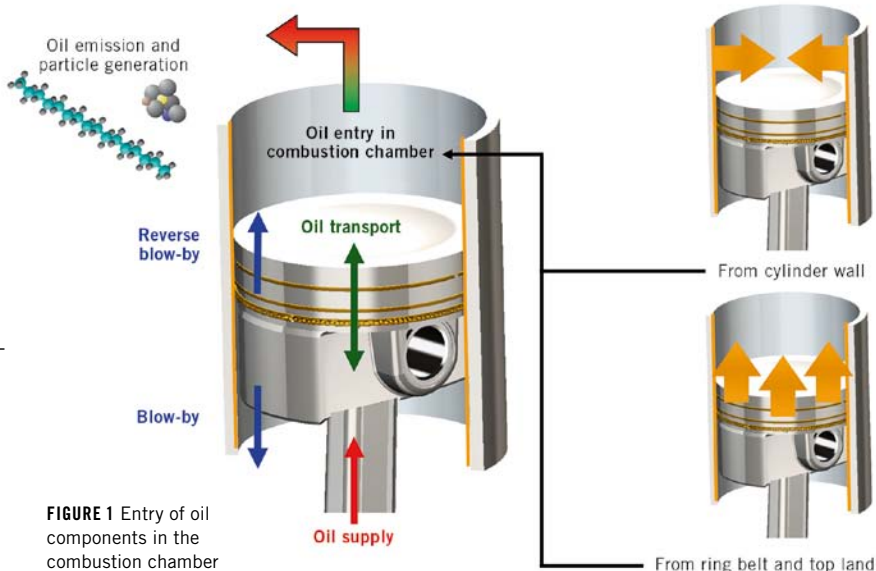


FIGURE 1 Entry of oil components in the combustion chamber

### OIL ENTRY THROUGH THE CYLINDER WALL

The lubricating oil on the cylinder wall can leave the engine through the evaporation mechanism. High gas temperatures in the combustion chamber and corresponding heat transfer coefficients lead to transport of matter over the phase boundary between oil and combustion gas during the combustion process and in the exhaust stroke.

The exchange is next to the speed of the gas at the surface significantly dependent on the temperature and pressure conditions as well as the oil formulation with the corresponding material properties like, for instance, vapour pressure and viscosity.

Applying low viscosity oils in the normal case significantly reduces friction

loss. The thereby achieved fuel consumption advantage, results in the actual state-of-the-art 0W-30 and 0W-20 oils [4]. FIGURE 2 shows the oil composition of conventional W-40 oil in comparison with modern W-20 oil analysed in the laboratory on the basis of simulated distillation. The oil formulation of the synthetic W-20 oil contains fewer fractions in the lower boiling range up to 420 °C. Based on the oil properties and the thermodynamic boundary conditions the vaporised amounts were calculated in different operating points. Especially at full load the W-20 oil shows up to 20 % lower evaporation rates.

By engines with manifold injection as well as by engines with direct injection the mixture formation can significantly

influence the lubricating oil emission [5]. The lambda value and the influence of the flow from swirl and tumble are important factors. FIGURE 3 shows the influence of an enrichment of the mixture on the measured oil emission. The additional fuel components interact with the oil wall film and by lambda = 0.7 they almost lead to a doubling of the emission. Besides the fuel entrainment in the oil wall film directly by the injection, there is also a permanent addition of fuel to the oil that doesn't completely evaporate. The resulting changed lubricant formulations and mixed viscosities have an effect on the evaporation behaviour as well as on the oil wall film heights and the oil transport behaviour around the piston rings.

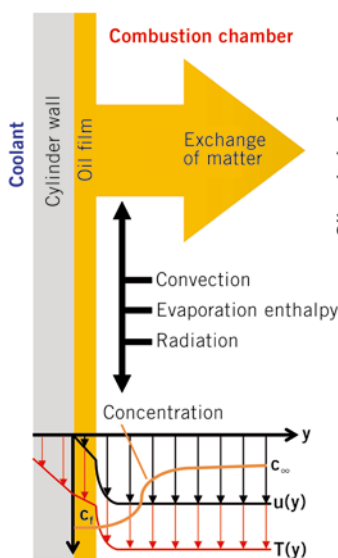
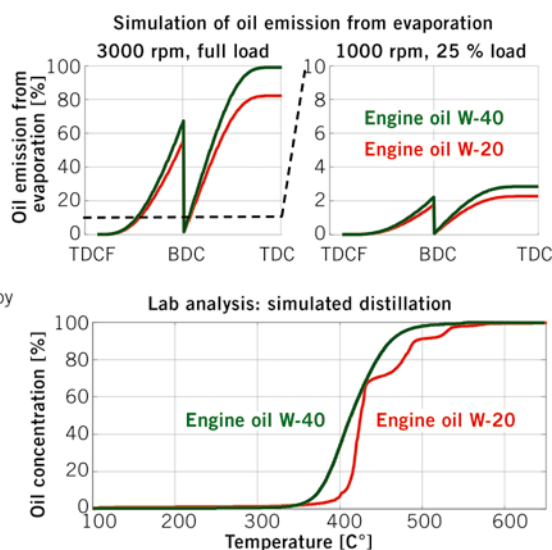


FIGURE 2 Comparison of oil emission by the evaporation mechanism



### OIL ENTRY OVER RING BELT AND TOP LAND

Due to mass forces from the piston movement, aided by the piston ring and gas dynamic lubrication, oil components from the ring belt can pass the top land and get into the combustion chamber. The amount that enters depends on the amount of oil which has gathered around the top ring. Different viscosities of the oil can have a significant influence on the oil transport mechanisms in this connection.

Particularly in overrun mode, the oil transfer to the cylinder is favoured due to a disadvantageous pressure drop between crankcase and combustion chamber as well as the reduced sealing effect of the piston rings from the missing combustion pressure.

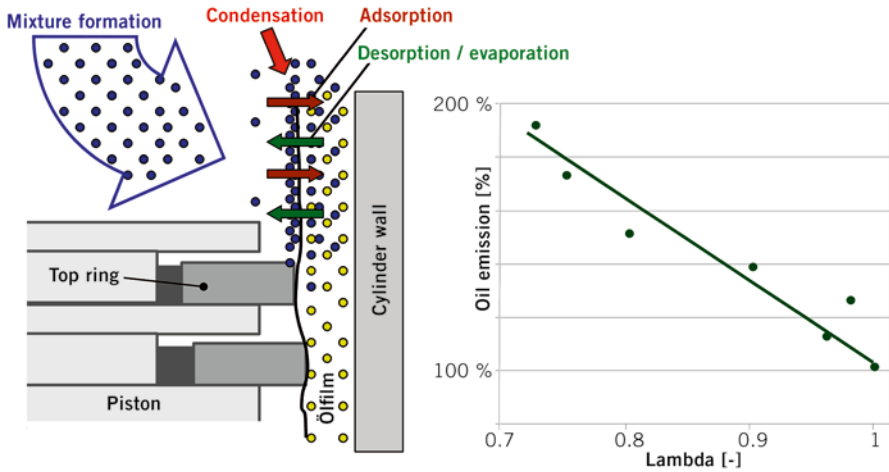


FIGURE 3 Influence of lambda on the resulting oil emission

The measurements with a white light aerosol spectrometer in the raw exhaust show emission of oil aerosol droplets in the size range 0.4 to 1.4  $\mu\text{m}$ , **FIGURE 4**. The total number shows a trend of growth with increasing engine speed. When using a W-20 oil in comparison to a W-40 oil, the concentration of aerosol increases in particular by higher engine speeds. Without the combustion in overrun mode there are no particles generated from the oil aerosol, but under transient conditions with changing load conditions between overrun and load this phenomenon cannot be ruled out.

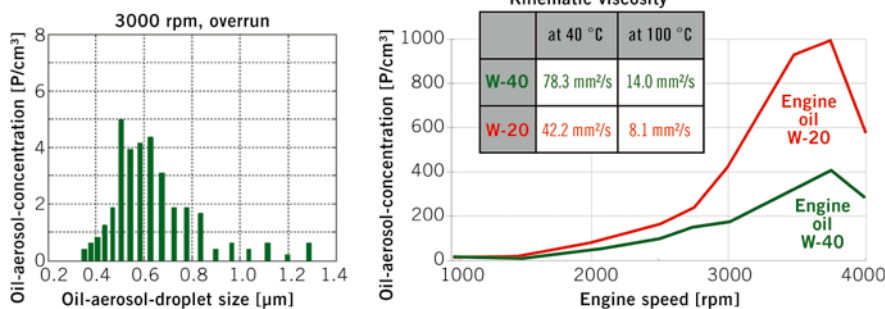
For targeted investigations of these dynamic effects individual operation profiles are made. **FIGURE 5** shows as an example synthetic load changes with different length overrun phases and subsequent operating with combustion. Oil components are getting into the combustion chamber during overrun phases and are, among other, due to the thermal boundary conditions not completely emitted. A part is not discharged until

after the recurrence of the combustion process in the subsequent operating point and is participating in the generation of particles. Just a small amount of lubricating oil can lead to a very high number of additional particles. This phenomenon is more pronounced by a W-20 oil than a W-40 oil. Optical investigations after prolonged overrun phases show in this connection also an increased oil wetting of the piston bottom and the cylinder wall.

A change to the oil formulation can have a negative influence on, for example, the oil supply from the piston cooling nozzles and the subsequent oil transport in the combustion chamber. To reduce emissions, often a combination of an overrun tolerant piston ring matching and calibration measures is the solution.

Similar effects can also be observed by load and speed changes. The splitting of the oil emission in stationary and dynamic portions allows for a prognosis of the engine behaviour under transient operating conditions.

FIGURE 4 Measurement of the emission of oil aerosols in overrun mode



**EXAMINATION OF DYNAMIC DRIVING CYCLES**

To evaluate the different influences on the emissions behaviour, both stationary maps over load and engine speed and individual synthetic operating profiles as NEDC and real driving cycles are examined [6].

Dynamic measurements of the different exhaust gas components are done to analyse the influences of the lubricating oil, the mechanical components and calibration measures.

**FIGURE 6** shows, as an example, the influence of different lubricating oils on the particle and oil emission in NEDC. Especially the dynamic phases show an increased oil emission and a consequent increasing number of particles. This behaviour is particularly significant by the W-20 oil.

By the calculative splitting of the oil emission in stationary and dynamic portions it is made clear that the oil formulation has a positive effect on the stationary evaporation behaviour. However, the change in viscosity leads to disadvantages in the transient phases, so that the accumulated oil emission is slightly higher over the cycle.

**CHAIN OF METHODS TO REDUCE EMISSIONS**

The APL Group has developed a complex chain of methods to specify and develop the mechanical properties and emission behaviour of powertrain systems. In regards to the engine mechanics the focus is on the numerous tribological contacts and the optimisation of the complete system under consideration of component structure, applied materials, surfaces and the lubrication properties including all interactions.

In the early development phase the system layout is accompanied by a simulation environment and the application of coupled MBS/ EHD as well as CFD simulation tools. This method is applied for the base design of the oil circuit and the tribological contacts as well as for the early optimisation in regards to undesired side effects like oil transport into the combustion chamber etc. The properties of relevant oil formulations are considered within the examined parameter space.

The first tests on component, full engine and tilt test stands for friction loss and function investigations are accompanied by elaborate laboratory analysis, in the laboratories of the APL Group, in regards to chemical properties of the oil over the run time as well as the before and after inspection of all components and surfaces. Combined with the high resolution radio-nuclide wear measurement technique (RNT) as well as the mass spectrometric analysis of unburned hydrocarbons and further exhaust measurement techniques on the

test stand, the engine behaviour as well as the functional interactions influenced by the oil can be described within the engine operating map and in representative dynamic cycles. If necessary, this can be supplemented by optical investigations in the combustion chamber for instance to early detect tendencies for combustion anomaly like pre-ignition [7]. The high information density of the described investigations is taken back into the simulation model and further optimisation potential is achieved through simulative-empirical coupled

approaches. The result is a targeted system layout in the early development phase with reduction of hardware variants and their numbers in the course of the project.

Irrespectively, in parallel to the specific development project, oils are intensely tested and evaluated in regards to its properties for engine use in the laboratories and on the test stands of the APL Group for the petroleum industry. The combined know-how leads to an effective project accompanying development process, which in the further course of the project plan for the early testing of the full powertrain in different simulated vehicle applications on the powertrain test stand. In regards to the design parameter oil and the corresponding oil emission behaviour, for instance particle generation, action, based on the above, can be taken at an early stage in regards to the calibration process and the interaction between fuel and oil wall film. Furthermore the APL Group intensely deal with the testing of alternative lubricants with the target of neutrality of lubricant caused emissions [8]. In summary the described activities contribute to the vision of the zero impact emission vehicle.

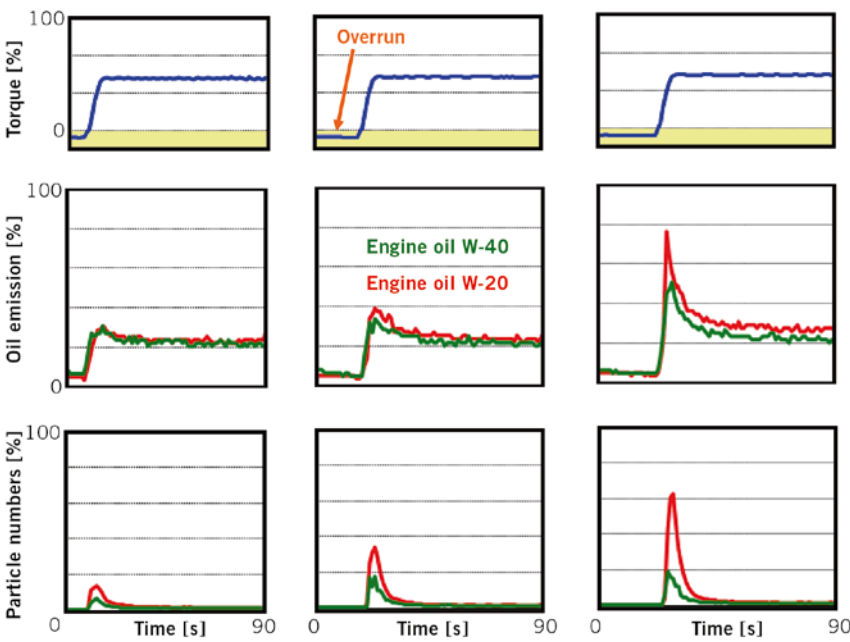


FIGURE 5 Effect of the oil emission on the particle generation

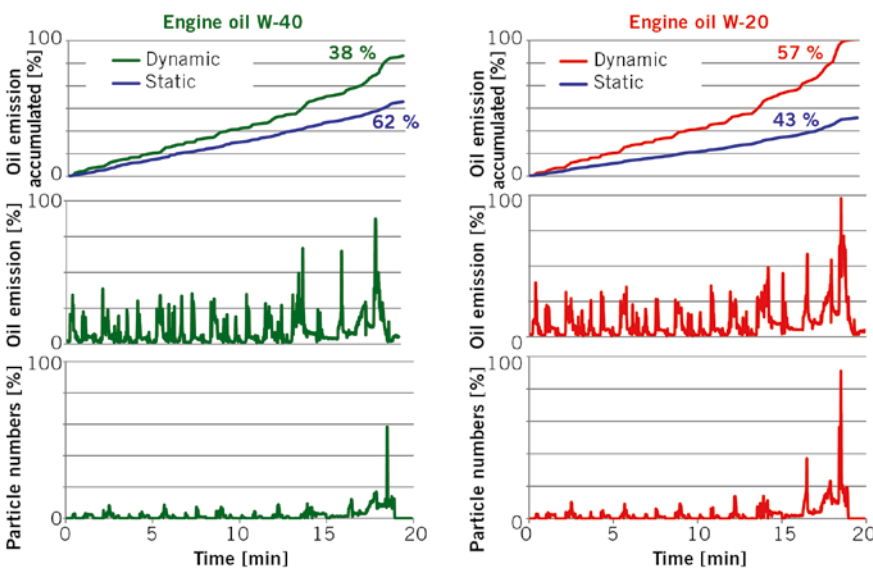
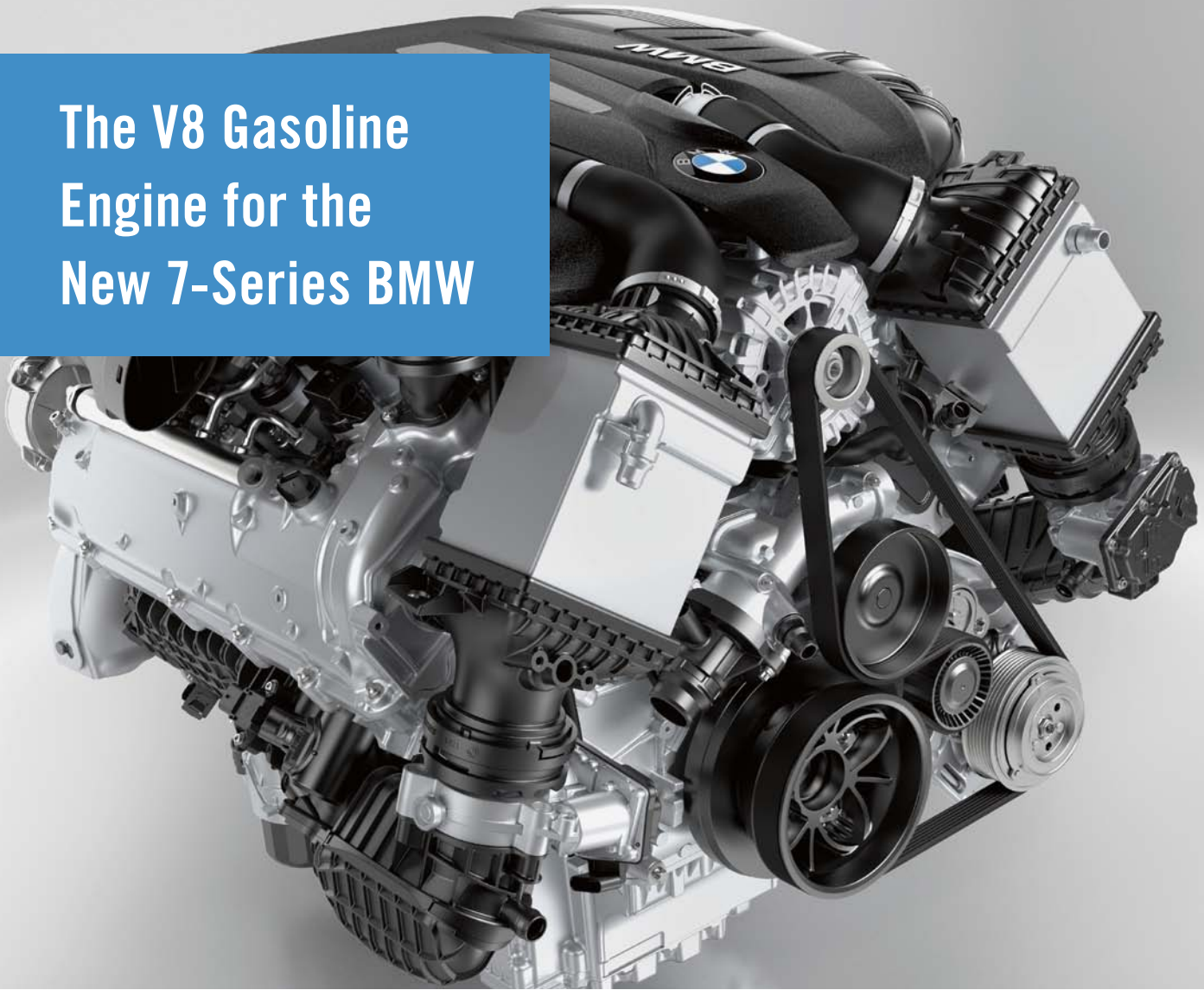


FIGURE 6 Emissions in NEDC by different oil formulations

REFERENCES

[1] Hadler, J.; Lensch-Franzen, C.; Kronstedt, M.: Emissionsbilanzen der Energieketten – Potenziale für nachhaltige Mobilität. 8. MTZ-Fachtagung “Der Antrieb von morgen”, Wolfsburg, 2013  
 [2] Hadler, J.; Lensch-Franzen, C.; Kronstedt, M.: Selektive Schadstoff- und Emissionsreduzierung entlang der Well to Wheel Kette. “Motor und Umwelt”, Graz, 2013  
 [3] Hadler, J.: Ölemissionsreduzierung – Ein signifikanter Faktor. In: MTZ 74 (2013), No. 11, p. 920  
 [4] Hadler, J.; Gohl, M.; Knoll, G.; Backhaus, K.: Development Tools for Base Engine Friction Reduction. In: MTZ worldwide 75 (2014), No. 3, pp. 32-37  
 [5] Gohl, M.; Brandt, S.; Budde, M.; Krause, S.: Influence of the Mixture Formation on the Lubricating Oil Emissions of Combustion Engines. In: MTZ worldwide 72 (2011), No. 1, pp. 46-51  
 [6] Hadler, J.; Lensch-Franzen, C.; Gohl, M.; Mink, T.: Concept for Analysing and Optimising Oil Emission. In: MTZ worldwide 75 (2014), No. 1, pp. 24-29  
 [7] Palaveev, S.; Magar, M.; Kubach, H.; Schiessl, R. et al.: Premature Flame Initiation in a Turbocharged DISI Engine - Numerical and Experimental Investigations. SAE Int. J. Engines 6 (1): pp. 54-66, 2013, doi: 10.4271/2013-01-0252  
 [8] Müller, G.; Stern, D.; Berlet, P.; Pöhlmann, K.: Praxisnahe Alterung von Motorölen und Auswirkung auf tribologisch relevante Eigenschaften. 54. Tribologische Fachtagung der Gesellschaft für Tribologie, Göttingen, 2013

# The V8 Gasoline Engine for the New 7-Series BMW



personal buildup for Force Motors Limited Library

The BMW V8 engine has been revised for integration into the new modular vehicle architecture. With its initial use in the new 7-series starting from August 2015, the engine shall be used in the following years in other series as well in a future-proof manner without the generation of derivatives. While maintaining proven design characteristics, the development focused on weight reduction and improved efficiency for a further reduction in fuel consumption in addition to the required vehicle integration.

## AUTHORS



**Dipl.-Ing. Johann Schopp**  
is Head of Engineering V-engines and Special Engines at the BMW AG in Munich (Germany).



**Dipl.-Ing. Rainer Dungen**  
is Sub-Project Manager V-engines at the BMW AG in Munich (Germany).



**Dr.-Ing. Martin Wetzel**  
is Team Manager Testing of Gas Exchange S.I. Engines at the BMW AG in Munich (Germany).



**Dipl.-Ing. Thomas Spieß**  
is Engineer for Engine-internal Thermal Management of V-engines at the BMW AG in Munich (Germany).

**OBJECTIVE**

For series implementation of the new 7-series in August 2015 as first derivative of a vehicle generation that is based on a common architecture platform also the 4.4-l V8 gasoline engine had to undergo further development in order to comply with the new package requirement and for integration into the new onboard electrical system architecture. Beyond that, the specification book prescribed requirements for higher efficiency to reduce fuel consumption, compliance with the latest exhaust emission regulations, weight reduction, improved quality, and cost reduction. In addition to greatest possible communality with the predecessor engine for production and assembly reasons, it should also be possible to derive a 4.0-l variant, while model-specific derivatives were to be avoided.

**CONCEPTUAL DESIGN**

With the introduction of the TwinPower Turbo technology in 2008, a new engine generation started up for BMW V8 gasoline engines [1, 2]. This engine features turned cylinder heads for the first time in volume production of passenger car engines. Turning of the heads enables the placement of exhaust turbocharger and

catalytic converter in the V-space between the cylinder banks. This arrangement has proven to be a key factor in the utilisation of package advantages. With the use of exhaust manifolds across the banks, the concept is also the ideal basis for performance improvements in motorsport variants. In the first revision of the BMW TwinPower Turbo V8 with direct gasoline injection and double Vanos in 2012, the Valvetronic technology was integrated into the engine for fully variable intake valve lift control [3]. This technology has already been used since 2001 in the predecessor generation of V8 naturally aspirated engines. The engine was now further developed while maintaining all mentioned future-proof design characteristics. This contains the integration of a new engine control unit generation, division of the cooling circuit into a head and block circuit, conversion to twinscroll turbocharger, active control of coolant and oil pump, the engine oil/water heat exchanger integrated into the engine V, and a completely new intake system concept. Additional components were designed in higher quality, with reduced costs or weight optimisation while maintaining their concept, or had to be adjusted only to the geometrical package requirements of the new vehicle generation.

**BASE ENGINE**

The crankcase design was completely revised while preserving the main engine dimensions, crank drive, and proven design principles, such as Alusil solid aluminium engine block with exposure-honed cylinder liners, double main bearing bolting with additional side wall connection, closed-deck technology, and cylinder head bolting in the base plate. Connections of an engine oil/water heat exchanger can now be found in the V-space, **FIGURE 1**. This replaces the external engine oil air cooler of the predecessor engine. The production quality of all oil channels in block and heads was improved, resulting in reduced friction due to optimised guidance. The coolant circuit was completely revised for warm-up optimisation and separate supply of cylinder jacket and heads. The pistons iron-plated by dipping are adjusted to the increase in compression from 10.0 to 10.5 and feature an additional oil collecting groove with eight drain holes each below the oil scraper ring for reduced oil consumption. The 4.0-l variant required for the Chinese market is realised by a crankshaft with shortened stroke and an adjusted connecting rod. The connecting rod to piston connection via bushing-less small

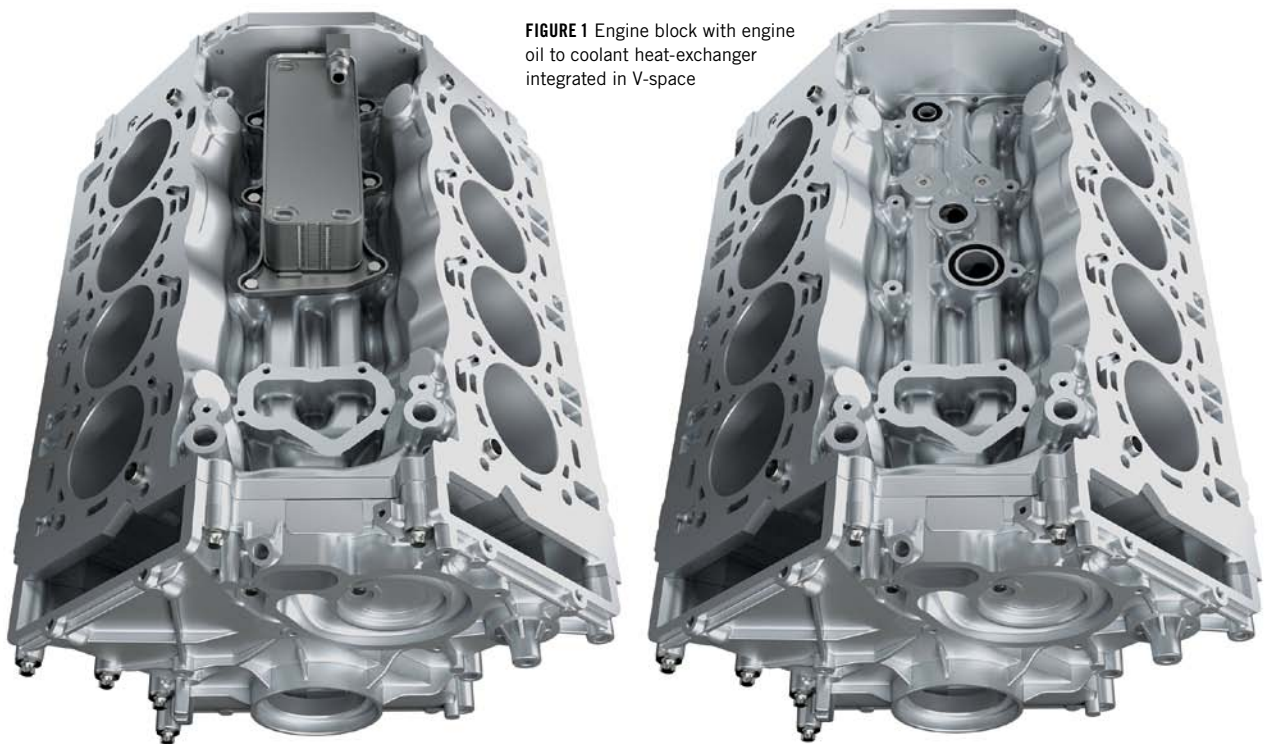


**FIGURE 1** Engine block with engine oil to coolant heat-exchanger integrated in V-space

trapezoid end was copied from the predecessor. The connecting rod is now connected to the crankshaft via anti-friction coated two-material bearings whereas in the main bearing area, the crankshaft runs on the proven three-material main bearings. The cylinder head was converted to central Vanos units while preserving the valvetrain. Oil bore production was optimised with respect to residual contamination. On its rear end, the intake camshaft on bank 1-4 drives the vacuum pump for brake vacuum provision using a dihedral coupling. A triple cam each at the exhaust camshafts is used as drive for fuel high-pressure pumps. For the first time in large-scale engine production for passenger cars, the intake system is partly integrated into the cylinder head. The result is 30 % shorter intake ports and a flow-optimised intake guide design.

**VALVETRAIN**

The fully variable Valvetronic valve-train and the chain drive with two acoustically optimised sleeve toothed chains and oil-pressure chain tensioners are copied from the predecessor engine, except for the conversion to central Vanos.

**ENGINE-INTERNAL THERMAL MANAGEMENT**

One of the influencing parameters for fuel consumption reduction is the thermal engine management during warm-up, **FIGURE 2**. Under the term “Split-Cooling – Combined”, the entire coolant routing of the base engine was revised, opening up new potentials. The parallel dual channel running towards the rear in opposite direction to the main oil channel above the crankshaft bearing tunnel was copied from the predecessor module. The coolant flows divide at its rear end into a flow each covering the head and cylinder jacket. A coolant channel located on the outside of the block accommodates approximately 80 % of the coolant flow and supplies the cylinder heads with lateral flow and the branching holes of the cylinder bridge cooling via the openings in the top. 20 % of the coolant flow flows from the rear to the front through the piston stroke jacket zones. The system resistance of the entire coolant circuit is reduced by 30 % thanks to the new channel design. The

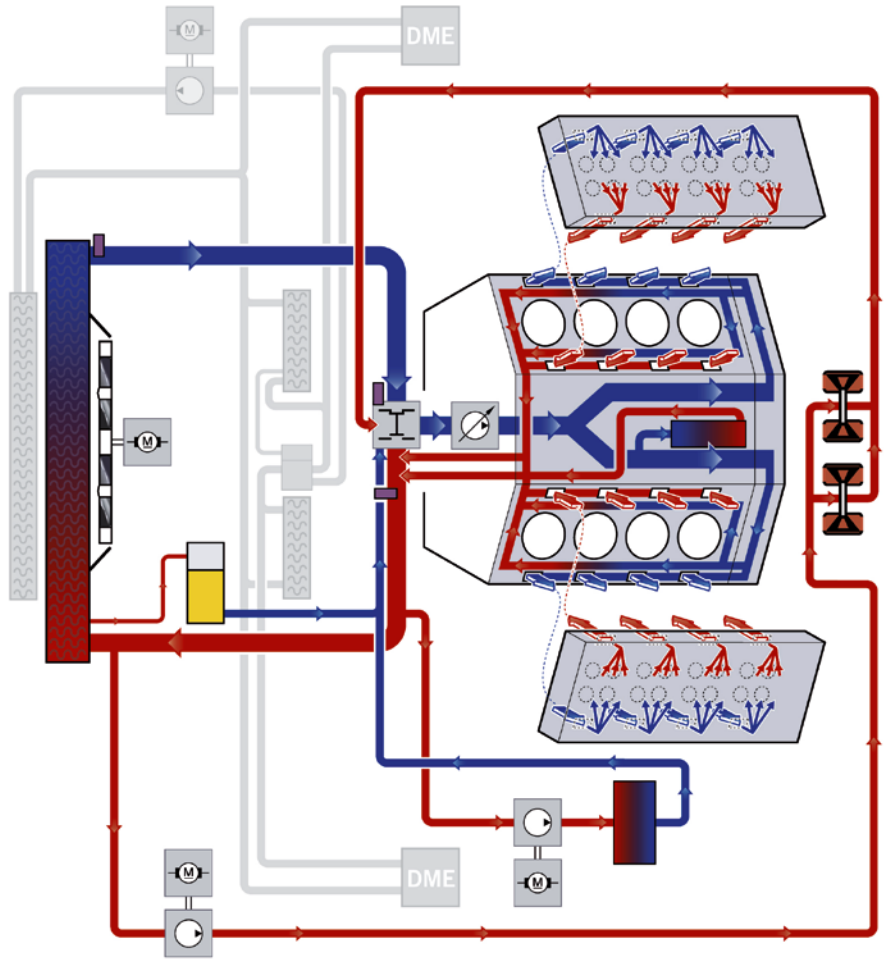


**FIGURE 2** Schematic representation of coolant circuit (DME: engine control unit)

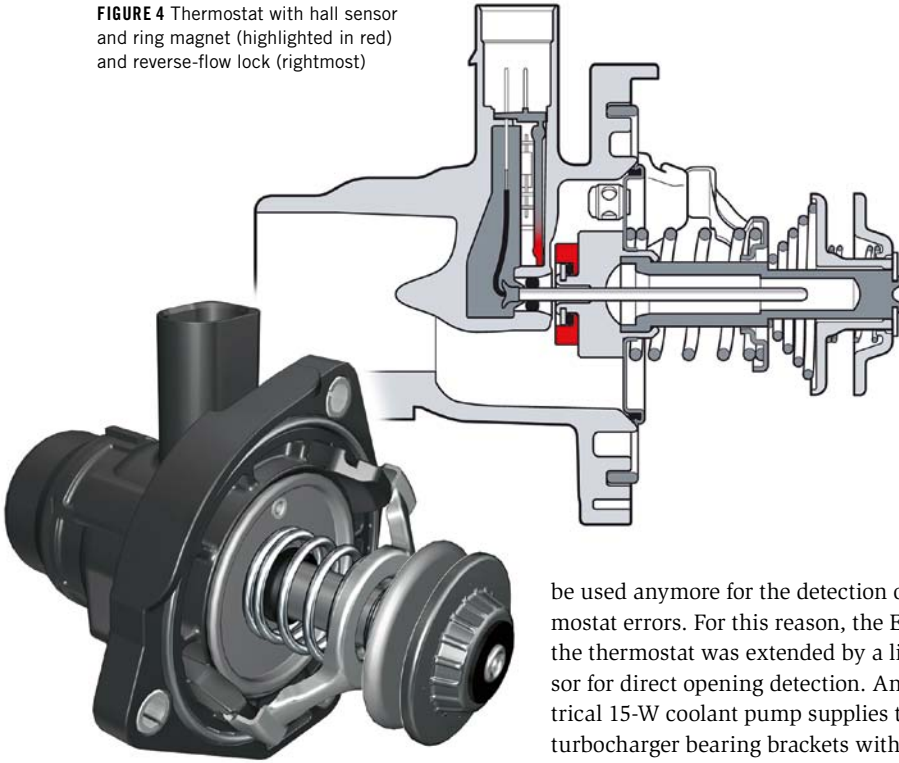


**FIGURE 3** Coolant pump control with actuator and annular slide valve

belt-driven coolant pump switching purely temperature-dependently via a wax element was converted into a map-controlled coolant pump by adding a heating element, **FIGURE 3**. As before, delivery can be reduced to a minimum amount of 10 % using a ring valve to avoid hot spots. Furthermore, this achieves the objective of a homogeneous thermal coupling within the base engine and always plausible temperature detection without an additional component sensor. Up to a cool-

ant temperature of 98 °C (predecessor 80 °C) the pump remains in an operating mode that focuses on heat preservation. It thus ensures a reduction in friction due to higher surface temperatures. In the case of higher outside temperatures or a high load requirement already during cold start, the delivery amount can be quickly switched to 100 % using the heating element. A pressure-dependent overload bypass switches to full delivery rate without delay in the case of a dynamic output request start-

**FIGURE 4** Thermostat with hall sensor and ring magnet (highlighted in red) and reverse-flow lock (rightmost)



be used anymore for the detection of thermostat errors. For this reason, the ECU of the thermostat was extended by a lift sensor for direct opening detection. An electrical 15-W coolant pump supplies the turbocharger bearing brackets with coolant after the engine is switched off.

ing from 3500 rpm regardless of the actuator position.

The engine thermostat, **FIGURE 4**, still opens at 105 °C, whereby the proven map-controlled concept via energised heating element has been preserved for demand-driven opening starting already from approximately 60 °C. Due to the required variability in thermal management, on-board diagnostics (OBD) that is based on temperature difference cannot

**OIL COOLING**

The engine oil/water heat exchanger was integrated into the engine-V to avoid external oil cooler, oil lines, and usually required vehicle-related diversification. As a result, the engine oil circuit, **FIGURE 5**, remains closed after filling at the end of engine assembly. Dirt accumulation and oil contamination are avoided in vehicle assembly. On the engine side, this results

in shorter channels integrated in the engine housing, a reduced number of seals, and an arrangement in flow direction upstream of the filter for risk minimisation due to residual production contamination despite the service-related spatially exposed position of the oil filter. The thermo-functional system coupling to the engine-internal thermal management is realised in dependence of coolant control, without additional thermostat.

**OIL PUMP AND SUMP**

The volume-controlled pendulum-slider pump with different chamber sizes driven using a sleeve chain was extended by map control. Monitored by an oil pressure sensor, a characteristic-map control valve installed on the oil sump and connected to the oil pump via holes actuates the pendulum slider. This avoids fault-prone cable ducts into the oil chamber. By controlling the oil pressure during warm-up to below 3.5 bar, map-dependent deactivation of the piston injection nozzles is possible for lowered particle emission, as well as a reduction in fuel consumption in many map ranges due to the corresponding reduction of the pump drive power. Thanks to the standardised vehicle architectures, only two oil sumps – one for two-wheel drive and one for all-wheel drive with integrated oil windage tray – are required for realising all possible vehicle integrations. The oil level is measured using a so-called PULS (Packaged Ultrasonic Level Sensor); an additional mechanical dip stick is available for service.

**OIL SEPARATION**

The oil absorbers are bolted in the two aluminium cylinder head covers. After preliminary separation in a labyrinth, the blow-by gas strongly deflected by the impactor and accelerated in the nozzles is efficiently deoiled using non-woven material.

In naturally aspirated engine operation, the venting gases of the crankcase are routed via the left oil absorber only to maintain the flow speed required for separation. They are next exhausted into the intake air guide of both cylinder banks via a crossing line. At the same time, fresh air is fed from the intake system to the crankcase via the second oil absorber to ensure a stable vacuum. By scavenging the crankcase with fresh air, chemical aging

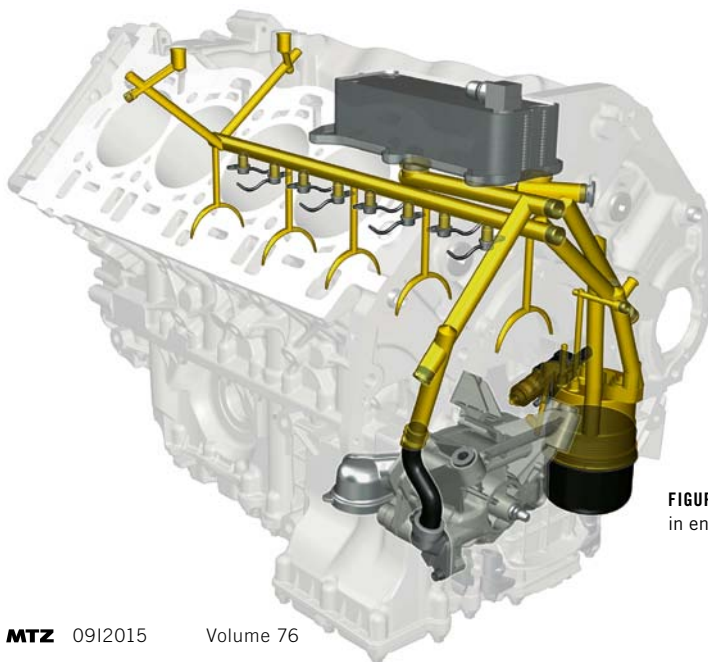


**FIGURE 5** Oil circuit in engine block

of the lubrication oil is delayed and the water content in the blow-by gas reduced. When switching from naturally aspired operation into charged operation, the cleaned gases are routed into the clean air bend upstream of the turbocharger.

**FUEL SYSTEM**

The so-called high-precision injection consisting of the coil injectors with adjusted spray pattern and return-free single-piston pumps works with a system pressure of 200 bar and was preserved without changes except optimised line routing.

**BELT DRIVE**

The mechanical power steering pump is omitted with the conversion of the new 7-series to electrical steering assistance. Due to the standardised modular vehicle architecture, the refrigerant compressor arranged on the left side of the vehicle now assumes the free space in the otherwise unchanged belt drive. The second belt drive was omitted.

**STARTER**

The starter proven in the predecessor was kept with a slightly rotated A-bearing shield. It meets the high requirements on comfortable engine start/stop operation and reliable initial starts at low outside temperatures.

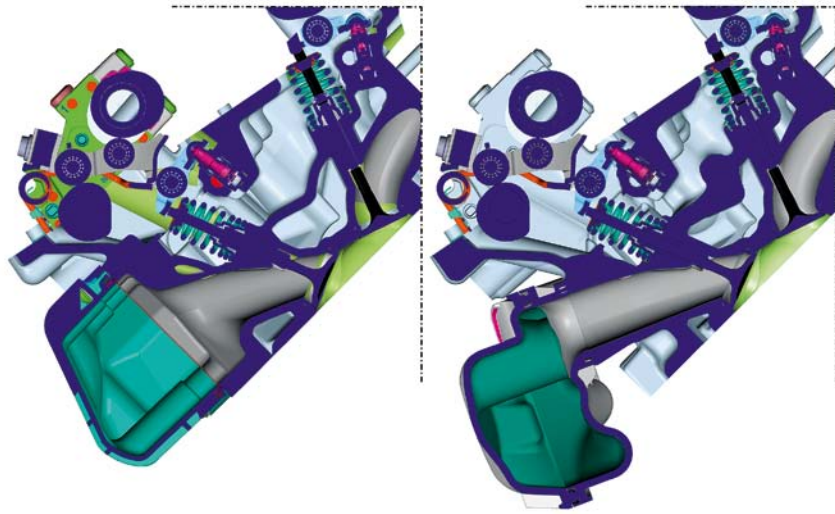
**GENERATOR**

To ensure a large fording depth, the generator remains placed in the engine-V. With its technology of active rectification, the generator represents a new technical development. It specially focuses on the increase of the generator's degree of efficiency by reducing the losses in the rectifier. For this purpose, the loss-generating diodes are replaced by actively actuated MOSFETs.

**TURBOCHARGING SYSTEM**

The newly developed twinscroll exhaust turbocharger is a common part on both engine banks. Thanks to application measures, still no diverter valve is required. The wastegate, electrically actuated for the first time for the V8, features a maximum opening angle of

FIGURE 6 Cylinder head and half-shell intake system in comparison with predecessor engine (right)



more than 40° to achieve optimum catalytic converter heating. It is actuated by an electrical actuator with integrated position sensor. For this reason, no vacuum system is required on the engine side. The connections of unfiltered air manifold and charge air hose to the compressor were converted to VDA quick-acting couplings.

It was possible to realise the bank-selective exhaust manifolds manufactured in the Lost Foam Casting process from high-temperature resistant, austenitic thin-walled cast steel with 20 % less weight each than their predecessors. On bank 1-4, they combine exhaust flows 1-3 and 2-4 and on bank 5-8 exhaust

flows 5-6 and 7-8, resulting in an optimised ignition sequence. The innovative sheet-metal bead sealing concept between manifold outlet and turbine inlet was designed based on FEM. It enables an extraordinary level of leak-tightness between the twinscroll flow ducts and thus ensures an excellent response.

The primary catalytic converters, also arranged in the V-space directly behind the turbines, quickly reach their operating temperature due to the short exhaust gas routing. They thus ensure compliance with the strict emission legislations Euro 6 and ULEVII, and enable the omission of underbody catalytic converters as well as a secondary air system. The highly effi-

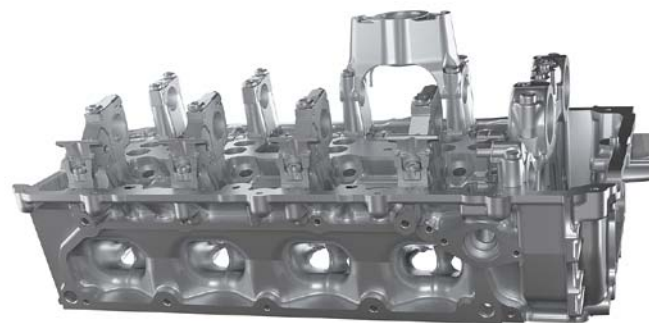


FIGURE 7 Intake side of cylinder head with inflow funnels and half-shell intake system

cient system enclosing the hot components, partly made of three-layer heat shields, was optimised based on CFD simulations and vehicle tests to ensure maximum heat dissipation from the V-space into the underbody area.

### INTAKE AIR FLOW AND INTAKE MANIFOLD

The dual unfiltered air flow of the intake air ends in a common engine-mounted intake silencer with integrated air filter insert. It is routed via the unfiltered air hoses, housing the valves for introduction of the crankcase venting gas to the exhaust turbochargers. The connection to the engine-mounted, water-cooled charge-air coolers with doubled volume is realised using fabric-enforced hoses. The throttle valve is mounted to a connection piece with three-hole flange on the plastic intake system using a VDA-similar coupling. The intake system implements a completely new concept for the first time, **FIGURE 6** and **FIGURE 7**. For this purpose, the intake system gallery usually located on the head side was relocated by design into the cylinder head. The result is shortened channels and a flow-optimised intake guide. The intake system itself consists of a half shell connected to the cylinder head via a circumferential sealing surface with connection piece for the throttle valve. Despite outer engine dimensions reduced due to the package, the intake system volume was increased by 0.5 l (15 %). With that, constrictions for the different steering spindle positions of the vehicle derivatives are widely removed.

### COOLING

In the vehicles of the new 7-series, the expansion tank of the main cooling circuit is located in front of the left wheelhouse. The expansion tank of the low-temperature circuit is engine-mounted in front of the generator. An auxiliary heat exchanger in the left wheelhouse supports the coolant radiator with 850-W e-fans. In the hot-land variant, it is supported by a second auxiliary heat exchanger in the right wheelhouse. The coolant radiator of the low-temperature circuit is located in front of the condenser of the automatic air conditioning. It cools the engine control units and the indirect charge-air coolers using an 80-W pump.

### EXHAUST SYSTEM

The continuous dual exhaust system features three silencers in absorption and/or mixed design and two map-controlled, electrically actuated exhaust gas valves. The four tailpipes protrude into two angular chrome covers integrated in the rear apron.

### ENGINE CONTROL UNIT

Two identical engine control units coupled via a bus are used as control according to the master-slave concept. The hardware is based on a completely newly developed platform, which is based on a six-cylinder variant. Based on the requirement, it supports all variants from three to twelve cylinders including diesel with the respective cylinder population.

Main characteristics of the engine electronics platform are:

- processor with multicore architecture (2 x 300 MHz, 1 x 200 MHz, 8 MB Flash)
- interfaces: FlexRay, CAN, LIN, SENT
- standardised connector system (254 pins)
- standard housing (air- and water-cooled variant possible)
- communal software modules up to standard programme version
- Autosar 4.

The platform development was a significant step in managing the increased complexity and variant diversity within the engine control systems for this V8 gasoline engine, as well as the applica-

tion. This reduces the previously complex engine-specific individual functionalities and thus creates advantages in flexibility, applicability, as well as testability across the entire engine control for gasoline and diesel engines, as well as hybrid drives.

### COMBUSTION PROCESS

The BMW V8 TwinPower Turbo gasoline engine combines the elements of turbocharging, variable Valvetronic valve control, double Vanos, and direct injection. As in the predecessor engine, the variabilities of Valvetronic and double Vanos are used to drive in a consumption-optimised manner in large ranges of the characteristic map by de-throttling the gas exchange at high internal EGR rates. Due to the separated flow ducts of the twincscroll exhaust turbocharger in combination with the increase in compression from 10.0 to 10.5, Vanos strategies can be applied that allow a further increase in the internal EGR rate and to open up further consumption potentials. At partial lift of the intake valves, phasing and masking generate an increased charge movement level. This ensures the required combustion stability.

### ENGINE FULL LOAD

The new BMW V8 gasoline engine distinguishes itself by a very uniform power delivery at a very high level across the entire speed range, **FIGURE 8**. The effective

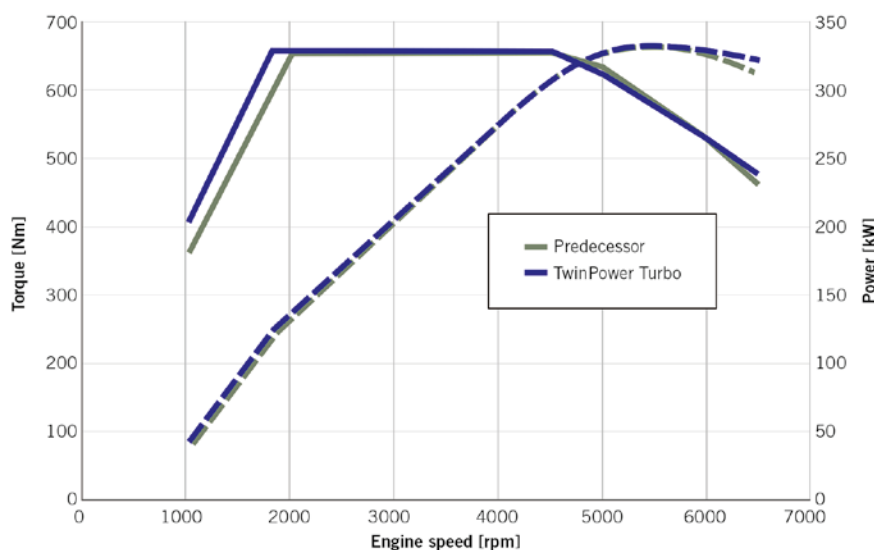


**FIGURE 8** Full-load curves in comparison with predecessor engine

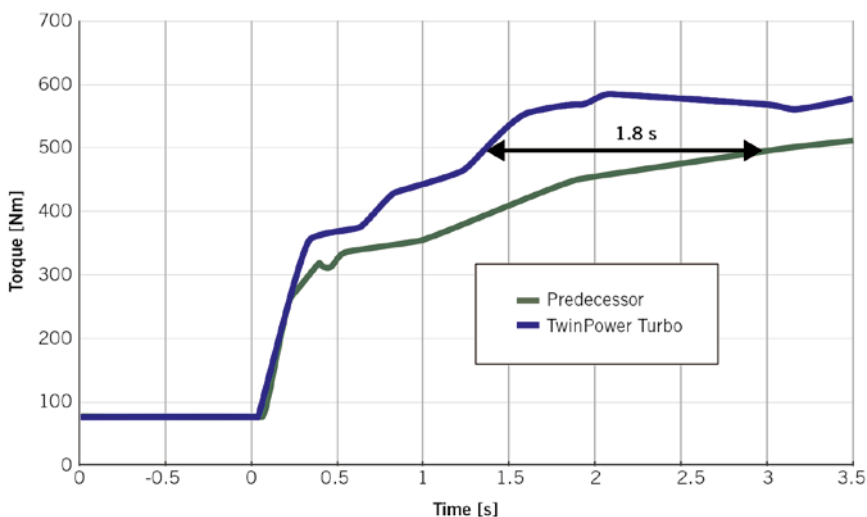


FIGURE 9 Response characteristics comparison with predecessor engine

power is 330 kW and is available between 5500 and 6000 rpm. The further development particularly focused on delay-free response from the lowest speed/load range. For this purpose, the monoscroll turbocharger was replaced with a twin-scroll turbocharger. As a result, the low-end torque (LET) is now available at 1800 rpm compared to the previous 2000 rpm and the response time in the case of a sudden abrupt load increase to 500 Nm from 1500 rpm is shortened by approximately 1.8 s, FIGURE 9. These improvements are the prerequisite for a superior driving experience in the new 7-series BMW. TABLE 1 shows the technical data of the new V8 engine.

**CONCLUSION**

The 4.4-l BMW V8 TwinPower Turbo gasoline engine was revised for adaptation to the architecture platform of the new BMW vehicles of the 7-series. In addition to the package requirements, this included the integration of a new engine control unit generation, as well as a further efficiency increase for reduction of fuel consumption and compliance

with the Euro 6 exhaust gas legislation. While preserving the proven design principle with the outlet side of the cylinder heads in the V-space, the concept that was successfully introduced in series production in 2008 was further developed in a future-proof manner: conversion to twin-scroll exhaust turbocharger, new combined cooling concept of separate head and block flow in combination with map-controlled coolant pump, and the intake system partly integrated into cylinder head. The standardised package will allow integration of the engine in vehicles of other model series in the coming years without the generation of derivatives.

**REFERENCES**

- [1] Langen, P.; Brox, W.; Br uner, T.; Fischer, H.; Hirschfelder, K.; Hoyer, U.: The New BMW V8 Gasoline Engine with Twin Turbo – Part 1: Design Features. In: MTZ worldwide 69 (2008), No. 11, pp. 4-11
- [2] Bock, C.; Hirschfelder, K.; Ofner, B.; Schwarz, C.: The New BMW V8 Gasoline Engine with Twin Turbo – Part 2: Functional Characteristics. In: MTZ worldwide 69 (2008), No. 12, pp. 42-49
- [3] Schopp, J.; D ngen, R.; Fach, H.; Sch nemann, E.: BMW V8 Gasoline Engine with Turbocharging, Direct Injection and Fully Variable Valve Gear. In: MTZ worldwide 74 (2013), No. 1, pp. 18-25

TABLE 1 Technical data of the new V8 engine

Parameter	Unit	V8 TwinPower Turbo
Engine displacement	cm <sup>3</sup>	4395 (3981)
Firing order	–	1-5-4-8-6-3-7-2
Power	kW	330
... at specified engine speed	rpm	5500-6000
Torque	Nm	650
... at specified engine speed	rpm	1800-4500 (TBE)
Max. engine speed	rpm	6500
Bore/stroke	mm	89/88,3 (80)
Compression ratio	–	10.5:1 (9.7:1)
Cylinder offset	mm	98
Main bearing diameter	mm	65
Con-rod bearing diameter	mm	54
Con-rod length	mm	138.5 (142.65)
Valve diameter (inlet/exhaust)	mm	33.2/29
Valve angle (inlet/exhaust)	°	21°/19°
Max. valve lift (inlet/exhaust)	mm	8,8/9,0
Camshaft spread (inlet/exhaust)	°CA	55°-125°/60°-126°
Admissible fuel min.	ROZ	91
Emission regulation	–	Euro 6 und ULEVII
Acceleration 0-100 km/h (BMW 750i/-Xdrive)	s	4.7/4.4
Fuel consumption (NEDC) (BMW 750i/-Xdrive)	l/100 km	7.9/8.1
CO <sub>2</sub> emission (BMW 750i/-Xdrive)	g/km	184/189

(Values in brackets for 4.0-l version)

# READ THE FUTURE



personal buildup for Force Motors Limited Library



**NUMBER 1 IN AUTOMOTIVE  
ENGINEERING SINCE 1898**

We offer the leading automotive engineering trade media for the entire sector – complete with the newest results from international research, development and manufacturing, as well as fascinating contributions from chosen experts. And because it is all about progress here, we have gone one step further: Thanks to their new design, the ATZ media are now even easier to read, even more clearly structured, and even more attractive. [www.ATZonline.com](http://www.ATZonline.com)

Source: Daimler AG

**ATZ**

Founded 1939 by Prof. Dr.-Ing. E. h. Heinrich Buschmann and Dr.-Ing. E. h. Prosper L'Orange

Organ of the Fachverband Motoren und Systeme im VDMA, Verband Deutscher Maschinen- und Anlagenbau e.V., Frankfurt/Main, for the areas combustion engines and gas turbines  
 Organ of the Forschungsvereinigung Verbrennungskraftmaschinen e.V. (FVV)  
 Organ of the Wissenschaftliche Gesellschaft für Kraftfahrzeug- und Motorentechnik e.V. (WKM)  
 Organ of the Österreichischer Verein für Kraftfahrzeugtechnik (ÖVK)  
 Cooperation with the STG, Schiffbautechnische Gesellschaft e.V., Hamburg, in the area of ship drives by combustion engine

09|2015 \_ Volume 76

Springer Vieweg | Springer Fachmedien Wiesbaden GmbH

P. O. Box 15 46 · 65173 Wiesbaden · Germany | Abraham-Lincoln-Straße 46 · 65189 Wiesbaden · Germany

Amtsgericht Wiesbaden, HRB 9754, USt-IdNr. DE811148419

Managing Directors Armin Gross, Joachim Krieger, Dr. Niels Peter Thomas

Managing Director Marketing & Sales Armin Gross | Director Magazines Stefanie Burgmaier | Director Production Dr. Olga Chiarcos

**SCIENTIFIC ADVISORY BOARD**

Prof. Dr.-Ing. Michael Bargende  
 Universität Stuttgart

Prof. Dr. techn. Christian Beidl  
 TU Darmstadt

Dr.-Ing. Ulrich Dohle  
 Rolls-Royce Power Systems AG

Dipl.-Ing. Markus Duesmann  
 BMW AG

Prof. Dr.-Ing. Lutz Eckstein  
 WKM

Dr.-Ing. Torsten Eder  
 Daimler AG

Dipl.-Ing. Friedrich Eichler  
 Volkswagen AG

Dipl.-Ing. Dietmar Goericke  
 Forschungsvereinigung  
 Verbrennungskraftmaschinen e.V.

Prof. Dr.-Ing. Uwe Dieter Grebe  
 AVL List GmbH

Prof. Dr.-Ing. Jens Hadler  
 APL

Prof. Dr.-Ing. Jürgen Hammer  
 Robert Bosch GmbH

Dr. Thomas Johnen  
 Adam Opel AG

Rainer Jückstock  
 Federal-Mogul Corporation

Prof. Dr.-Ing. Heinz K. Junker  
 Mahle GmbH

Prof. Dr. Hans Peter Lenz  
 ÖVK

Prof. Dr. h. c. Helmut List  
 AVL List GmbH

Dipl.-Ing. Wolfgang Maus  
 Continental Emitec GmbH

Peter Müller-Baum  
 VDMA e.V.

Prof. Dr.-Ing. Stefan Pischinger  
 FEV GmbH

Prof. Dr. Hans-Peter Schmalz  
 Pankl-APC Turbosystems GmbH

Dr. Markus Schwaderlapp  
 Deutz AG

Prof. Dr.-Ing. Ulrich Seiffert  
 WiTech Engineering GmbH

Dr. Michael Winkler  
 Hyundai Motor Europe  
 Technical Center GmbH

**EDITORIAL STAFF**

**EDITORS IN CHARGE**

Dr. Johannes Liebl, Wolfgang Siebenpfeiffer

**EDITOR IN CHIEF**

(responsible for editorial content)

Dr. Alexander Heintzel  
 phone +49 611 7878-342 · fax +49 611 7878-462  
 alexander.heintzel@springer.com

**DEPUTY EDITOR IN CHIEF**

Dipl.-Journ. (FH) Martin Westerhoff  
 phone +49 611 7878-120 · fax +49 611 7878-462  
 martin.westerhoff@springer.com

**MANAGING EDITOR**

Kirsten Beckmann M. A.  
 phone +49 611 7878-343 · fax +49 611 7878-462  
 kirsten.beckmann@springer.com

**EDITORS**

Angelina Hofacker  
 phone +49 611 7878-121 · fax +49 611 7878-462  
 angelina.hofacker@springer.com  
 Dipl.-Ing. Ulrich Knorra  
 phone +49 611 7878-314 · fax +49 611 7878-462  
 ulrich.knorra@springer.com  
 Dipl.-Ing. Michael Reichenbach  
 phone +49 611 7878-341 · fax +49 611 7878-462  
 michael.reichenbach@springer.com  
 Markus Schöttle  
 phone +49 611 7878-257 · fax +49 611 7878-462  
 markus.schoettle@springer.com

**PERMANENT CONTRIBUTORS**

Dipl.-Ing. (FH) Richard Backhaus,  
 Andreas Burkert, Dipl.-Ing. (FH) Andreas Fuchs,  
 Roland Schedel, Stefan Schlott

**ENGLISH LANGUAGE CONSULTANT**

Paul Willin

**ONLINE | ELECTRONIC MEDIA**

Portal Manager Automotive  
 Christiane Brüninglinghaus  
 phone +49 611 7878-136 · fax +49 611 7878-462  
 christiane.brueninglinghaus@springer.com

Editorial Staff

Katrin Pudenz M. A.  
 phone +49 6172 301-288 · fax +49 6172 301-299  
 redaktion@kpz-publishing.com

**SPECIAL PROJECTS**

Managing Editorial Journalist  
 Markus Bereszewski  
 phone +49 611 7878-122 · fax +49 611 7878-462  
 markus.bereszewski@springer.com

Editorial Staff | Coordination

Dipl.-Reg.-Wiss. Caroline Behle  
 phone +49 611 7878-393 · fax +49 611 7878-462  
 caroline.behle@springer.com  
 Christiane Imhof M. A.  
 phone +49 611 7878-154 · fax +49 611 7878-462  
 christiane.imhof@springer.com

**PROJECT MANAGEMENT | ASSISTANCE**

Yeliz Konar  
 phone +49 611 7878-180 · fax +49 611 7878-462  
 yeliz.konar@springer.com  
 Martina Schraad  
 phone +49 611 7878-276 · fax +49 611 7878-462  
 martina.schraad@springer.com

**ADDRESS**

Abraham-Lincoln-Straße 46 · 65189 Wiesbaden  
 P. O. Box 1546 · 65173 Wiesbaden, Germany  
 redaktion@ATZonline.de

**ADVERTISING**

**SALES MANAGEMENT**

(responsible for advertising)  
 Volker Heselndenz  
 phone +49 611 7878-269 · fax +49 611 7878-78269  
 volker.heselndenz@best-ad-media.de

**MEDIA SALES**

Frank Nagel  
 phone +49 611 7878-395 · fax +49 611 7878-78395  
 frank.nagel@best-ad-media.de

**KEY ACCOUNT MANAGEMENT**

Rouven Bastian  
 phone +49 611 7878-399 · fax +49 611 7878-78399  
 rouven.bastian@best-ad-media.de

**DISPLAY AD MANAGER**

Nicole Brzank  
 tel +49 611 7878-616 · fax +49 611 7878-78164  
 nicole.brzank@best-ad-media.de

**AD PRICES**

Advertising ratecard from October 2014.

**MARKETING | OFFPRINTS**

**HEAD OF MARKETING  
 MAGAZINES + EVENTS**

Jens Fischer  
 phone +49 611 7878-340 · fax +49 611 7878-407  
 jens.fischer@springer.com

**OFFPRINTS**

Martin Leopold  
 phone +49 2642 907-596 · fax +49 2642 907-597  
 leopold@medien-kontor.de

**PRODUCTION | LAYOUT**

Heiko Köllner  
 phone +49 611 7878-177 · fax +49 611 7878-78177  
 heiko.koellner@springer.com

All persons specified may be contacted by post at the publisher's address.

**SUBSCRIPTIONS**

Springer Customer Service Center GmbH  
 Haberstraße 7 · 69126 Heidelberg · Germany  
 phone +49 6221 3454-303 · fax +49 6221 3454-229  
 Monday to Friday, 8 a.m. to 6 p.m.  
 springervieweg-service@springer.com  
 www.my-specialized-knowledge.com/automotive

**ORDERING OPTIONS**

The eMagazine MTZworldwide appears 11 times a year for subscribers. Ordering options and details on the subscription conditions can be found at www.my-specialized-knowledge.com/MTZworldwide.

All rights reserved.

Reproduction: This magazine and all its contents, including all images, graphics and photographs, are protected by copyright. Unless its usage is, in exceptional cases, expressly permitted by copyright law, no part of this magazine may be reproduced without the prior written consent of the publisher. This applies in particular to copies, reprints, adaptations, translations, microfilms, provision of public access and the storage and processing of this magazine in whole or in part in databases and other electronic systems and its distribution or usage via electronic systems.

**YOUR HOTLINE  
 TO MTZ**

Editorial Staff

+49 611 7878-120

Customer Service

+49 6221 3454-303

Advertising

+49 611 7878-395

The articles published in MTZworldwide are produced with the greatest possible care and attention. However, the editors do not accept any liability for the correctness, completeness and current accuracy of the content printed. The content of advertisements is the sole responsibility of the advertiser.

Every annual subscription includes access to the online archive at Springer für Professionals. Access is available exclusively to the individual subscriber and is not transferable.

No liability can be accepted for the unsolicited submission of manuscripts, photographs or illustrations.

© Springer Vieweg | Springer Fachmedien Wiesbaden GmbH, Wiesbaden 2015

Springer Vieweg is part of Springer Science+Business Media.

Springer Vieweg

## PEER REVIEW

Peer Review Process for Research Articles  
in ATZ, MTZ and ATZelektronik

## STEERING COMMITTEE

Prof. Dr.-Ing. Lutz Eckstein	RWTH Aachen University	Institut für Kraftfahrzeuge Aachen
Prof. Dipl.-Des. Wolfgang Kraus	HAW Hamburg	Department Fahrzeugtechnik und Flugzeugbau
Prof. Dr.-Ing. Ferit Küçükay	Technische Universität Braunschweig	Institut für Fahrzeugtechnik
Prof. Dr.-Ing. Stefan Pischinger	RWTH Aachen University	Lehrstuhl für Verbrennungskraftmaschinen
Prof. Dr.-Ing. Hans-Christian Reuss	Universität Stuttgart	Institut für Verbrennungsmotoren und Kraftfahrwesen
Prof. Dr.-Ing. Ulrich Spicher	MOT	
Prof. Dr.-Ing. Hans Zellbeck	Technische Universität Dresden	Lehrstuhl für Verbrennungsmotoren

## ADVISORY BOARD

Prof. Dr.-Ing. Klaus Augsburg	Dr. Malte Lewerenz
Prof. Dr.-Ing. Michael Bargende	Prof. Dr.-Ing. Markus Lienkamp
Prof. Dipl.-Ing. Dr. techn. Christian Beidl	Prof. Dr. rer. nat. habil. Ulrich Maas
Prof. Dr. sc. techn. Konstantinos Boulouchos	Prof. Dr.-Ing. Markus Maurer
Prof. Dr. Dr. h.c. Manfred Broy	Prof. Dr.-Ing. Martin Meywerk
Prof. Dr.-Ing. Ralph Bruder	Ao. Univ.-Prof. Dr. Gregor Mori
Dr. Gerhard Bruner	Prof. Dr.-Ing. Klaus D. Müller-Glaser
Prof. Dr. rer. nat. Heiner Bubb	Dr. techn. Reinhard Mundl
Prof. Dr. rer. nat. habil. Olaf Deutschmann	Prof. Dr. rer. nat. Peter Neugebauer
Prof. Dr.-Ing. Klaus Dietmayer	Prof. Dr. rer. nat. Cornelius Neumann
Dr. techn. Arno Eichberger	Prof. Dr.-Ing. Nejila Parspour
Prof. Dr. techn. Helmut Eichseder	Prof. Dr.-Ing. Peter Pelz
Prof. Dr. Wilfried Eichseder	Prof. Dr. techn. Ernst Pucher
Dr.-Ing. Gerald Eifler	Dr. Jochen Rau
Prof. Dr.-Ing. Wolfgang Eifler	Prof. Dr.-Ing. Konrad Reif
Prof. Dr. rer. nat. Frank Gauterin	Prof. Dr.-Ing. Stephan Rinderknecht
Prof. Dr. techn. Bernhard Geringer	Prof. Dr.-Ing. Jörg Roth-Stielow
Prof. Dr.-Ing. Uwe Dieter Grebe	Dr.-Ing. Swen Schaub
Dr. mont. Christoph Guster	Prof. Dr. sc. nat. Christoph Schierz
Prof. Dr.-Ing. Holger Hanselka	Prof. Dr. rer. nat. Christof Schulz
Prof. Dr.-Ing. Horst Harndorf	Prof. Dr. rer. nat. Andy Schürr
Prof. Dr. techn. Wolfgang Hirschberg	Prof. Dr.-Ing. Ulrich Seiffert
Prof. Dr. techn. Peter Hofmann	Prof. Dr.-Ing. Hermann J. Stadtfeld
Prof. Dr. rer. nat. Peter Holstein	Prof. Dr.-Ing. Karsten Stahl
Prof. Dr.-Ing. Volker von Holt	Prof. Dr. techn. Hermann Steffan
Prof. Dr.-Ing. habil. Werner Hufenbach	Prof. Dr.-Ing. Wolfgang Steiger
Prof. Dr.-Ing. Armin Huß	Prof. Dr.-Ing. Peter Steinberg
Dr. techn. Heidelinde Jetzinger	Dr.-Ing. Peter Stommel
Prof. Dr.-Ing. Roland Kasper	Dr.-Ing. Ralph Sundermeier
Prof. Dr.-Ing. Prof. E. h. mult. Rudolf Kawalla	Prof. Dr.-Ing. Wolfgang Thiemann
Prof. Dr.-Ing. Tran Quoc Khan	Prof. Dr.-Ing. Dr. h.c. Helmut Tschöke
Dr. Philip Köhn	Prof. Dr.-Ing. Georg Wachtmeister
Prof. Dr.-Ing. Ulrich Konigorski	Prof. Dr.-Ing. Jochen Wiedemann
Prof. Dr. Oliver Kröcher	Prof. Dr. rer. nat. Gerhard Wiegler
Prof. Dr.-Ing. Peter Krug	Prof. Dr. techn. Andreas Wimmer
Dr. Christian Krüger	Prof. Dr. rer. nat. Hermann Winner
Prof. Dr. techn. Thomas Lauer	Prof. Dr. med. habil. Hartmut Witte
Prof. Dr. rer. nat. Uli Lemmer	Dr.-Ing. Michael Wittler

Scientific articles of universities in ATZ Automobiltechnische Zeitschrift, MTZ Motortechnische Zeitschrift and ATZelektronik are subject to a proofing method, the so-called peer review process. Articles accepted by the editors are reviewed by experts from research and industry before publication. For the reader, the peer review process further enhances the quality of the magazines' content on a national and international level. For authors in the institutes, it provides a scientifically recognised publication platform.

In the Peer Review Process, once the editors has received an article, it is reviewed by two experts from the Advisory Board. If these experts do not reach a unanimous agreement, a member of the Steering Committee acts as an arbitrator. Following the experts' recommended corrections and subsequent editing by the author, the article is accepted.

In 2008, the peer review process utilised by ATZ and MTZ was presented by the WKM (Wissenschaftliche Gesellschaft für Kraftfahrzeug- und Motorentechnik e. V./ German Professional Association for Automotive and Motor Engineering) to the DFG (Deutsche Forschungsgemeinschaft/German Research Foundation) for official recognition. ATZelektronik participates in the Peer Review since 2011.



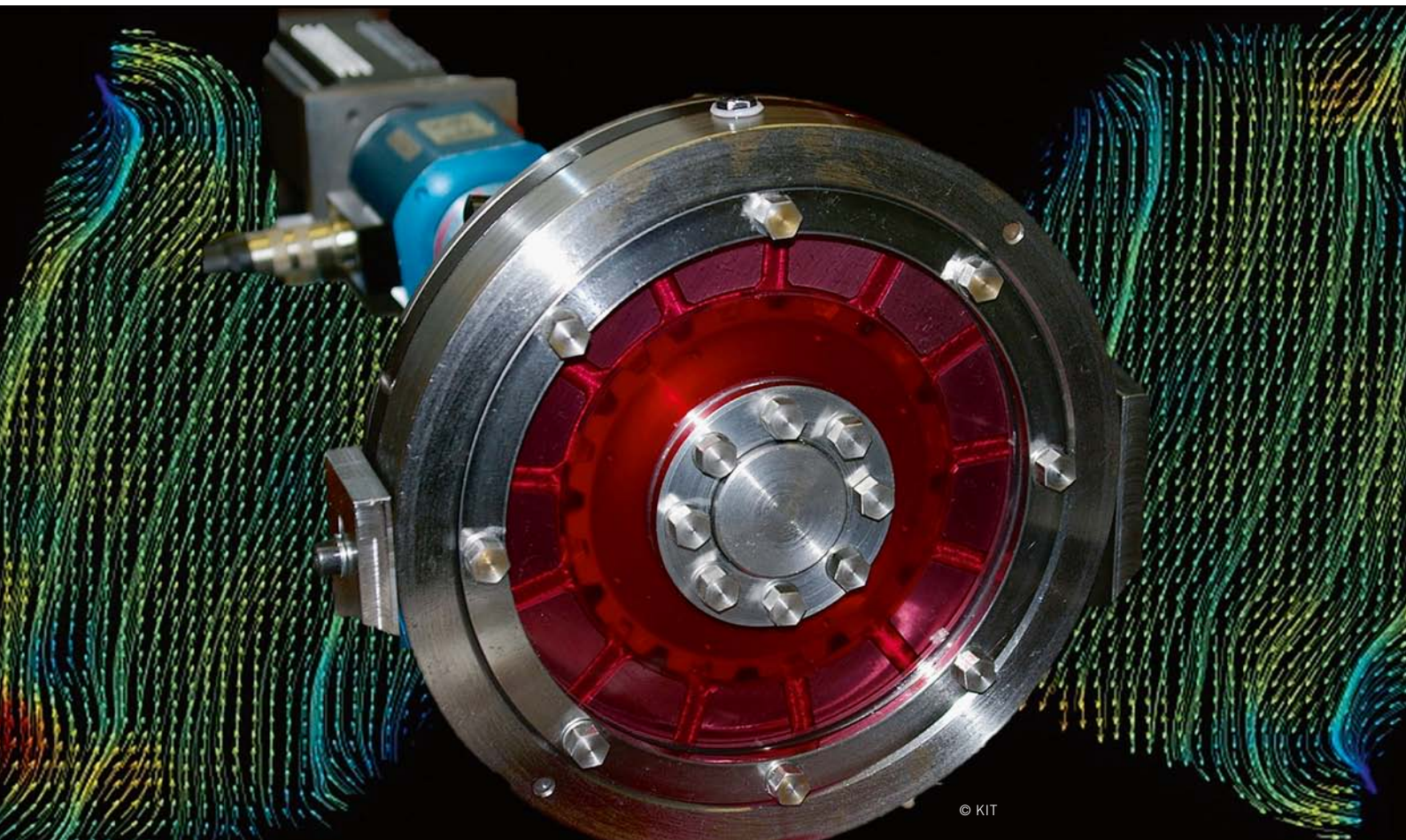
## Advanced Development of Hybrid Drivetrains

AUTHOR



**Dr.-Ing. Friedrich Brezger** obtained his Ph.D. at the IPEK – Institute of Product Engineering of the Karlsruhe Institute of Technology (KIT) Germany in the Field of Drive Systems.

The clutch systems used in hybrid vehicles must comply with amended or extended tasks in the various new propulsion systems. The new general conditions are worked out and studied by means of a product development model and the Contact & Channel & Connector-Approach, which allows the necessary product development processes and their resource system to be synthesised. For the case of a wet multiple-disc clutch of a parallel hybrid vehicle with an electric motor at the transmission input, a new validation environment is created for CFX simulations of the special clutch discs, and an existing modelling approach is added the possibility of modelling incompressible hydraulics. The Ph. D. thesis won the Hermann Appel Prize of the IAV in 2014.



© KIT

1	MOTIVATION
2	STATE OF THE ART
3	DEVELOPMENT ENVIRONMENT FOR WET CLUTCHES
4	IMPORTANCE OF DISC SHAPE IN THE CLUTCH OF A VEHICLE
5	SUMMARY

## 1 MOTIVATION

Since January 2010, a new legal regulation has been in force in motor vehicle tax applied to passenger cars which demands CO<sub>2</sub> emissions below 120 g/km in the new European Driving Cycle (NEDC) if the vehicle is to be granted tax exemption. Internal combustion engine efficiencies mostly suffer in the part-load regimes occurring in this certification cycle or others. As hybrid vehicles continue to be certified in different ways, it is obvious that they will not be optimised for one cycle. The clutch system of alternative vehicles is to be developed further in this study with a view to the drivetrain, and special consideration will be given to real customer behaviour in order to ensure reliable performance.

The motivation for optimising specific clutch systems can be derived from considerations of power loss in a sports car in the NEDC. [8] have shown that a torque converter in a conventional passenger car converts 2 % of the traction power into losses. When the power loss is expressed relative to the mechanical power at the engine output end, the percentage of power loss in the converter in this case is 7.4 %. When this converter of a conventional passenger car is replaced by a special clutch for energy-efficient modelling of the hybrid functions in a hybrid car, special attention must be paid to its power loss in the certification cycles as well as in the cycles relevant to customer expectations. New development and validation methods as well as the results generated will be described below.

## 2 STATE OF THE ART

### 2.1 X-IN-THE-LOOP FRAMEWORK

One possible environment for development and validation is the X-in-the-Loop framework (XiL) developed at the IPEK. This XiL is to advance the learning curve in product development as far ahead as possible and, in this way, save costs and expense. A kind of test chain is created for this purpose which allows development and validation of the relevant pairs of power transmission surfaces via subsystems, components, up to the whole system. Applicability to the early phases of product development requires modelling so that a simulated residual system can be studied in its interaction with the System Under Development (SUD) as required [6]. The SUD constitutes the design space within which development may be carried out. In this way, a holistic approach is created in which suitable studies can be performed under continuous inclusion of the driver, environment, and test cases/manoeuvres systems. **FIGURE 1** shows the XiL framework: The different levels are shown in the vehicle system.

A working surface pair (WSP), for instance, could be a clutch lining with the matching friction partner. This does not have to be the complete clutch disc, but could be a study of the pair of materials under various simulated boundary conditions. If the example is chosen at a higher level, this would be a clutch disc with a friction plate to match. Depending on the objective of a study, these subsystems can be extended up to the drivetrain. At the next higher level, the vehicle is in the loop, for instance on a roller dynamometer (virtual environment), a test track, or in a real physical environment. It is always possible to distinguish between physical and virtual in the vehicle system. The SUD, for instance, is on the physical and virtual roller dynamometer, respectively as a simulation model or as a physical component. This is where the XiL approach derived its name: the transitions between the physical and virtual domains are fluid.

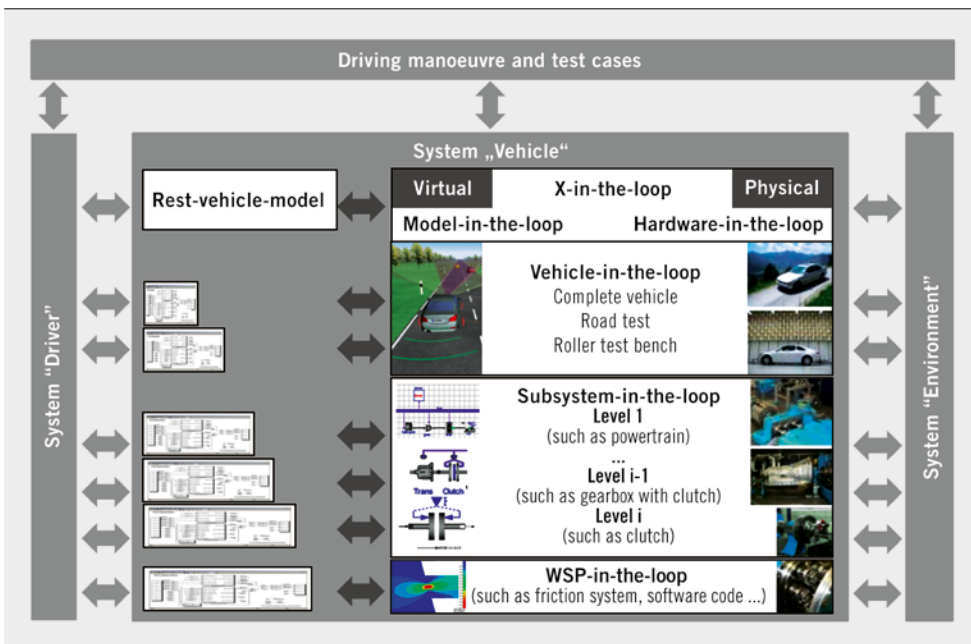


FIGURE 1 X-in-the-Loop framework (© KIT)

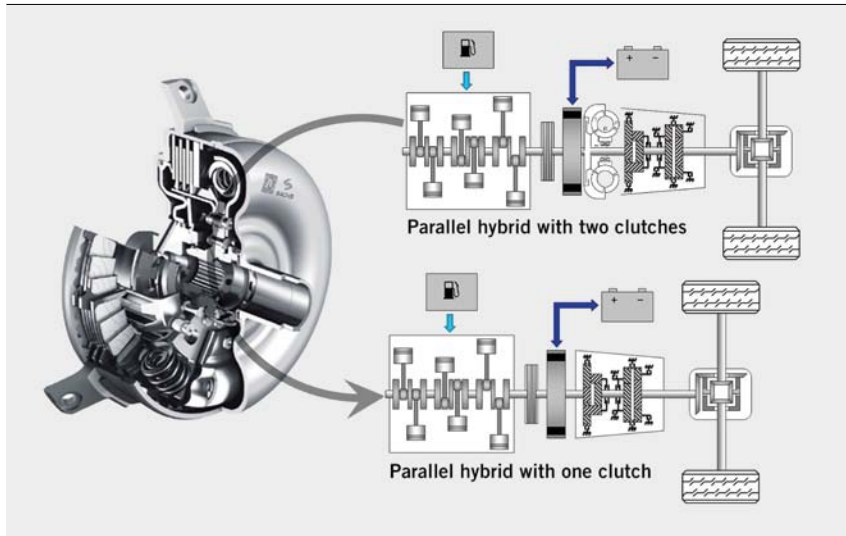


FIGURE 2 Wet multiple-disc clutch (left) and P2 hybrid variants (right) (© clutch left: ZF Sachs; right KIT)

2.2 WET MULTIPLE-DISC CLUTCH IN A PASSENGER CAR

In wet, switchable, externally operated friction clutches [1] oil serves as the coolant between discs extracting the friction power as heat from the system in order to avoid damage to the friction partners. The flow of the oil coolant determines the oil volume in the friction gap. Depending on the mode of operation, air may enter in classical clutches. As a consequence, the characteristic development of the drag torque in the disengaged state of such clutches can be subdivided into three phases:

- Phase 1: Nearly linear rise of the drag torque as a function of speed, then plateau formation
- Phase 2: Steep decline of the drag torque as a result of air entering. Low, pronounced plateau
- Phase 3: Slight increase in the drag torque and further increase in speed as a result of disc wobble.

One special design of a wet clutch is of special interest as a model of the methods later shown for the advanced development of clutch systems for hybrid drivetrains. It is a wet multiple-disc clutch whose housing is closed so that a closed oil coolant volume flow can be achieved. This has been designed for use in passenger cars with high power inputs and without a torque converter. In parallel full-hybrid vehicles, the torque converter and a clutch additionally required are to be replaced by this clutch system, **FIGURE 2**. This means that the clutch system has to perform other special functions: separating the internal combustion engine from the drivetrain; comfortable engagement of the clutch and possibility of longer slip phases. As a result of its duties and its position in the drivetrain, this system is referred to as a mix of torque converter and wet clutch [3]. In this design, the helical turbulent oil flow moving in a circumferential direction is to ensure highly effective cooling during synchronising. This hydrodynamic effect (Hydrodynamically Cooled Clutch, HCC) is to allow the oil coolant flow applied externally to be kept much lower than in comparable wet clutch systems.

2.3 CONTACT & CHANNEL & CONNECTOR-APPROACH

The purpose of the Contact & Channel & Connector-Approach (C&C<sup>2</sup>-A) is to find a standardised model language for technical

systems. It combines a number of studies from systems theory and claims to be continuous. In this way, the C&C<sup>2</sup>-A can be used to describe the connection between observed functioning and its design, and it serves for analysis and synthesis of technical (sometimes mechanical) systems, and is made up of the in **FIGURE 3** showed model elements [9]. This research language has been validated in innumerable examples of mechanical processes [4]. This study is to show for the first time that this language can also be used for incompressible fluids.

3 DEVELOPMENT ENVIRONMENT FOR WET CLUTCHES

Some first studies of the clutch system within the XiL context were carried out to quantify potentials for optimisation of the system. For this purpose, the clutch was installed in an in-line test rig and operated in various configurations (components, operating parameters etc.). At the same time, a model with plain discs was implemented on the basis of the model presented and in the light of the situation known from the state of the art. This latter model happens to match exactly the drag torque of the grooved discs in the experiment. The model was expanded by a heating model [7] based on the energy conservation formula, thus allowing the temperature rise in the oil coolant in the clutch during the manoeuvre to be simulated as well. Above a differential speed of approx. 1000 rpm a highly divergent drag torque is obtained. In the end, the simulated drag torque of the expanded

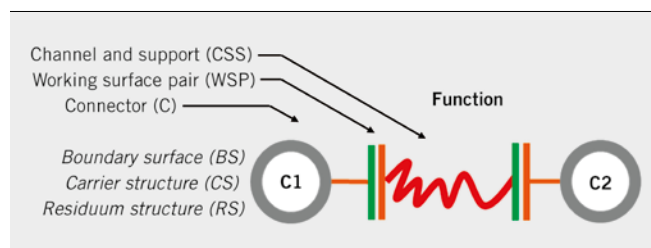
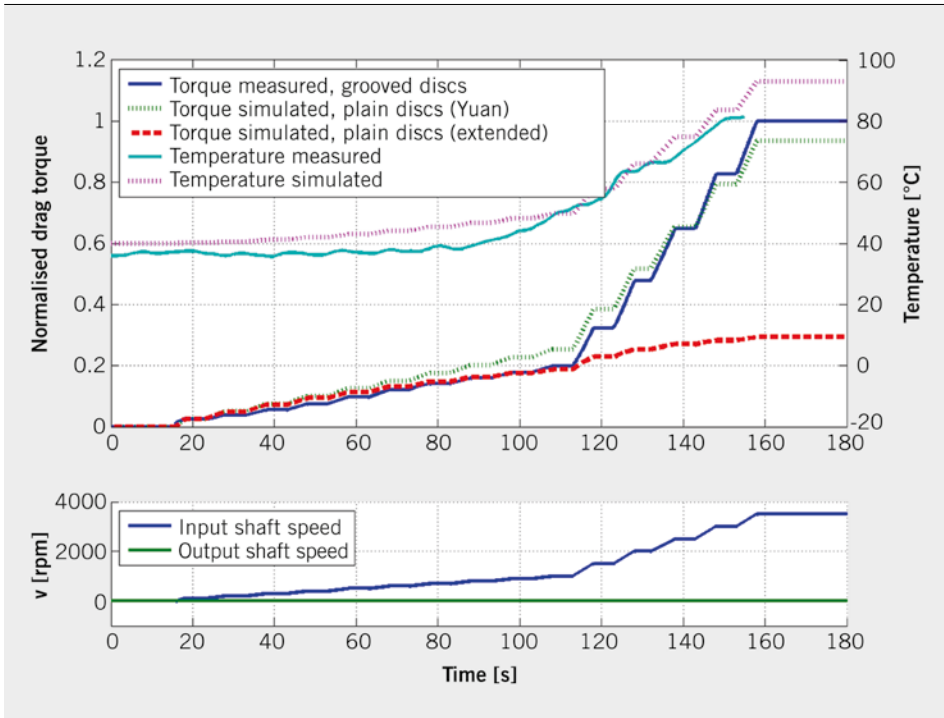


FIGURE 3 Elements of the C&C<sup>2</sup> Approach and the simplest representation of the function (© KIT)



**FIGURE 4** Measurement and simulation of the drag moment produced at various differential speeds (© KIT)

model is only 30 % of the measured torque. The valid model approach in this way shows that the temperatures generated in the oil coolant flow are compared, **FIGURE 4**. The simulated temperature (dotted pink) relative to the measured drag torque (blue) initially rises slightly after the differential speed has been set. Energies are low. The curve deviates only slightly from the temperature measurement (turquoise), which initially is a bit lower. As speeds become higher, temperatures develop more or less alike. These minor deviations may be due to the point of temperature measurement and the thermal masses hot from operation. However, as the differences turn out to be minimal, and the influences are known, the model was not formulated in a more precise way. A variety of hypotheses can be derived from this study, a combination of experiment and simulation.

- At low relative speeds (in this case  $\leq 1000$  rpm), the difference in drag torque between the grooved and the plain discs is very small for this clutch system, i.e. it is negligible. This hypothesis is in agreement with the findings by Oerleke et al. [2] in phase 1 (before air enters the disc set) of their test rig design. Moreover, the relatively low drag torques and speeds also make for relatively slight heating of the oil.
- The grooved discs designed for the HCC effect produce this effect fully only above a differential speed of more than 1000 rpm in the clutch system under investigation. This hypothesis is derived from the idea that the fully developed helical oil flow through pumps and turbines generates the drag torque because of increased friction.
- The measurement was compared in simulation with ideally distributed plain discs. Simulation predicts a rise of the drag torque, on the basis of Newton's shear stresses, in the case of inhomogeneous distribution of the discs (as  $M \sim 1/h$ ). As deviations obviously are slight, a relatively uniform disc distribution can be assumed for this clutch system at low relative speeds.

- If the relative speed is raised to 1000 rpm, there are significant differences in the drag torques as measured and as simulated in the extended model. This may be due to two effects: The discs abandon their rather ideal arrangement for a very inhomogeneous

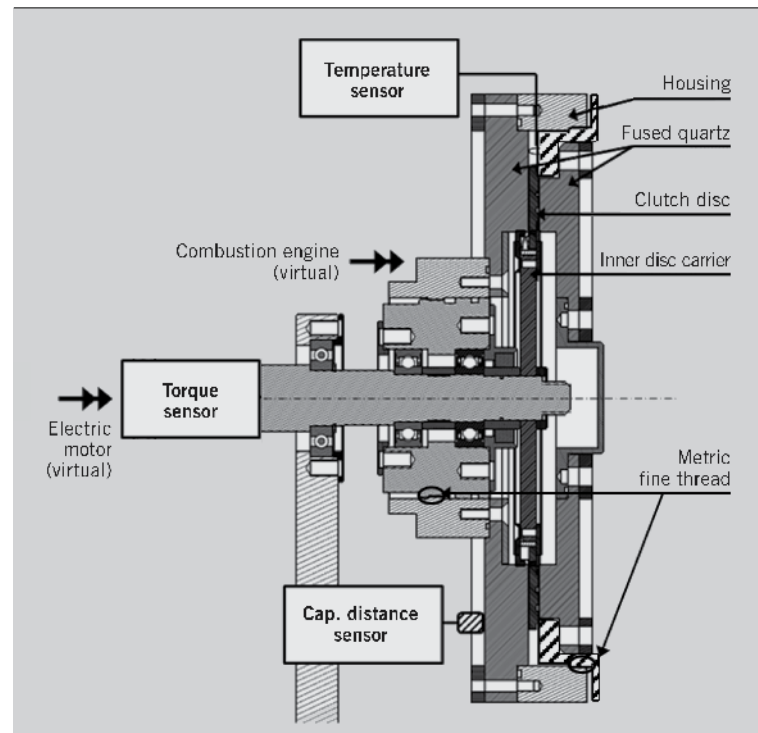


**FIGURE 5** Sectional view of the probe of the single-disc test rig with an inner disc in place (© KIT)

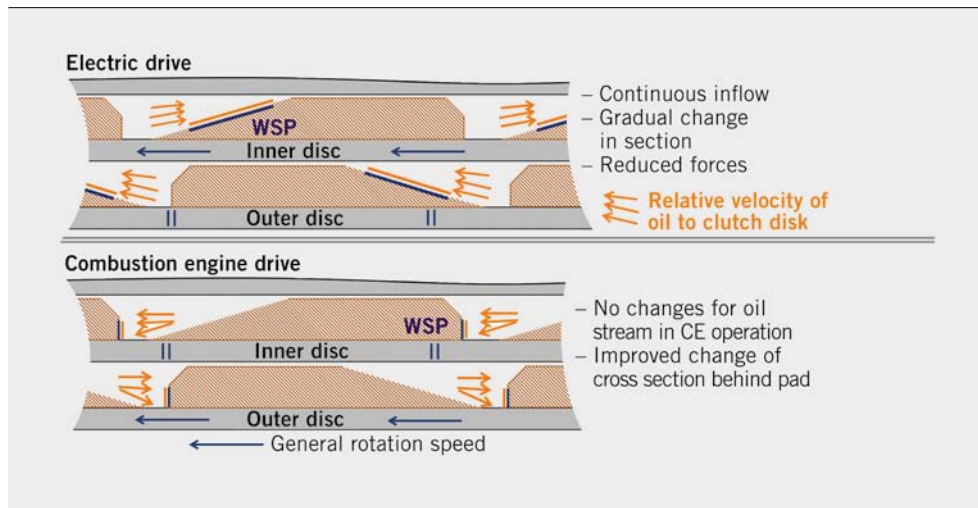


**FIGURE 6** Schematic representation of disc design and disk installation (© KIT)

geneous distribution, perhaps with incipient mixed friction: The energy is consumed for the pumping effects in the clutch and associated viscous friction. Or compared to ideally distributed plain discs, this phenomenon may amount to 70 % of the drag moment at a relative speed of 3500 rpm in this clutch.

For verification of the hypotheses, a single-disc test rig has been developed which is characterised by its optical accessibility and exact position detection by means of capacitive sensors, **FIGURE 5**. This test rig allows CFD simulations to be compared with measurements and different disc designs to be varied and measured by means of a representation merely of milled discs. It was demonstrated that, in a clutch filled with oil, neither fabrication nor the material generate different drag torques or flows on a macroscopic scale [5]. This was demonstrated by measurements of a single disc and after introduction of another disc. The effect discovered, i.e. that the single-sided disc changes its point of contact as a function of oil temperature and speed, occurs in the original disc and in the milled disc. It was also shown that much of the drag torque is caused by self-induced axial forces. Models generated from the C&C<sup>2</sup> Approach were used as a basis for a design then corroborated in the single-disc test rig. Afterwards, this was validated at vehicle level (XiL).

#### 4 IMPORTANCE OF DISC SHAPE IN THE CLUTCH OF A VEHICLE

This design, which is shown in **FIGURE 6**, activates the HCC effect only in the preferential direction of the differential speed if the VKM runs at a higher speed. In addition, unnecessary backflow regions of the disc grooves are restricted. The HCC effect is clearly reduced in the electric mode of operation. In addition, it is possible for defined modes (ranges of temperature and differential speed) in electric operation to achieve hydrodynamic distancing of the discs. This must be harmonised with the overall vehicle system in terms of frequencies of operating points and, hence, operating strategy (temperature and differential speeds); in that case, it is possible to reduce further drag losses.

#### 5 SUMMARY

It has been shown that clutch systems for hybrid vehicles mean new requirements. The clutch system is optimised in the context of the overall system and in the light of the planned operating strategy. This requires knowledge of the disc pairs and the entire clutch in the system and also of the residual system (such as electric motor, gearbox etc.). Specific optimisation of a parameter can be achieved in a single-disc test rig if the type of superposition is known and has been proven. This requires detailed modelling both in the physical and in the virtual domains. Intelligent asymmetric arrangement of a tapered lining design permits the HCC effect to be tied to the direction of relative speed. In the XiL environment, in which the simulation of the entire vehicle with the operating strategy, driver, and subsystem, is coupled, it is seen that the losses arising at the clutch can be reduced by 16 % in the hands of the customer.

#### REFERENCES

- [1] N. N.: Wellenkupplungen. Systematische Einteilung nach ihren Eigenschaften. VDI-Richtlinie 2241, Blatt 1, Düsseldorf: VDI-Verlag, 1982
- [2] Oerleke, C.; Funk, W.: Leerlaufverhalten ölgekühlter Lamellenkupplung. FVA, Forschungsvorhaben no. 290, 1998
- [3] Sasse, C.; Sudau, J.: Nasslaufende Anfahrkupplung für Automatikgetriebe durch innovatives Kühlkonzept. In: ATZ 111 (2009), no. 12, pp. 914–921
- [4] Alink, T.: Bedeutung, Darstellung und Formulierung von Funktion für das Lösen von Gestaltungsproblemen mit dem C&C-Ansatz. Karlsruhe: IPEK, 2010, Forschungsberichte, vol. 48
- [5] Albers, A.; Brezger, F.; Koch, C.: Development of a new validation environment for CFD simulations on the example of a lubricated clutch. VDI Getriebe in Fahrzeugen, Friedrichshafen, 2012
- [6] Albers, A.; Brezger, F.; Geier, M.; Freudenmann, T.; Stier, C.: Phenomena-Based Methods in Powertrain Validation. Innovative Automotive Transmissions and Hybrid & Electric Drives, vol 10, 2011
- [7] Albers, A.; Brezger, F.: Modelling of oil heating of disengaged lubricated clutches in hybrid vehicles. Fisita, 2012
- [8] Schommers, J.; Doll, G.; Weller, R.; Behr, T.; Scheib, H.; Löffler, M.; Böhm, J.; Hartweg, M.; Bosler, A.: Reibleistungsoptimierung – Basis für die Zukunftsfähigkeit der Verbrennungsmotoren. 33. Internationales Wiener Motorenkomposium, vol. 33., 2012
- [9] Albers, A.; Sadowski, E.; Chakrabarti, A.; Blessing, L.: The Contact and Channel Approach (C&C2-A) – relating a system's physical structure to its functionality. Springer, 2013

# IT'S TIME FOR EXPERT KNOWLEDGE WITH MORE FLEXIBILITY.



## ATZ eMAGAZINE.

© creativa republic 2015

personal buildup for Force Motors Limited Library



**THE FASTEST INFORMATION IS DIGITAL.**

The **ATZ eMagazine** for the technology-oriented management in the automotive industry is loaded with the latest findings in research, development and production – for every aspect of passenger car and commercial vehicle engineering, for every branch and specialty. The **ATZ eMagazine** is fast and up-to-date: easily find topics with keyword searches, read up on feature articles in the online archives or create a PDF with extracted information.

[www.my-specialized-knowledge.com/ATZworldwide](http://www.my-specialized-knowledge.com/ATZworldwide)

# ATZ

AUTHORS



**Dipl.-Ing. Mathias Diefenthal**  
 is Scientific Research Engineer in the Field of Numerical Simulations at the Institute for Power Plant Technology, Steam and Gas Turbines at the RWTH Aachen University (Germany).



**Dipl.-Ing. Christian Rakut**  
 is Scientific Research Engineer in the Field of Theoretical Investigations at the Institute for Power Plant Technology, Steam and Gas Turbines at the RWTH Aachen University (Germany).



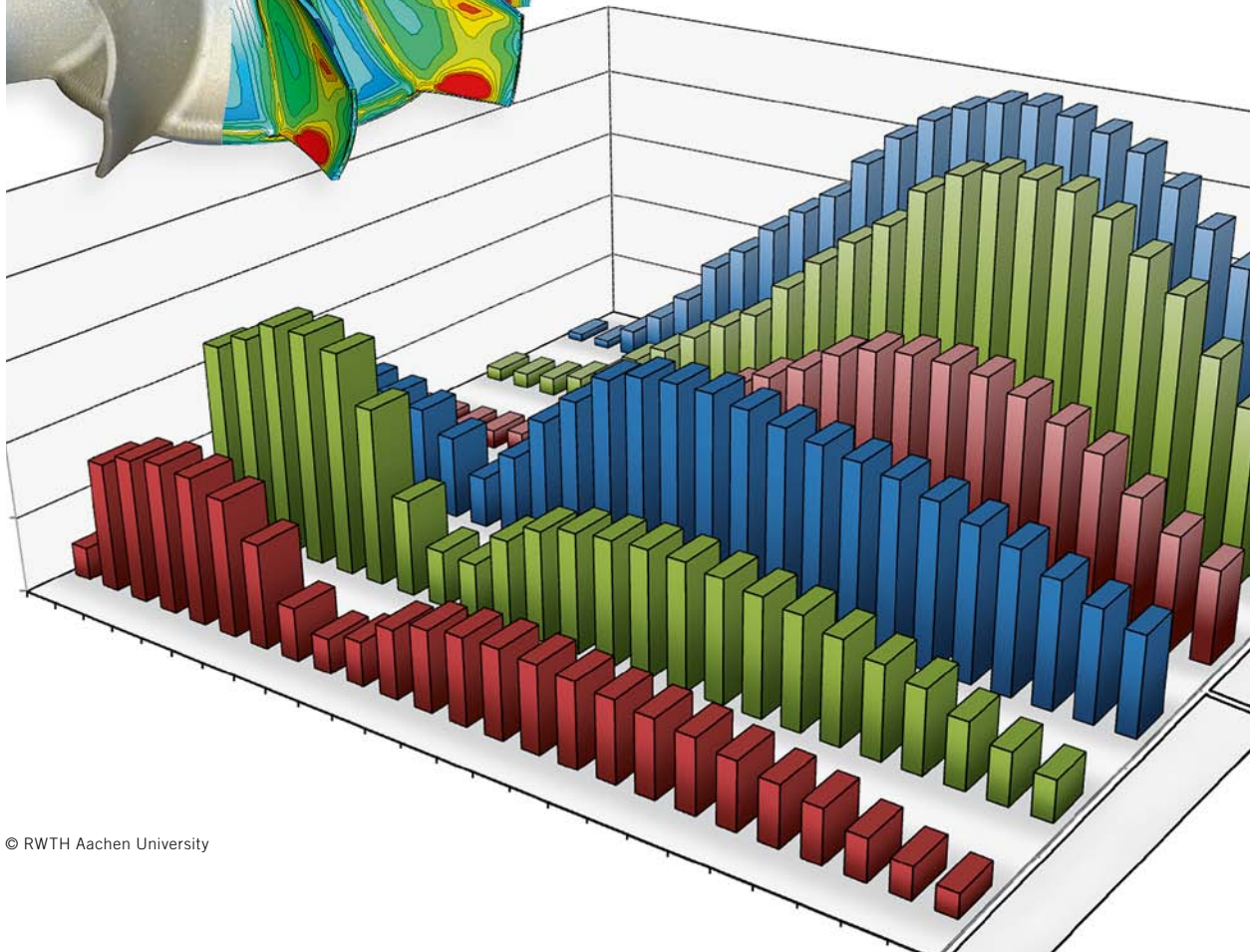
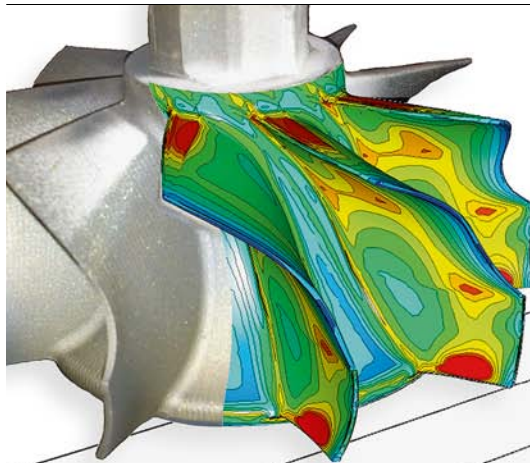
**Dipl.-Ing. Hailu Tadesse**  
 is Scientific Research Engineer in the Field of Experimental Investigations at the Institute for Power Plant Technology, Steam and Gas Turbines at the RWTH Aachen University (Germany).



**Univ.-Prof. Dr.-Ing. habil. Manfred Wirsum**  
 is Head of the Institute for Power Plant Technology, Steam and Gas Turbines at the RWTH Aachen University (Germany).

# Temperature Distribution in a Radial Turbine Wheel During Transient Operation

In recent decades the efficiency increase of combustion engines for mobile vehicles and stationary industrial applications has become more important due to the growing demand for the reduction of CO<sub>2</sub> emissions and fuel consumption. Exhaust gas turbochargers make a great contribution in this context since the kinetic and thermal energy of the exhaust gas is used to increase the efficiency of the engine by increasing the boost pressure. As part of a FVV research project the transient and steady-state temperature fields were examined in the turbine of a turbocharger at the RWTH Aachen.



© RWTH Aachen University

1	MOTIVATION
2	EXPERIMENTAL INVESTIGATIONS
3	NUMERICAL MODEL
4	SIMULATION METHOD
5	THERMAL LOADS OF THE TURBINE WHEEL
6	SUMMARY AND OUTLOOK

## 1 MOTIVATION

The requirements for turbochargers are manifold. In order to achieve a good response characteristic of the turbocharger and thus a reduction of the turbo lag, the rotating components have to be constructed as lightweight as possible. Simultaneously higher exhaust gas temperatures are implemented for the purpose of a better efficiency which results in higher thermal loads. According to [1] gas temperatures up to 1050 °C can be reached in gasoline engine exhausts. The thermal loads are particularly important in mobile applications because in this case turbochargers operate inherently dynamic. In acceleration and deceleration phases load changes of the engine occur, resulting in strong variations of the exhaust gas temperatures and thus in inhomogeneities of the turbine component temperatures. As described in [2] and [3] these high thermal loads cause stresses in the components that superimpose upon the centrifugal stresses. Neglecting these stresses can lead to damage of the turbocharger caused by Low Cycle Fatigue. To investigate the influence of the thermal stresses on the durability of the turbine components, an understanding of the inhomogeneous steady-state and transient temperature fields in the components is necessary.

The transient and steady-state temperature fields in the turbine of a turbocharger were investigated in a FVV research project. For this purpose experimental and numerical investigations were conducted. The objectives were the development of a simulation method for determining the transient temperature fields and an analysis of the relevant heat transfer phenomena with regard to the thermal loads. With an understanding of these effects, a method for the fast estimation of the thermal loads can be developed in future research.

## 2 EXPERIMENTAL INVESTIGATIONS

In the experimental part of the project a test rig was designed and built which allows the approximation of the real transient operation of the turbocharger by thermal shock tests. In these tests, the inlet temperature of the turbocharger is changed rapidly in order to initialise a heating or a cooling process with a change in rotor speed. **FIGURE 1** shows a schematic illustration of the hot gas turbocharger test rig. The depicted combustion chamber is supplied with air by a turbo compressor. During the whole thermal shock test the combustion chamber operates stationary at the upper temperature level ( $T = 450\text{--}600\text{ °C}$ ). Behind the combustion chamber the hot gas mass flow is split into two parts. In the first part, the temperature level remains almost unchanged (hot strand). In the second part, the exhaust gas mass flow is mixed with cold air from a screw compressor in order to reduce the temperature level (cold strand). In all conducted investigations the exhaust gas temperature was set to 200 °C in this strand. By a system of throttle valves equal mass flow rates are achieved in both strands. The exhaust gas that is not needed is directed to the stack by a bypass.

With the described design of the test rig it is possible to switch between the two strands (hot and cold), which results in a rapid change of the gas temperature at the inlet of the turbocharger. By a flow conditioner in front of the turbine inlet the swirl that is generated by the Y-pipe between the two strands can be minimised and thus a good quality of the flow profile at the inlet of the turbocharger is ensured.

The investigated turbocharger is designed for commercial vehicles and the radial turbine wheel has a scallop back. The turbine housing contains no guide wheel and no wastegate. The chosen size of the turbocharger is necessary for the application of the instrumentation in the turbine wheel. To determine the boundary conditions for the numerical investigations the inlet and outlet conditions of the turbine, the compressor and the bearing housing are recorded. This comprises the measurement of the temperatures, the static pressures and the mass flow rates. In addition, four solid temperatures are measured on the turbine wheel and six on the turbine housing. **FIGURE 2** shows the positions of the equidistantly measuring points at the housing and the measuring points at the turbine wheel schematically. For all temperature measurements thermocouples of type K were used. The diameters of the thermocouples

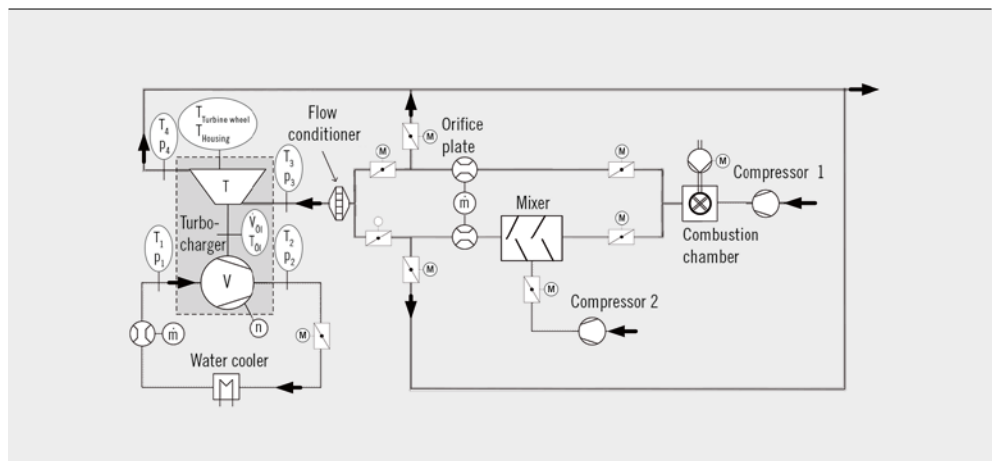


**FIGURE 1** Flow sheet of the exhaust turbocharger test rig (© RWTH Aachen University)

vary with the regard of the location. The data of the rotating system are transferred by means of a four-channel-telemetry system.

### 3 NUMERICAL MODEL

Based on the experimental data, the numerical models were validated and their accuracy was assessed. In order to achieve a high accuracy of the numerical simulations and thus to generate a suitable data base for the analysis of the heat transfer mechanisms and the temperature fields, conjugate heat transfer calculations were performed. The model used for this purpose is shown in **FIGURE 3**. It consists of the turbine volute, a segment of the turbine wheel with periodic boundary conditions and the turbine inlet and outlet pipe. The coupling of the volute and the rotating turbine wheel is made by peripheral averaging (Mixing Plane). Compressor and bearing housing are not included in the simulations. For that reason thermal boundary conditions have to be defined at the interface between the turbine and the bearing housing to describe the heat transfer from the turbine into the bearing housing and the compressor. Therefore at the wall of the volute and of the shaft heat transfer coefficients and corresponding reference temperatures are used. These boundary conditions were determined iteratively based on the measured data. The fluid state is calculated as ideal gas. To model the turbulence the  $k\omega$ -SST turbulence model is implemented. The material properties of fluid and solid are defined as a function of the temperature.

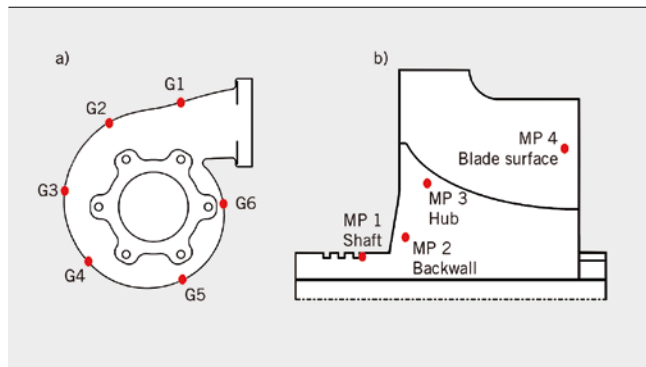


**FIGURE 2** Positions of the temperature measuring points on the turbine (a: turbine housing, b: turbine wheel and shaft) (© RWTH Aachen University)

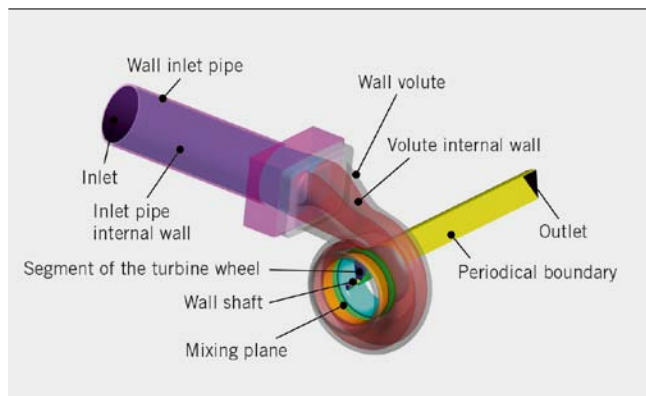


**FIGURE 3** Used numerical model of fluid state and solid body of the turbine side of the turbocharger (© RWTH Aachen University)

### 4 SIMULATION METHOD

In a transient heating or cooling process fluid and solid react very different to changes of the operating point. According to [4] the timescales differ about a factor of  $10^4$ . Due to these differences transient conjugate heat transfer simulations of the thermal shock tests are very time-consuming and cannot be carried out with reasonable computational effort. Therefore, simplifications have to be made that allow a reduction of the computation time. Compared to the fluid state the solid body reacts very slowly when varying the operating point. Therefore, the influence of temperature changes in the solid body on the fluid state can be neglected over wide periods and the fluid state can be assumed as quasi-stationary in these intervals. In detail, this means that the pressures and velocities in the fluid state do not change in these intervals. With that assumption, mass and momentum equations do not need to be solved for these periods and much larger time steps can be used, which means that the computing time can be considerably reduced. In the literature this methodology is known as the Frozen Flow or Only Energy [5].

In the investigations it could be found that the duration of the quasi-stationary simulation sections has a significant impact on the accuracy of the solution. Therefore, periods were defined for the thermal shock simulations in which the assumption of a quasi-stationary fluid state is valid. To evaluate the accuracy of the fluid simulation, the Reynolds number was used because it is essential for the heat transfer. It was defined that the error in the mean relative Reynolds number in the blade channel due to the assumption of a quasi-stationary fluid must not be greater than 3.0 %. Based on this criterion, a very good correspondence between the experiments and the simulations could be achieved. In **FIGURE 4** the measured and simulated temperature profiles at two exemplary measuring points on the turbine wheel are compared.

A very good agreement between the temperature profiles over the entire simulation period was achieved. The root mean square deviation of both measurement points is less than 7.0 K.

### 5 THERMAL LOADS OF THE TURBINE WHEEL

The validated simulations were used to analyse the transient temperature fields in the turbine wheel and the relevant heat transfer mechanisms. In the scope of these investigations, four thermally highly loaded areas were identified. These are listed below, sorted in descending order according to the quantity of the temperature gradients.

- undercut between the turbine wheel back and the shaft
- trailing edge at the hub
- pressure side near the leading edge
- hub at suction side at the narrowest cross section.

At the undercut between the turbine wheel back and the shaft most of the heat from the turbine wheel flows to the bearing housing respectively to the compressor. These large heat fluxes result in high temperature gradients and accordingly high thermal loads in the turbine wheel. The maximum loads in this area are caused by a high difference in the mean temperature of the turbine wheel and the shaft and therefore occur already in the steady-state operating points. Thus, in this area a transient consideration of the turbocharger is not necessary to quantify the maximum thermal loads. In the other three areas, the maximum loads occur during the transient operation of the turbocharger. These loads are

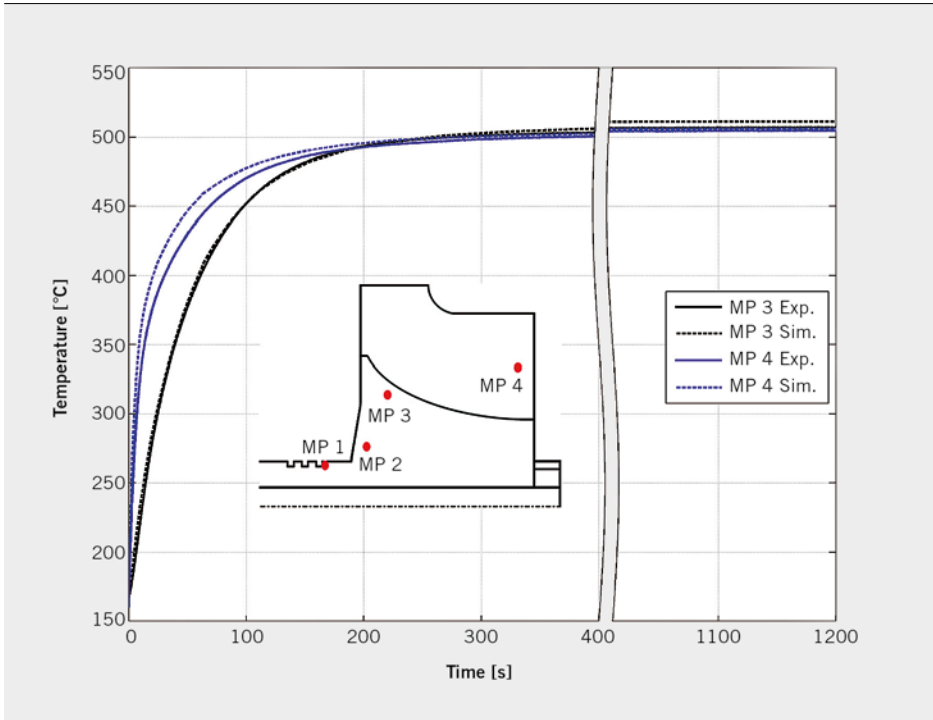


**FIGURE 4** Comparison of measurement and simulation at two measuring points on the turbine wheel (© RWTH Aachen University)

caused by secondary flows. The relationship between the thermal loads and the secondary flows is described below using the example of the trailing edge at the hub.

Due to the separation of the flow at the trailing edge a local area of turbulence (wake) occurs, **FIGURE 5**. This area of turbulence

leads locally to very small Reynolds numbers compared to those in the main flow. It is well established that the Reynolds number is directly related to the heat transfer coefficients. Consequently, there are locally very small heat transfer coefficients at the blade trailing edge compared to the main flow that influence the heat

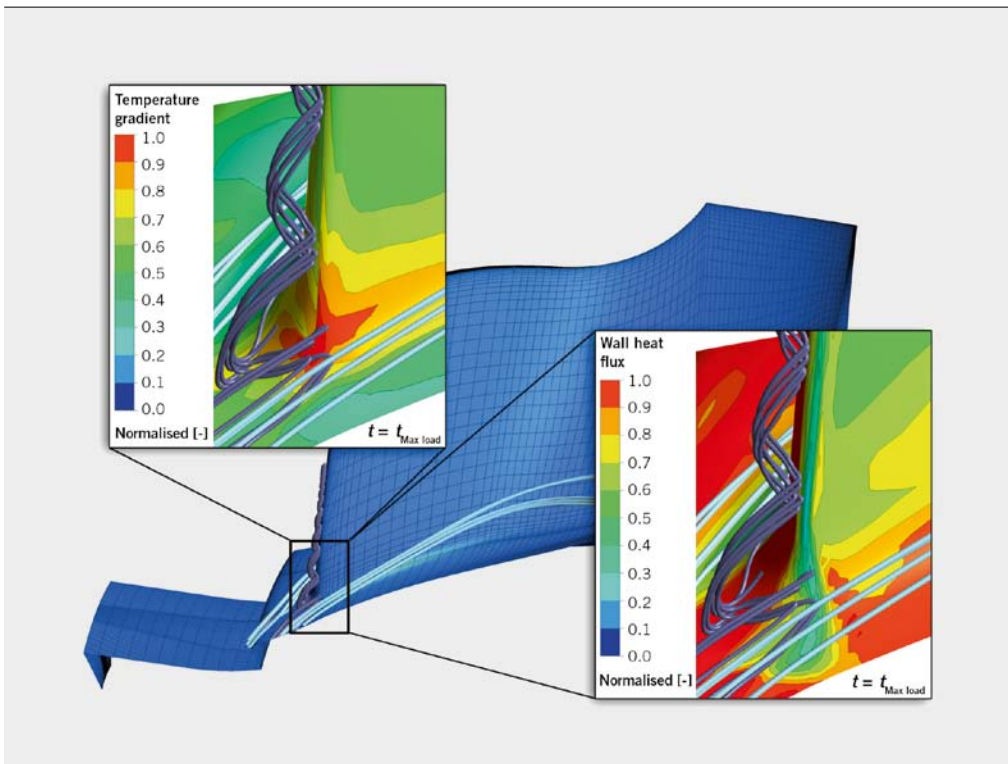


**FIGURE 5** Heat fluxes, temperature gradients and the separation flow at the the trailing edge (© RWTH Aachen University)

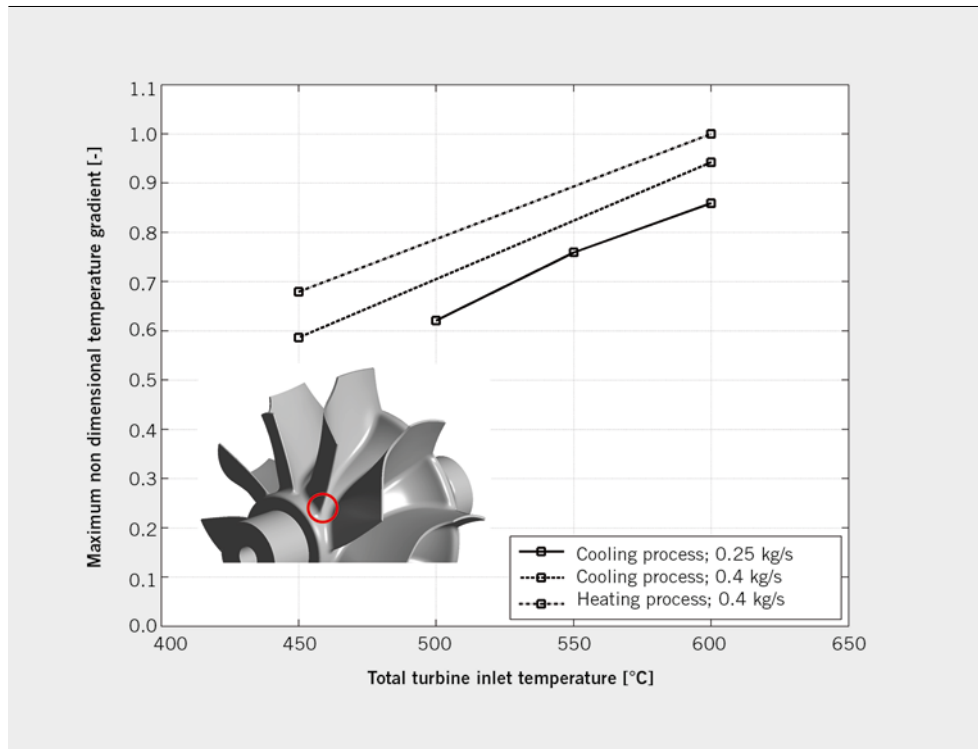


**FIGURE 6** Maximum temperature gradient at the trailing edge on the hub for different operating parameters (© RWTH Aachen University)

input or output at the blade. **FIGURE 5** shows the heat fluxes at the time point of the maximum thermal loads. It can be seen that, due to the reduced heat transfer coefficients, significantly smaller heat fluxes occur at the trailing edge compared to those on the blade surface that interact with the main flow. As a result of this strong variation of the heat fluxes in a very small area high temperature gradients occur inside the material.

High temperature differences between the fluid state and the solid body occur in the transient operation of the turbocharger compared to the steady-state operation. These temperature differences lead to correspondingly high heat fluxes. The locally reduced heat transfer coefficients at the trailing edge have particularly high impact in this case since the differences between the heat fluxes of the mainstream and those of the area of turbulence are considerably higher. Therefore, the maximum temperature gradients in this area arise during the transient operation of the turbocharger. Similar effects also occur in the other two areas mentioned above. Here, secondary flows cause locally reduced heat fluxes that lead to high temperature gradients in the solid body as well.

The thermal loads are strongly dependent on the operation process of the turbocharger. To investigate the influence of different operating parameters on the thermal loads, various thermal shock processes were measured and simulated. The total inlet temperature, the mass flow and the operation mode were varied. The operation comprises cooling and heating processes. In **FIGURE 6**, the maximum non dimensional temperature gradients at the trailing edge at the hub are compared for different operating parameters in the thermal shock processes. For non-dimensional representation of the gradients they are divided by the maximum value. It is apparent that the thermal stressors increase with both the inlet temperature and the mass flow rate. An increase in the mass flow rate with a constant inlet temperature leads to higher mean Rey-

nolds numbers and therefore to higher heat fluxes and temperature gradients. An increase in the turbine inlet temperature leads to increased driving temperature differences between the fluid state and the solid body. This also results in higher heat fluxes and thermal loads. As a final influence parameter the operation mode was investigated. It turned out that a heating process shows higher temperature gradients than a cooling process. In the heating process higher driving temperature difference between fluid state and solid body occur, which result, as described above, in higher temperature gradients. Thus, operation under full load is particularly critical with regard to the thermal loads. An engine brake operation, however, is less critical since smaller mass flow rates there occur in this case and the turbocharger is cooled.

## 6 SUMMARY AND OUTLOOK

In the FVV research project, a test rig was constructed, which allows to approximate the real transient operation of a turbocharger by thermal shock tests. In these tests material temperatures were measured in the turbine, which serve as a validation basis of the numerical simulations. A simulation methodology was developed which achieves very accurate results compared to the measured data and which allows a detailed analysis of the heat transfer mechanisms. Based on these simulations four thermally highly loaded areas were identified. Furthermore, it was shown that the thermal stressors in three of the four critical areas are caused by secondary flows that lead to locally reduced heat fluxes in the turbine wheel and thus causes high temperature gradients in the solid body.

In future investigations structural mechanics simulations of the turbine wheel will be carried out using the known transient temperature fields. Based on these simulations, the influence of the thermal stressors compared to the centrifugal force stressors will

be investigated in order to assess the necessity of considering the thermal stressors in the design process of a turbocharger. Furthermore, a method will be developed which allows a faster approximation of the thermal loads, so that the thermal loads can be included in the design process of a turbocharger.

#### REFERENCES

- [1] Dornhöfer, R. et al.: Der neue R4 2,0l 4V TFSI-Motor im Audi A3. 11. Aufladetechnische Konferenz, Dresden, 2006
- [2] Heuer, T. et al.: Numerical Analysis of the Heat Transfer in Radial Turbine Wheels of Turbochargers. ASME Turbo Expo GT2007-27835, Montreal, Canada, 2007
- [3] Ahdad, F. et al.: Analytical Approach of TMF Prediction for Complex Loading. ASME Turbo Expo GT2010-23440, Glasgow, UK, 2010
- [4] He, L. et al.: Unsteady Conjugate Heat Transfer Modelling. ASME Turbo Expo GT2009-59174, Orlando, 2009

- [5] Sun, Z. et al.: Efficient Finite Element Analysis/Computational Fluid Dynamics Thermal Coupling for Engineering Applications. ASME Journal of Turbomachinery, Vol. 132, 2010

---

## THANKS

The authors would like to thank the research association Forschungsvereinigung Verbrennungskraftmaschinen e. V. (FVV), the Association Industrial Research (AiF), BorgWarnerTurbo Systems Engineering GmbH and the JARA-HPC award committee for supporting this work. Especially the authors thank the chairman of the project Dr. Tom Heuer.